CONTRACT SERIAL NO.
23440-8-9176-01-SS
FINAL REPORT
CONTRACTOR: LAVAL UNIVERSITY

[redacted]

DÉPARTEMENT DE GÉNIE CHIMIQUE

UNIVERSITÉ LAVAL

QUÉBEC, QUÉ., CANADA, G1K 7P4

91-06110/

QUANTITATION OF XPS INTENSITY RATIOS FOR SUPPORTED CATALYSTS

A. SAYARI AND S. KALIAGUINE

Final Report

Project conducted for the
Canada Centre for Mineral and
Energy Technology
Energy, Mines and Resources Canada

File No. (DSS): 064SS-23440-8-9176
Project No. (CANMET) 23440-8-9176

CANMET Scientific Authority: Dr. James R. Brown

THIS WORK WAS SUPPORTED BY
THE FEDERAL PANEL ON ENERGY R&D (PERD)

Department of Chemical Engineering
Université Laval

126 pp

November 1990

MICROMEDIA

CONTENTS

ABSTRACT iii

RESUME. iv

EXECUTIVE SUMMARY v

LIST OF TABLES vii

LIST OF FIGURES. viii

I. INTRODUCTION 1

II. BACKGROUND. 3

III. EXPERIMENTAL 11

III.1. Catalyst preparation. 11
III.1.1. Support materials 11
III.1.2. Pd/HZSM-5. 13
III.1.3. Pt/HZSM-5. 14
III.1.4. Other catalysts. 14

III.2. Characterization of catalysts. 16
III.2.1. Analysis: atomic absorption and x-ray fluorescence. 16
III.2.2. X-ray photoelectron spectroscopy 16
III.2.3. BET and external surface areas. 18
III.2.4. Hydrogen chemisorption 20
III.2.5. Electron microscopy 21

IV. RESULTS AND DISCUSSION. 22

IV.1. General considerations. 22
IV.1.1. General procedure for XPS quantitation. 22
IV.1.2. External surface areas. 25

IV.2. Experimental results and discussion 41
IV.2.1. Pd/HZSM-5 catalysts. 41
IV.2.1.1. Experimental data. 41
IV.2.1.2. Application. 46
IV.2.1.3. Effect of various parameters on C_2 and x_1. . 49
IV.2.1.4. Conclusions. 56
IV.2.2. Pt/HZSM-5 catalysts. 62
IV.2.3. Silica- and alumina-supported Pt catalysts . . . 71
IV.2.4. Other catalysts 64

V. CONCLUSIONS AND RECOMMENDATIONS. 80

REFERENCES. 85

APPENDIX 1 - SOFTWARE DESCRIPTION AND OPERATIONS.

APPENDIX 2 - TRANSMISSION ELECTRON MICROGRAPHS OF SOME SELECTED Pt AND Pd CONTAINING CATALYSTS.

APPENDIX 3 - XPS SPECTRA OF ALL CATALYSTS.

ABSTRACT

This work dealt with the use of XPS intensity data to quantitative determination of mean particle sizes (and dispersion) of active materials in supported catalysts. A major novelty of the model developed here as compared to previous models is its ability to allow for surface segregation of supported materials and therefore to determine bimodal distributions. A general approach to solve the mathematical equations is also proposed. This method uses in addition to the XPS intensity ratios, the BET and the external surface areas of catalysts under both the as-synthesized and the ground forms. Method developments for measurements of external surface areas for zeolite-based catalysts were carried out. Experimental procedures for the pore plugging technique were determined.

The XPS model was applied to a series of Pt, Pd, Ni and Mo supported catalysts. It was found to be particularly suitable for zeolite-based catalysts.

R E S U M E

Ce travail a été consacré à l'utilisation quantitative des rapports d'intensité des pics obtenus en spectroscopie des photoélectrons (XPS) pour déterminer la taille moyenne (et la dispersion) des particules d'espèces actives dans les catalyseurs supportés. La principale nouveauté du modèle développé ici est sa capacité de tenir compte de la segrégation superficielle et par conséquent d'analyser des distributions bimodales. Une approche générale pour résoudre les équations mathématiques est aussi proposée. Cette méthode utilise en plus des rapports d'intensité des pics XPS, la surface BET et la surface spécifique externe du catalyseur avant et après broyage. Des méthodes pour mesurer la surface spécifique externe de catalyseurs à base de zéolithes ont été développées. La procédure expérimentale pour la technique du remplissage des pores a été déterminée.

Le modèle XPS a été utilisé pour une série de catalyseurs contenant l'un des métaux suivants: Pt, Pd, Ni, Mo. Ce modèle a été trouvé particulièrement adapté aux catalyseurs à base de zéolithes.

EXECUTIVE SUMMARY

X-ray photoelectron spectroscopy (XPS) has been used extensively to characterize catalytic materials. Several models have been proposed to extract quantitative information from XPS data with regard to the particle sizes of the active phase in supported catalysts. In particular the so-called sheet stacking model has attracted much attention. In these models however, the supported material was considered as comprised of particles having the same size and homogeneously distributed throughout the support. Therefore, bimodal distributions arising from surface segregation, a phenomenon that occurs in real catalysts almost systematically cannot be addressed using such models. Zeolite-supported catalysts are particularly prone to surface segregation; they often exhibit bimodal distributions with large particles on the external surface and small particles well dispersed within the zeolite micropore structure.

Kaliaguine and his coworkers have proposed an improved version of the sheet stacking model that is capable of accomodating surface segregation and bimodal distributions. In this model, the active phase is regarded as a combination of two populations with different particle sizes, C_1 and C_2. The crystallites of size C_1 are homogeneously distributed throughout the support, while the particles with the larger dimension C_2 are segregated on the external surface of the support.

The mathematical derivation of this model leads to an equation involving three independent variables, namely C_1, C_2 and the weight percent of one of the two crystallite populations, say x_1. A general approach has been developed to determine C_2 and x_1 based on an arbitrarily chosen value for C_1. This method involves the determination of XPS intensity ratios of a photoline for the dispersed phase and a photoline of the support, as well as the external and the BET surface areas of the catalyst before and after grinding.

Method developments for measurements of external surface areas for zeolite-based catalyst were carried out. The study dealt in particular with the t-plot and the pore plugging methods. Experimental procedures for the pore plugging technique were determined.

The XPS model was applied to a series of Pt, Pd, Ni and Mo supported catalysts after various pretreatments. In the case of reduced samples, comparison with results obtained by transmission electron microscopy and hydrogen chemisorption showed that the model as it stands now is particularly suitable for zeolite-based catalysts.

A systematic study of the effect of various parameters on the distribution characteristics (C_2 and x_1) calculated using the XPS model has been carried out. It included the effect of the value of C_2 , which is usually given an arbitrary value, the upper limit of which should not exceed the zeolite micropores size. Other factors such as the effect of the external surface area before and after grinding and the XPS intensity ratios were also studied.

This model is very promising particularly with regard to the characterization of non metallic catalysts such as supported oxides, sulfides and other salts. More work is however still needed for example in the area of the external surface area (definition and measurements). Applications to catalysts based on non zeolitic materials should also be made possible.

LIST OF TABLES

Tables	TITLE	Page
I	Conditions for the preparation of ZSM-5 zeolites. . . .	12
II	Silica- and alumina-supported catalysts.	15
III	Chemical analysis	17
IV	Nitrogen physisorption data for samples A and B	33
V	XPS data for Pd/HZSM-5 catalysts	43
VI	Textural properties of Pd/HZSM-5 catalysts.	44
VII	XPS data for Pt/HZSM-5 catalysts	61
VIII	Textural properties of Pt/HZSM-5 catalysts.	63
IX	Data for XPS quantification for reduced Pt/ZSM-5 catalysts.	64
X	XPS data for Pt/SiO_2 and Pt/Al_2O_3 catalysts.	67
XI	Textural properties of Pt/SiO_2 and Pt/Al_2O_3.	68
XII	XPS data for Ni/Al_2O_3.	70
XIII	XPS data for Mo/Al_2O_3.	71
XIV	Textural properties of Ni/Al_2O_3 and Mo/Al_2O_3 catalyts . .	74
XV	Data for XPS quantification for NiO/Al_2O_3 catalysts. . .	76
XVI	Data for XPS quantification for MoO_3/Al_2O_3 catalysts. . .	77

LIST OF FIGURES

Figure	TITLE	Page
1.	Schematic representation of the XPS model.	7
2.	t-plot: effect of meso- and microporosity.	28
3.	Nitrogen adsorption-desorption isotherms for sample A before and after benzene preadsorption.	31
4.	t-plots for sample A before and after benzene preadsorption.	32
5.	BET suface areas of sample A as a function of the benzene residual pressure, P_B (torr)	34
6.	Adsorption-desorption isotherm of benzene for sample A at 301 K.	36
7.	Nitrogen adsorption-desorption isotherm for CPG 120. . . .	38
8.	Pore size distributions for CPG 120, (a) before benzene adsorption, (b) after benzene preadsorption (P_B = 85 torr) .	39
9.	XPS spectra of Pd(3d) in sample 142B (2.43% Pd/HZSM-5) (a) oxidized, (b) reduced	42
10.	Hydrogen chemisorption isotherms for sample 142B (2.43% Pd/HZSM-5).	48
11.	Transmission electron micrograph of sample 142B (2.43% Pd/HZSM-5) after reduction.	50
12.	Particle size distribution from TEM micrograph of sample 142B (2.43% Pd/HZSM-5)	51
13.	Calculated effect of the size of dispersed particles (C_1) on (a) the size of segregated particles (C_2), (b) the particles distribution. Sample 142B (2.43% Pd/HZSM-5).	52

14. Calculated effect of the external surface area A_u at a constant A_u/A_g ratio on
(a) the size of segregated particles (C_2),
(b) the particles distribution.
Sample 142B (2.43% Pd/HZSM-5). 54

15. Calculated effect of the external surface area A_u at a constant A_g on
(a) the size of segregated particles (C_2),
(b) the particles distribution.
Sample 142B (2.43% Pd/HZSM-5). 55

16. Calculated effect of the XPS intensity ratio $(I_p/I_s)_g$ at a constant $(I_p/I_s)_u/(I_p/I_s)_g$ ratio on

(a) the size of segregated particles (C_2),
(b) the particles distribution.
Sample 142B (2.43% Pd/HZSM-5). 57

17. Calculated effect of the XPS intensity ratio $(I_p/I_s)_g$ at a constant $(I_p/I_s)_u$ ratio [$(I_p/I_s)_u$ = .3017] on

(a) the size of segregated particles (C_2),
(b) the particles distribution.
Sample 142B (2.43% Pd/HZSM-5). 58

18. XPS quantification results for
(upper figure) sample 142A (3% Pd/HZSM-5), and
(lower figure) sample 180A (3% Pd/HZSM-5). 60

19. XPS quantification results for sample 151B
(2.93% Pd/HZSM-5). 61

20. XPS spectra of Pt(4d) in sample 140A (1.85% Pt/HZSM-5)
(a) oxidized, (b) reduced, (c) reduced and ground 63

21. XPS quantification results for
(upper figure) sample 140A (1.85% Pt/HZSM-5), and
(lower figure) sample 140B (2.53% Pt/HZSM-5) 68

22. Calculated effect of the external surface area A_u at a constant A_g on
(a) the size of segregated particles (C_2),
(b) the particles distribution.
Sample 140A (1.85% Pt/HZSM-5). 69

23. Calculated effect of the external surface area A_u at a constant A_u/A_g ratio on the size of segregated particles (C_2). Sample 140Å (1.85% Pt/HZSM-5). 70

24. XPS spectra of Ni(3p) in sample 182 (3.36% Ni/Al_2O_3) (a) oxidized, (b) oxidized and ground 77

25. XPS spectra of Mo(3d) in sample 183 (9.30% Mo/Al_2O_3) (a) oxidized, (b) oxidized and ground 78

QUANTITATION OF XPS INTENSITY RATIOS

FOR SUPPORTED CATALYSTS

I. INTRODUCTION

Ideally, the characterization of a catalyst comprised of different chemical phases should include the determination of the surface area exposed by each of these phases, together with their particle size distributions. For unsupported catalysts with one single phase, the combined use of the BET and for example electron microscopy techniques may be appropriate to reach this objective.

For supported catalysts however, the success is primarily dependent on the nature of the phases present. Supported metals are usually relatively easy to characterize in terms of dispersion and particle size distribution. Chemisorption methods are quite effective for a number of metals (1). In addition, several physical techniques including electron microscopy and X-ray methods (diffraction line broadening and small angle scattering) may provide the same kind of information (2-4).

As for other types of catalysts such as supported alloys, oxides, sulfides and other salts, the problem may be much harder to overcome. Chemisorption techniques are of a very limited use and not always reliable. Most of the physical characterization methods have also strict criteria to be met before contemplating their use. The X-ray photoelectron spectroscopy (XPS) seems however, to be a quite general technique that can be readily used to characterize heterogeneous catalysts regardless of their nature. In this case, the information that can be obtained is limited primarily by the inability of the current models to translate the XPS data in terms of dispersions and particle size distributions.

The potential usefulness of this technique to address many problems in relation to heterogeneous catalysis cannot be overemphasized. Several areas that may benefit from the development of a model, based on XPS intensity ratios, that can accurately estimate the dispersion and other

structural characteristics of a supported active phase were identified in the original proposal. These were:

1. Comparison of methods of preparation of supported catalysts.
2. Effect of pretreatments.
3. Structural changes associated with the catalytic reactions at steady state or even in transient situations.
4. Catalyst deactivation (sintering, coking, poisoning by nitrogen, sulfur, phosphorus, heavy metals, etc.).
5. Simulation of catalyst regeneration.

Beyond the suitability of the model in terms of whether or not it is a realistic representation of real catalysts, the use of XPS as tool for quantitative characterization has been severely hampered by the many uncertainties and imprecisions accompanying the various parameters involved. This points out to the urgent need to assess and eventually correct these problems.

This work was carried out at the Catalyst Laboratory of Laval University (Prof. S. Kaliaguine) and supported by CANMET, Departemnt of Energy, Mines and Resources Canada and the Program of the Federal Panel on Energy Research and Development (Dr. J.R. Brown) under contract # 23440-8-9176. The main objectives of this work were twofold:

- to develop an elaborate model for the quantitative description of XPS intensity ratios for supported catalysts. Such a model should account for at least two phenomena frequently observed in real catalysts. These are the segregation of active materials at the external area and the resulting bimodal distribution of these species.

- to assess and find ways to minimize the uncertainties associated

with a series of experimental parameters.

The various tasks as defined in the contract were as follows:

TASK 1: Model development. Mathematical derivation. Elimination of uncertainties.
TASK 2. Experimental verification of the model:
TASK 2A. Pd/Zeolite catalysts.
TASK 2b. Pt/zeolite catalysts.
TASK 3b. Other catalysts: Pt/SiO_2, Ni/Al_2O_3, Mo/Al_2O_3.
TASK 3. Delivrables: reports, computer programs, etc.

It is hoped that this work would provide a much needed tool to characterize supported catalysts regardless of their nature.

II. BACKGROUND

Since the early seventies, X-ray photoelectron spectroscopy has been used extensively to characterize catalytic materials. Early applications dealt mostly with the qualitative analysis of the outmost layers of catalysts. The first quantitative applications appeared with the development of the solid solution model proposed by Carter *et al.* (5). In this model, it was assumed that at least within the thickness of the surface layer actually analyzed, the solid is homogeneous and its composition is constant. The surface composition of an element p relative to a reference element s can be calculated using equation [1] in which I_p/I_s stands for the intensity ratio of the selected photolines of electrons ejected from elements p and s.

$$\left(\frac{I_p}{I_s}\right)_{XPS} = \left(\frac{n_p}{n_s}\right)_{SURF.} \frac{\sigma_p}{\sigma_s} \frac{\lambda_p}{\lambda_s} \frac{D(E_{kp})}{D(E_{ks})} \qquad [1]$$

n_i, σ_i, λ_i and $D(E_{ki})$ designate the surface relative atomic concentration of species i, the ionisation cross section, the inelastic mean free path and the detector efficiency of a selected electron ejected from species i, respectively.

Equation [1] is used routinely to analyse catalyst surfaces. Some of the most interesting applications were:

- The detection of surface segregation during the preparation (6) or post-synthesis modifications (7) of zeolite based catalysts.
- The detection of aluminum surface enrichment in certain zeolites (8, 9).
- The homogeneity of alloys and bimetallics or the surface segregation thereof (10, 11).
- The identification and quantitation of acid sites by adsorption of pyridine (12, 13).

One of the first attempts to extract the average metallic particle size of supported metal catalysts from XPS data was made by Delgass *et al.* (14). In their model, the catalyst was regarded as a uniform distribution of cubic particles of promoter p, on a flat, semi-infinite layer of support s. This model has been extended to other shapes of particles (15). The general equation allowing for the determination of the average particle size C is:

$$\left(\frac{I_p}{I_s}\right)_{XPS} = k\frac{w}{\rho_p S_{BET}}\frac{\lambda_p}{\lambda_s}\frac{D(E_{kp})}{D(E_{ks})}\Psi(C,\ \lambda_p) \qquad [2]$$

where k designates a constant describing the distribution of the promoter p; w is the weight of p per gram of catalyst; ρ_p is the density of p and S_{BET} is the BET surface area of the support. This model did not meet much success because it ignored the effect of surface roughness and the support porosity on the XPS intensity data. As shown by Defosse (16), it can at best be used for catalysts supported on materials of relatively low surface areas, say less than 100 m^2g^{-1}.

A more elaborate model that better simulates the porous nature of supported catalysts has been proposed by Defosse *et al.* (17). Here, the support was described as a stacking of non-porous particles or sheets, the size or the thickness of which is such that the surface-to-mass ratio of these particles or sheets is equal to the surface-to-mass ratio of the actual support. Note however, that the sheet stacking model that has been further improved by Kerkhof and Moulijn (18) attracted more attention than the models based on the stacking of particles.

Recent developments of this model were reported by Davis (19-21). Assessment of metallic particle sizes in the range 10 - 60 Å was made using one of the following XPS data, (i) XPS intensity ratio of two core levels of the supported phase with different kinetic energy, (ii) XPS intensity ratio of photoelectons from the dispersed phase and the support, (iii) the influence of inelastic scattering on the photoemission line shape.

In these models, the supported material was considered as comprised of particles having the same size and homogeneously distributed throughout the support. Therefore, even though the sheet stacking model as originally proposed was considered as a significant step forward in enhancing our ability to extract quantitative information from XPS data, it failed to address problems arising from surface segregation and bimodal distributions which occur in real catalysts almost systematically.

These shortcomings incited Kaliaguine and his coworkers (22) to propose an improved version of this model that is capable of accomodating both concerns. As schematically shown in Figure 1, in this model the promoter is regarded as a combination of two populations with different particle sizes, C_1 and C_2. The crystallites of size C_1 are homogeneously distributed throughout the support, while the particles with the larger dimension C_2 are segregated on the external surface of the support.

The mathematical derivation of this model leads to the following equation:

$$\left(\frac{I_p}{I_s}\right)_{XPS} = \frac{K_p}{K_s}\frac{\left(1-P_{ss}P_{sp}^2\right)}{\left(1-P_{ss}\right)P_{sp1}}\left\{\left(1-P_{pp1}\right)+P_{pp1}\frac{P_{ps}\left(1-P_{pp}^2\right)}{1-P_{ps}P_{pp}^2}\right\} \qquad [3]$$

where

$$\frac{K_p}{K_s} = \frac{n_p\sigma_p\lambda_{pp}D\left(E_{kp}\right)}{n_s\sigma_s\lambda_{ss}D\left(E_{ks}\right)} \qquad [4]$$

Here P_{is} stands for the probability for electrons originating from the material i (support or promoter) to pass through a continuous layer of support of thickness t, while P_{ip} refers to the probability for the same electrons to travel through a discontinuous layer of promoter having a thickness of C_1 and occupying a fraction f_1 of the support surface area. P_{ip1} represents the probability for an electron from material i to pass through the outermost layer of promoter. In contrast to the inner layers of promoter, this layer is comprised of two different populations having average particle sizes C_1 and C_2,

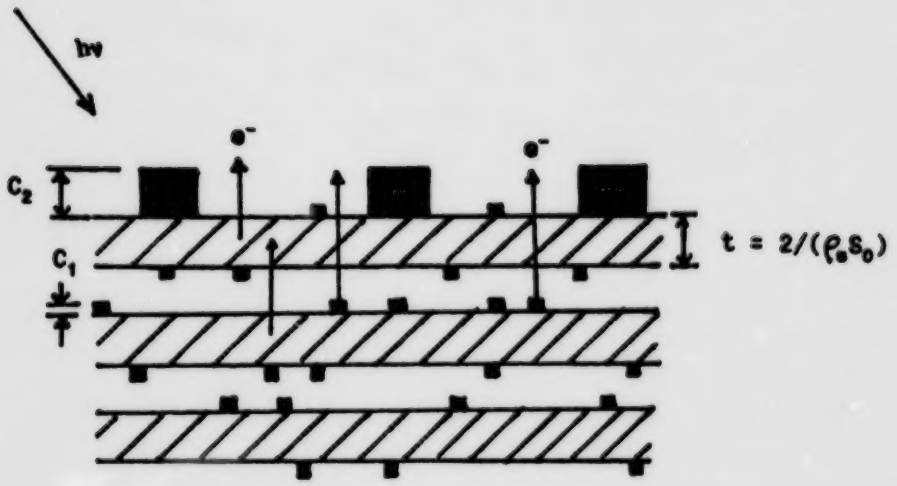

Figure 1. Schematic representation of the sheet stacking model with surface segregation.

respectively. The fractions f_1 and f_2 of the outermost layer of the support that are occupied by the two promoter populations are calculated on the basis of the total BET and the external surface area, respectively. This assumption is based on the fact that the small particles of the promoter can be accomodated anywhere on the support, whereas the large particles cannot penetrate into the porous structure of the support, and therefore they can be accomodated only on the external surface. Finally, n_p and n_s are the atomic densities of the analyzed elements in promoter and support, respectively. In this context, the atomic density means the number of g.atoms of the analyzed element per cubic centimeter of the actual chemical component containing that element, and not the number of g.atoms per volume of catalyst. The atomic density of an element A in a compound C, the formula and density of which are A_aB_b and ρ_C, is given by:

$$n_a = a*\rho_C/M_C$$

For example, in an oxidized PdO/ZSM-5 sample, if the analyzed elements are Pd and Si, then n_p and n_s would be the atomic densities of Pd in PdO and that of Si in SiO_2 (assuming a silica-rich zeolite), respectively:
$n_p = \rho_{PdO}/M_{PdO} = 8.3/122.4 = .0678$ g.atom/cm^3.
$n_s = \rho_{SiO2}/M_{SiO2} = 2.4/60 = .04$ g.atom/cm^3.
If the catalyst were reduced n_p would be equal to ρ_{Pd}/M_{Pd}.

No attempts have been made to solve equation [3] before further simplifications. For example, it is usually possible to find in a XPS spectrum a photoline originating from the promoter that is close in terms of kinetic energy to a photoline from the support. If these two photolines are chosen for the quantitation of the XPS intensity ratio, the following simplifications can be made (11):

$$\lambda_{pp} = \lambda_{sp} = \lambda_p; \qquad \lambda_{ss} = \lambda_{ps} = \lambda_s \quad \text{and}$$

$$P_{ss} = P_{ps} = P_1; \quad P_{sp} = P_{pp} = P_2; \quad P_{sp1} = P_{pp1} = P_3$$

Under these conditions equation [3] becomes

$$\left(\frac{I_p}{I_s}\right)_{XPS} = \frac{K_p}{K_s}\left(\frac{1-P_1P_2^2}{(1-P_1)P_3}-1\right) \qquad [5]$$

with

$$P_1 = e^{-t/\lambda_s} \qquad [6]$$

$$P_2 = 1-f_1+f_1e^{-C_1/\lambda_p} \qquad [7]$$

$$P_3 = 1-f_1-f_2+f_1e^{-C_1/\lambda_p}+f_2e^{-C_2/\lambda_p} \qquad [8]$$

Moreover f_1 and f_2 are given by

$$f_1 = x_1/S_0(1 - x_B)\rho_pC_1 \qquad [9]$$

$$f_2 = x_2/A_0(1 - x_B)\rho_pC_2 \qquad [10]$$

where x_1 and x_2 designate the weight percent of the dispersed and the segregated population, respectively, whereas x_B represents the total weight percent of the promoter. The BET and the external surface areas of the

catalyst are referred to as S_0 and A_0, respectively.

In equation [5], three independent variables are involved, namely the crystallite sizes of the dispersed (C_1) and the segregated (C_2) fractions of the promoter and the weight percent of one of these fractions, say x_1. Several approaches were used to extract quantitative information using XPS data in conjunction with equation [5].

In a successful application that dealt with a homogeneous series of zeolite-supported ruthenium catalysts, C_1 was arbitrarily taken as 3 Å because of the pore size restrictions (22). Moreover, x_1 was assumed to be proportional to the percent of exchanged Bronsted acid sites which can be determined from infrared measurements. The proportionality factor was calculated by chosing among the catalysts a reference for which x_1 was arbitrarily taken as 50 %. This study revealed two important findings, (i) for C_1 values ranging from 3 to 10 Å, the calculated values for C_2 hardly change, (ii) the estimated value of C_2 is strongly dependent on the external surface area A_0.

In another study dealing with iron-loaded ZSM-5 catalysts, Kaliaguine *et al.* (23) used equation [5] in combination with the equivalent equation that one would derive if both populations of the promoter were homogeneously distributed throughout the support, that is

$$\left(\frac{I_p}{I_s}\right)_{XPS} = \frac{K_p}{K_s}\frac{(1-P_4)}{(1-P_1)}\left(\frac{1+P_1P_4}{P_4}\right) \qquad [11]$$

where

$$P_4 = 1 - f_1 - f_3 + f_1 e^{-C_1/\lambda_p} + f_3 e^{-C_3/\lambda_p} \quad [12]$$

and

$$f_3 = x_2/S_0(1 - x_B)\rho_p C_2 \quad [13]$$

It was shown that the XPS intensity ratios satisfy equation [11] if catalysts are submitted to a lengthy grinding period. Note that in this approach, XPS measurements have to be carried out on catalysts in both their ground and as-prepared forms and yet one has to allow for an arbitrary value of C_1.

In the present work, a more general approach has been adopted whereby grinding has not to be lengthy or even controlled as long as it induces a change in the XPS intensity ratio. Detailed description of the procedure will be provided later.

III. EXPERIMENTAL

III.1. CATALYST PREPARATION

III.1.1. Support Materials

Two ZSM-5 zeolites were prepared following published procedures (24). Three solutions, the composition of which are gathered in Table 1 were mixed together under vigorous stirring. The mixture was then shaked for two more hours before it was poured in stainless steel autoclaves and kept at a temperature of 140 °C for several days (Table 1) during which the alumino-silicic gel crystallizes into a ZSM-5 structure. The solid thus obtained was thoroughly washed with distilled water, dried, then air-calcined at 500 °C for 15 h.

TABLE I. Conditions for the Preparation of ZSM-5 Zeolites

	Sample A	Sample B
Solution I		
Sodium silicate (g)	712.12	272.8
Water (g)	333	127
Solution II		
NaCl (g)	90.57	0
CsCl (g)	0	100
Water (g)	333	127
Solution III		
Water	333	127
$Al_2(SO_4)_3$, $18H_2O$ (g)	53.32	20.43
H_2SO_4 (g)	56,95	21.8
TPABr[a] (g)	80	30.66
Crystallization		
Time (days)	4	9
Temperature (°C)	140	140

(a) tetrapropylammonium bromide

As shown in Table 1, the major differences in the preparation procedures of samples A and B are the nature of solution II and the autoclavation time. According to Gabelica *et al.* (13), the use of CsCl instead of NaCl together with a longer crystallization time leads to a ZSM-5 sample with larger and more perfect crystallites.

III.1.2. Pt/HZSM-5

Platinum-containing zeolites were prepared using the ion-exchange technique. In a typical procedure, an aqueous solution containing the required amount of $Pt(NH_3)_4Cl_2$ was added dropwise at room temperature to a vigorously stirred suspension of 1 g of zeolite per 100 ml of water. The mixture was kept under continuous stirring for an additional 15 h-period. The solid was then filtred, thoroughly washed and dried. The resulting platinum catalyst precursor was then decomposed in air while heating at 1 $K.mn^{-1}$ up to 400 °C. This temperature was maintained overnight. As stressed by several authors (25, 26), the experimental conditions during the calcination step (rate of temperature increase and maximum temperature) are of paramount importance for a well dispersed catalyst to be obtained upon reduction. Activation conditions similar to those used in this work have been reported to yield highly dispersed Y-zeolite supported platinum catalysts (10, 25, 26).

Subsequent to the sample calcination, the remaining Na^+ or Cs^+ cations in the sample were extensively exchanged with NH_4^+ using 1 M aqueous solutions of NH_4NO_3 at 80 °C. Finally, the catalyst was calcined again at 500 °C for 15 h in order to decompose the ammonium cations and obtain the acid form of the sample. The crystallinity of both samples was checked by comparing their X-ray diffraction patterns (diffraction angles and relative energies) to a standard spectrum of the ZSM-5 structure.

III.1.3. Pd/HZSM-5

Two series of palladium-loaded zeolites were prepared. For the first series, the ion-exchange technique using $Pd(NH_3)_4(NO_3)_2$ was adopted. All the preparation steps were the same as those described for the platinum-containing catalysts.

As for the second series, the gas phase adsorption-decomposition technique was selected. In this method, the hydrogen form of the zeolite is dry-mixed (under vacuum or controlled atmosphere, if necessary) with the required amount of an organometallic compound of the desired metal. The mixture is then sealed under vacuum and heated gradually up to a temperature high enough for the organometallic complex to decompose completely. This final temperature is usually maintained for 24 h before cooling down the sample which should then undergo a final calcination in air at 500 °C for 15 h. In the present work both zeolites (A and B) were used and the organometallic source of Pd was either allyl cyclopentadienyl palladium or palladium acetate.

III.1.4. Other Catalysts

As listed in Table II, several samples consisting of Pt supported on γ-alumina or on a large-pore silica gel were also prepared. In a typical preparation, an aqueous solution containing the required amount of H_2PtCl_6, xH_2O was mixed with the support under vigorous stirring. The mixture was then heated until dryness in a rotating evaporator. Subsequently, the sample was calcined in air at 500 °C for 15 h.

Two more catalysts consisting of Mo/Al_2O_3 and Ni/Al_2O_3 were prepared according to similar recipes (Table II). Nickel nitrate and Ammonium molybdate were used as precursors for Ni and Mo, respectively.

TABLE II. Silica- and Alumina-Supported Catalysts

Designation	Description	Precursor	wt% Metal[a]
185A	Pt/alumina	H_2PtCl_6, xH_2O	1.85
185B	Pt/alumina	" " "	0.96
186A	Pt/silica	" " "	2.97
186B	Pt/silica	" " "	1.10
182	Ni/alumina	$Ni(NO)_3$, $6H_2O$	3.36
183	Mo/alumina	$(NH_4)_6Mo_7O_{24}$, $4H_2O$	9.30

(a) determined by atomic absorption

III.2. CHARACTERIZATION OF CATALYSTS

III.2.1. Analysis: Atomic Absorption and X-Ray Fluorescence

Complete analyses of all samples were carried out mostly by atomic absorption using a 1100B Perkin Elmer spectrometer. Usually, a known amount of the sample to analysed is digested at 90 °C in a solution containing concentrated HCl and HNO_3 and a 40% HF solution, their volumic proportions being 10/10/1. Quantitative analyses were made by comparing actual data to data of calibrated solutions of the various elements of interest.

Palladium contents were determined by X-ray fluorescence using a LINK XR200 apparatus. For calibrated purposes, samples of known Pd concentrations were prepared by thoroughly grinding mixtures containing the required amounts of palladium acetate and pure HZSM-5 zeolite. The results of these analyses are summarized in Table III.

III.2.2. X-Ray Photoelectron Spectroscopy (XPS)

All Pt- and Pd-containing samples were studied by XPS under four different forms:

- oxidized
- oxidized then ground
- reduced
- reduced then ground

As for Ni/Al_2O_3 and Mo/Al_2O_3, it is known that H_2 treatment of such samples often leads to incomplete reduction and the occurrence of various Ni and Mo species. Therefore, it is felt that the study of reduced samples would be too complicated to carry out at this stage of development. The study will be confined to the oxidized forms of these two catalysts.

TABLE III. Chemical Analysis

Designation	Description	%Me	%Si	%Al
A	HZSM-5	0.009 (Na)	38.0	2.6
		0.008 (Cs)		
B	HZSM-5	1.63 (Cs)	39.1	2.6
		0.038 (Na)		
140A	Pt/A	1.85		
140B	Pt/B	2.53		
142A	Pd/A	3.00		
142B	Pd/B	2.43		
151A[a,b]	Pd/A	2.93		
151B[a]	Pd/B	2.98		
180A[c]	Pd/A	3.00		

(a) Prepared by gas phase adsorption (GPA) of allyl cyclopentadienyl palladium, *(b)* this sample was not homogeneous, it was replaced by sample 180A, *(c)* prepared by GPA of Pd acetate.

In practice, samples were deposited in small stainless steel cups and introduced into the spectrometer chamber for analysis. The residual pressure inside the analysis chamber was kept below 10^{-7} Torr at all time. The XPS spectra were recorded using a VG Scientific Escalab Mark II system with a hemispherical analyzer operated in the contant pass energy mode (20 eV). In most cases, a MgKα X-ray source (h_ν = 1253.6 eV) was used and the spectometer was operated at 20 mA and 15 kV. The calibration of the instrument was frequently checked using Au, Ag and Cu samples.

For all zeolite- and silica-supported catalysts, a binding energy of 103.3 eV for Si(2p) was used as an internal reference, while for alumina-supported samples a binding energy of 74.4 eV for Al(2p) was adopted. The intensity of the various XPS bands needed to carry out the calculations was determined using linear background substraction and integration of the peak area (VG software). The area measurement was then used to calculate the so-called normalized area according to the following relationship:

$$A_{NORM} = A_{MEASURED} \frac{\Delta}{n_c t_c s} \qquad [14]$$

where Δ, n_c, t_c and s stand for the scan width, the number of channels, the time per channel and the number of scans respectively.

III.2.3. BET and External Surface Areas

BET surface areas were determined using the conventional technique of nitrogen physisorption at liquid nitrogen temperature. As for the external surface area, because of its dramatic effect on the dispersions as calculated using the model described previously, and also because of the limited number of previous investigations dealing with the experimental determination of the

external surface areas of zeolites, it was necessary to carry out some method development studies. Techniques such as the t-plot or the micropore plugging methods (27) were carefully assessed. In particular, the experimental conditions under which these methods may be safely applied to zeolites have been determined.

Prior to adsorption measurements, samples were heated under vacuum at 300 °C for 2 h. About 0.1 g batches were used for the nitrogen BET and t-plot methods. Nitrogen adsorption-desorption experiments were carried out using a computer controlled sorption analyzer (Omnisorp 100) operating in the dynamic mode. Software programs for data reduction included BET surface area analysis, t-plot analysis with reference to a non-porous silica, and micropore and mesopore distributions according to the model of Horvath and Kawazoe (28) and Barrett *et al.* (29), repectively.

For the micropore plugging technique, batches of 0.4 to 1.0 g were needed. When using benzene as pore filling adsorbate, the outgassed sample was exposed for 1 h at room temperature to gaseous benzene at its saturated vapor pressure in an all-glass vacuum system. Subsequently, the sample-containing cell was transferred to the Omicron adsorption system and the residual pressure of benzene (P_B) above the sample was adjusted to a desired value in the range 1 - 70 torr. As suggested by Suzuki *et al.* (30, 31), helium was introduced into the cell to a final pressure of about 700 torr before cooling the cell to 77 K. Finally, the helium was pumped off and a conventional nitrogen adsorption-desorption isotherm was determined. It is important to mention that the dead volume of the sample cell was small enough so that the extra hydrocarbon that condenses onto the sample when it is cooled to 77 K was, regardless of P_B, negligible in comparison to the micropore volume of the sample.

Experiments involving the use of n-nonane as a pore filling

sorbate were untertaken according to the same procedure except that the hydrocarbon was adsorbed at a vapor pressure of ca. 5 torr for 2 hours, then evacuated at room temperature for 1 hour as recommended by several authors while studying microporous carbon and titania (14).

The benzene adsorption-desorption isotherm for HZSM-5 (sample A) was measured at 301 K using the same Omnisorp 100 analyzer which was adapted for measurements in the static mode.

III.2.4. Hydrogen Chemisorption

Chemisorption of hydrogen was carried out on several Pt- or Pd-containing samples using either static or dynamic volumetric techniques. In the static mode, helium was used for dead-volume determination. The prereduced samples were first evacuated at 10^{-6} torr and 300 °C, then held at that temperature for 2 hours in the presence of about 300 torr of hydrogen to ascertain that the catalysts were fully reduced. The samples were outgassed at 350 °C for 1 hour, then cooled to room temperature. The total uptake of hydrogen was determined up to 350 torr and the high-pressure linear part of the isotherm was extrapolated to zero pressure. A second isotherm was then performed in the same manner after evacuating the sample for a 5 min-period of time. The difference between the two isotherms, at zero pressure gave the amount of irreversibly chemisorbed hydrogen.

In the dynamic chemisorption technique, the catalysts were reduced as in the previous method, then the hydrogen was swept away with a flow of dry and oxygen-free argon. The samples were then cooled to room temperature under flowing argon, and pulses of hydrogen were admitted into the argon stream. For any given pulse, any hydrogen that did not adsorb on the catalyst surface was directed to a previously calibrated TCD detector to be quantitatively analyzed. Pulses of hydrogen were stopped once the TPD signal levelled off.

The total amount of adsorbed hydrogen was taken as the amount of irreversibly chemisorbed hydrogen.

The use of the irreversibly held hydrogen as a means for metallic dispersion measurements has long been recognized (32). Despite some disagreement, there is a large consensus that for Pt and Pd, the stoichiometry of hydrogen chemisorption is fairly well accounted for by $H_{irr}/Me_s = 1$ where Me_s stands for a metallic surface atom (32, 33). In all calculations of metallic dispersions, the metal surface atom number density was assumed to be 1.27×10^{-19} m^{-2} for Pd and 1.25×10^{-19} m^{-2} (1). These values were calculated on the basis of equal contributions of the main low index crystal planes to the exposed surface. The relationship $d_p = S\rho$, where ρ is the density of the metal and S is the metallic surface per gram of metal was used to assess the average metallic crystallite size, d_p.

III.2.5. Electron Microscopy

Several zeolite-supported samples were characterized by transmission electron microscopy at Ecole Polytechnique de Montreal using a MET JEOL 2000 FX microscope operated at 200 kV. The extractive replica technique was used (4). In brief, the catalyst is first deposited on a mica sheet freshly cleaved and covered with a carbon film. The support is then dissolved selectively in a dilute solution of HF. The metallic particles that are located on the external surface of the support remain "glued" to the carbon film, which is then separated from the mica sheet, washed and mounted on a grid for microscope obsevation.

palladium and platinum particle size distributions were obtained from electron mocrographs using a ZEISS I BAS image analyzer.

IV. RESULTS AND DISCUSSION

IV.1. GENERAL CONSIDERATIONS

IV.1.1. General Procedure of XPS Quantitation

As stated in the Background Section, the simplified version of XPS intensity ratio based on the sheet-stacking model with surface segregation (equation [5]) has three independent adjustable parameters, for example C_1, C_2 and x_2. For zeolite-based catalysts, an arbitrary value for C_1 in the range 3 to 10 Å can be justified on the ground of their regular pore structures. Moreover, it was found that the actual value of C_1 within these limits has little effect on the calculated value of C_2 (22). Therefore, in the present investigation, C_1 will continue to be fixed arbitrarily at 3 Å.

To determine x_1 and C_2, another independent equation is needed. In the procedure published earlier (23), we used equation [11]. For this equation to be fulfilled, it was necessary to submit the catalyst to a lengthy grinding until it reached homogeneity, i.e., no further changes in the relative intensities of the XPS peaks took place upon additional grinding. In the approach used in the present work, the catalyst is also ground and analyzed again by XPS. However, the method does no longer require that the ground sample be homogeneous as far as XPS intensities are concerned. The grinding conditions no longer play a critical role provided a significant change in the XPS intensity ratio in comparison to the unground sample is brought about. Under these conditions an equation comparable to equation [5] and involving the XPS ratio as well as other characteristics of the ground catalyst can be derived.

It is assumed that during grinding, the sizes of all metallic particles are preserved, while the external and/or the BET surface areas of

the catalyst undergo some changes. Under these conditions, the model representing the ground catalyst would involve support sheets of thickness t' different from t. Moreover, since the BET and/or the external surface change upon grinding, the surface fractions occupied by both populations of particles will no longer be the same as in the original sample. As a result, all the probabilities P_i (i = 1-4) defined in equation [5] will change to P_i' (i = 1-4). The simultaneous resolution of the following two equations should lead to x_1 and C_2:

$$\left(\frac{I_p}{I_s}\right)_{UNGRND} = K\left(\frac{1-P_1P_2^2}{(1-P_1)P_3}-1\right) = Y_1 \qquad [15]$$

$$\left(\frac{I_p}{I_s}\right)_{GRND} = K\left(\frac{1-P_1P_2^2}{(1-P_1)P_3}-1\right) = Y_2 \qquad [16]$$

Y_1 and Y_2 designate the XPS intensity ratios for the sample in unground and ground forms, respectively. Equation [15] gives:

$$P_3 = \frac{K}{Y_1+K}\frac{(1-P_1P_2^2)}{(1-P_1)} \qquad [17]$$

and from equations [7] and [8], we have

$$P_3 = P_2 - \frac{X_2}{A_u(1-X_B)\rho_p C_2}\left(1-e^{-C_2/\lambda_p}\right) \qquad [18]$$

Therefore, we have:

$$\frac{x_2}{(1-x_B)\rho_p C_2}\left(1-e^{-C_2/\lambda_p}\right) = \left[P_2 - \frac{K}{K+Y_1}\left(\frac{1-P_1P_2^2}{1-P_1}\right)\right]A_u \qquad [19]$$

$$\frac{x_2}{(1-x_B)\rho_p C_2}\left(1-e^{-C_2/\lambda_p}\right) = \left[P_2 - \frac{K}{K+Y_2}\left(\frac{1-P_1'P_2'^2}{1-P_1'}\right)\right]A_g \qquad [20]$$

where A_g and A_u designate the external surface area of the ground and unground samples, respectively.

From the expressions of P_2 (equation [7]) and its counterpart P_2', we have

$$\frac{P_2'-1}{P_2-1} = \frac{f_1'}{f_1} = \frac{S_u}{S_g} = R \qquad [21]$$

where S_u and S_g are the BET surface area of the unground and the ground forms of the sample, respectively.

Finally, from equations [19], [20] and [21] we have

$$AP_2^2+BP_2+C = 0 \qquad [22]$$

where

$$A = \frac{KP_1A_u}{(K+Y_1)(1-P_1)} - \frac{KP_1'R^2A_g}{(K+Y_2)(1-P_1')} \qquad [23]$$

$$B = A_u + \frac{2KR(R-1)P_1'A_g}{(K+Y_2)(1-P_1')} - RA_g \qquad [24]$$

$$C = -\frac{KA_u}{(K+Y_1)(1-P_1)} + \left(\frac{K\left(1-P_1'(R-1)^2\right)}{(K+Y_2)(1-P_1')} + (R-1)\right)A_g \qquad [25]$$

Since P_2 is a probability, acceptable solutions for equation [22] should be in the range 0-1. This value is used to calculate x_1 according to equation [7]. The segregated fraction of supported material (x_2) is then deduced as the difference between x_s and x_1. The size of the segregated particles (C_2) is calculated by iteration using equation [19] and a numerical method. A computer program has been designed to carry out such calculations. The operating guide of the software and other related information are given in the Appendix.

IV.2.2. External Surface Areas

The distinction between external and internal surface is not always clear. Gregg and Sing (27) defined the external surface as the surface that includes all the cracks which are wider than they are deep. In many instances such a definition is difficult to use as pores having the same diameter may be included or not in the external surface depending on their depth to width ratios. Another definition of the external surface area (S_e)

would be the area that is available for multilayer physical adsorption. With regard to our quantification model of XPS data (22,23), the most appropriate definition of S_e would be the overall BET surface area without the contribution of micropores.

Well crystallized zeolites are strictly microporous, and therefore have very low external surface areas that may be approximated by their apparent geometrical areas as measured directly by scanning electron microscopy (30,31,34). However, more often than not zeolite samples are less than perfectly crystalline and may exhibit mesopores and consequently external surface areas much higher than their apparent geometrical areas. Mesopores can also be created by most dealumination procedures (9,35).

Several techniques have been devised to determine S_e of adsorbents, and a great deal of the earlier applications dealt with carbon samples (27,36). It is only recently that attempts have been made to apply some of these techniques to zeolites (30,31,34,36-43). Hudec et al. (37) used the t-plot method while Carrott and Sing (38) and others (39,40) used the α_e-method to measure S_e for series of ZSM-5, erionite, mordenite and Y-type zeolites. The application of these two methods rests on the availability of a nonporous reference material of known surface area (27). Ideally, the results should be checked by another independent method since there is no guaranty as far as the suitability of the reference material is concerned.

A brief description of the origin and usefulness of the t- and α_e-plots is needed. A t-plot is in fact an adsorption isotherm drawn as the amount of adsorbed nitrogen versus t, instead of p/p^0. The statistical thickness of the adsorbeb layer t at a given relative pressure p/p^0 is taken from a standard t-curve of a suitable nonporous material. Relative pressures can also be converted into t-values using the following equation (44):

$$t = [13.99/\log(p/p^0) + 0.034]^{0.5}$$

The independent variable t is related to the number n of adsorbed nitrogen molecules as follows: $t = \sigma * n/n_m$, where n_m and σ stand for the monolayer capacity and the thickness of a nitrogen monolayer, respectively. Without going into much detail, there is a fairly large consensus on using a nonporous hydroxylated silica as a standard material (27).

The exact shape of the t-plot of a given adsorbent depends on the pore structure of the material. There are three limiting situations, (i) if the solid under study is nonporous and its isotherm has the same shape as the standard isotherm (Figure 2a), the t-plot will be a straight line the equation of which is $n = b*t$. The slope b is related to the BET surface area; $S_{BET} = 3.45*10^5*b$, (ii) If mesopores are introduced (Figure 2b), the capillary condensation that occurs at relative pressures higher than ca. 0.45 induces an upward deviation of the t-plot in the same range of relative pressures. The low pressure section of the t-plot will be the same as if the solide was nonporous, and the same information as in the previous case can be extracted, (iii) If the adsorbent contains micropores, a strong nitrogen uptake takes place at low pressure, and consequently the t-plot will shift upward at in the same relative pressure range. As shown in Figure 2c, the slope of the linear high pressure section of the t-plot can still be used to calculate the BET surface area, the same way as for nonporous solids. The linear extrapolation to the adsorption axis gives the micropore volume. If the solid contains both meso- and micropores, it may become hard to find a linear section of the t-plot in the range of medium pressure.

The concept of α_s-plot is very similar to the t-plot approach (27). Because, to compare a given adsorption isotherm to a standard isotherm, it is not necessary to know the monolayer capacity n_m, any amount n_s adsorbed at a chosen relative pressure $(p/p^0)_s$ may be used as a normalizing factor. Usually,

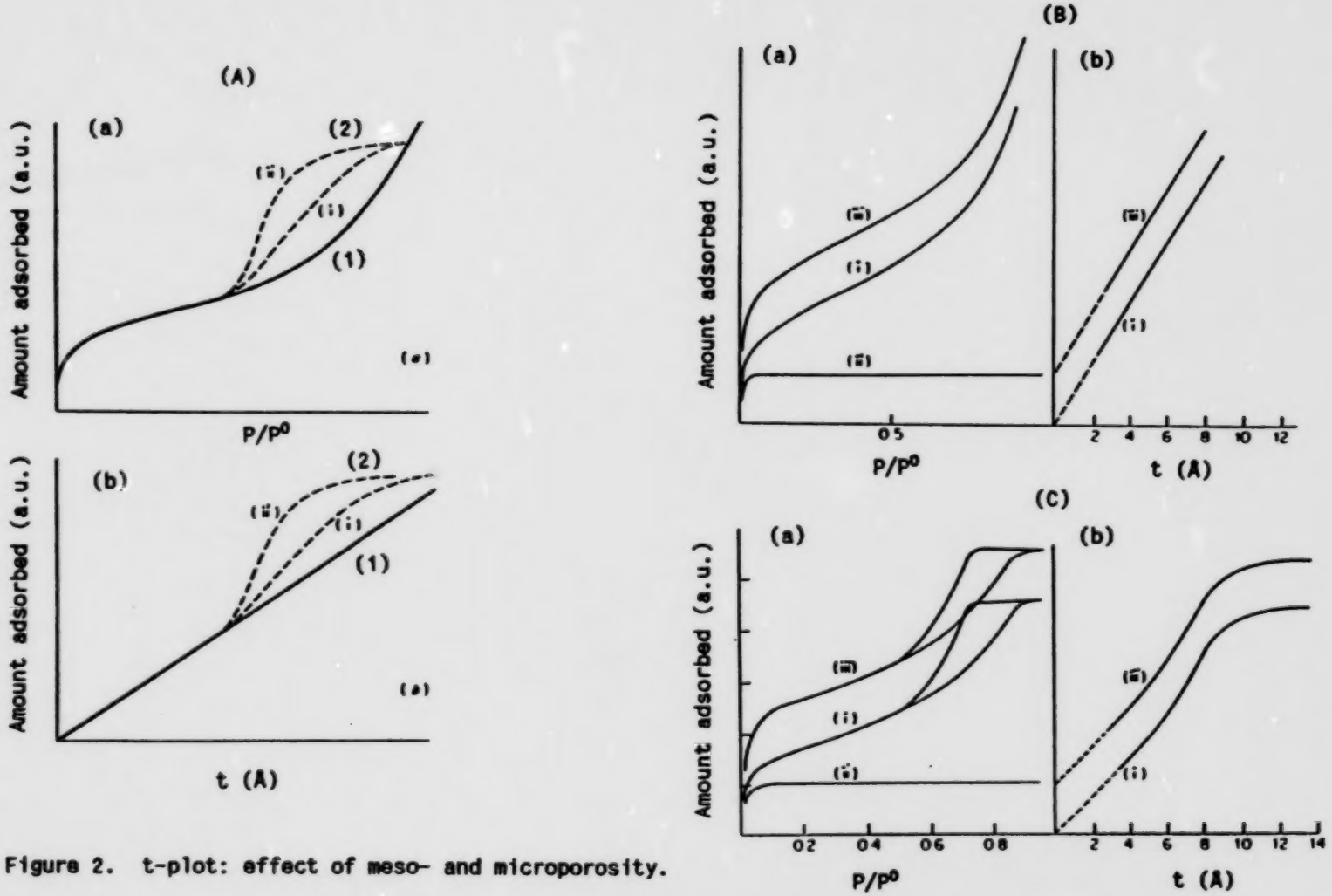

Figure 2. t-plot: effect of meso- and microporosity.

(A) *effect of mesoporosity on the t-plot.* (a) (1) adsorption isotherm on a nonporous adsorbent, (2) isotherm of the same solide after introduction of mesoporosity, (i) adsorption, (ii) desorption; (b) the t-plots corresponding to the isotherms in (a).
(B) *effect of microporosity on the t-plot.* (a) (i) nonporous adsorbent, (ii) a wholly microporous solid, (iii) a solid with the same external surface area as (i) and the same micropore volume as (ii); (b) the corresponding t-plots.
(C) *simultaneous effect of micro- and mesoporosity.* (a)(i) mesoporous solid, (ii) microporous solid, (iii) a solid with the same mesoporous system as in (i) and having the micopore volume as (ii); (b) the corresponding t-plots.

the relative pressure $(p/p^0)_s$ is taken as 0.4. The standard α_s-curve is then obtained from the standard isotherm by plotting $n/n_{0.4}$ (= α_s) vs. p/p^0. The α_s-plot can then be derived by following the same steps as for the t-plot and can provide the same kind of information.

The second technique that has been used for the same purpose consists of plugging the micropores with a strong adsorbate before determining the remaining surface area by the conventional nitrogen BET technique (30,31, 34). Here also, problems may arise because of unsuitability of the pore filling sorbent or of experimental conditions. For example, Inomata et al. (31) reported that for a series of zeolites, water becomes a less and less suitable pore filler as the silicon-to-aluminum ratio of the adsorbents increases. This was related to the fact that as their silicon content goes up, the zeolites turn to be more and more hydrophobic.

A third procedure of determining S_e of zeolites was used by Suzuki et al. (30,31). This method is based on the adsorption kinetics of relatively large molecules such as neopentane (30). Alternatively, nitrogen can be used if the micropores have been previously filled with another sorbent (31). For this method, it is essential that the adsorption process be monitored at its very early stages.

It has also been reported that adsorbates with large molecules may be used under equilibrium conditions, and the external surface area may be calculated from the corresponding BET equation (41) or by comparison to a nonmicroporous amorphous aluminosilicate (42). For small pore zeolites, titration of the external acid sites was also used for the same purpose and compared to direct methods such as adsorption of larges molecules or mercury porosimetry (42,43).

In the present investigation, method development for the

determination of external surface areas of zeolites was carried out using mostly the two ZSM-5 samples (A and B) mentioned above. Particular emphasis has been put on the evaluation the t-plot and the pore plugging methods.

The adsorption-desorption isotherm for sample A (Figure 3, upper curve) shows a high uptake of nitrogen at very low relative pressures and a hysteresis loop at higher pressures. These two properties are characteristic of microporous and mesoporous materials, respectively. Using the linear portion of the t-plot corresponding to a film thickness higher than 4-5 Å (Figure 4), a micropore volume of 0.18 cm^3g^{-1} and a S_e of 35.5 m^2g^{-1} were determined (Table IV). Hall et al. (45) reported a theoretical value of 0.18 cm^3g^{-1} for ZSM-5 micropore volume, while experimental data in the range 0.13 to 0.23 cm^3g^{-1} have been found for various ZSM-5 zeolites (37-39,45,46). As for the external surface areas of ZSM-5 zeolites, data ranging from 1 to 120 m^2g^{-1} have been reported (30,31,34,37-43).

Typical nitrogen isotherms measured after preadsorption of benzene are plotted in Figure 3. The corresponding BET surface areas are plotted in Figure 5 against the residual pressure of benzene. It is seen that at pressures below 3 torr, high surface areas were obtained. For pressures ranging from 3 to 10 torr, the BET surface area leveled off at 40 ± 2 m^2g^{-1}. This area decreased steadily when increasing benzene pressures were applied. At near saturation, i.e. P_B of about 70 torr, a surface area of 4 m^2g^{-1}, very close to the apparent geometrical area (4.4 m^2g^{-1}), was measured.

The extrapolated linear branches of the t-plots as redrawn from the nitrogen adsorption isotherms of samples that had been exposed to benzene then outgassed to a final pressure $P_B < 3$ torr had positive intercepts on the adsorption axis indicating that the micropores were not effectively filled. However, for P_B in the range of 3 to 10 torr, no remaining micropores were detected while the mesopore volume amounted to about 60 % of its original

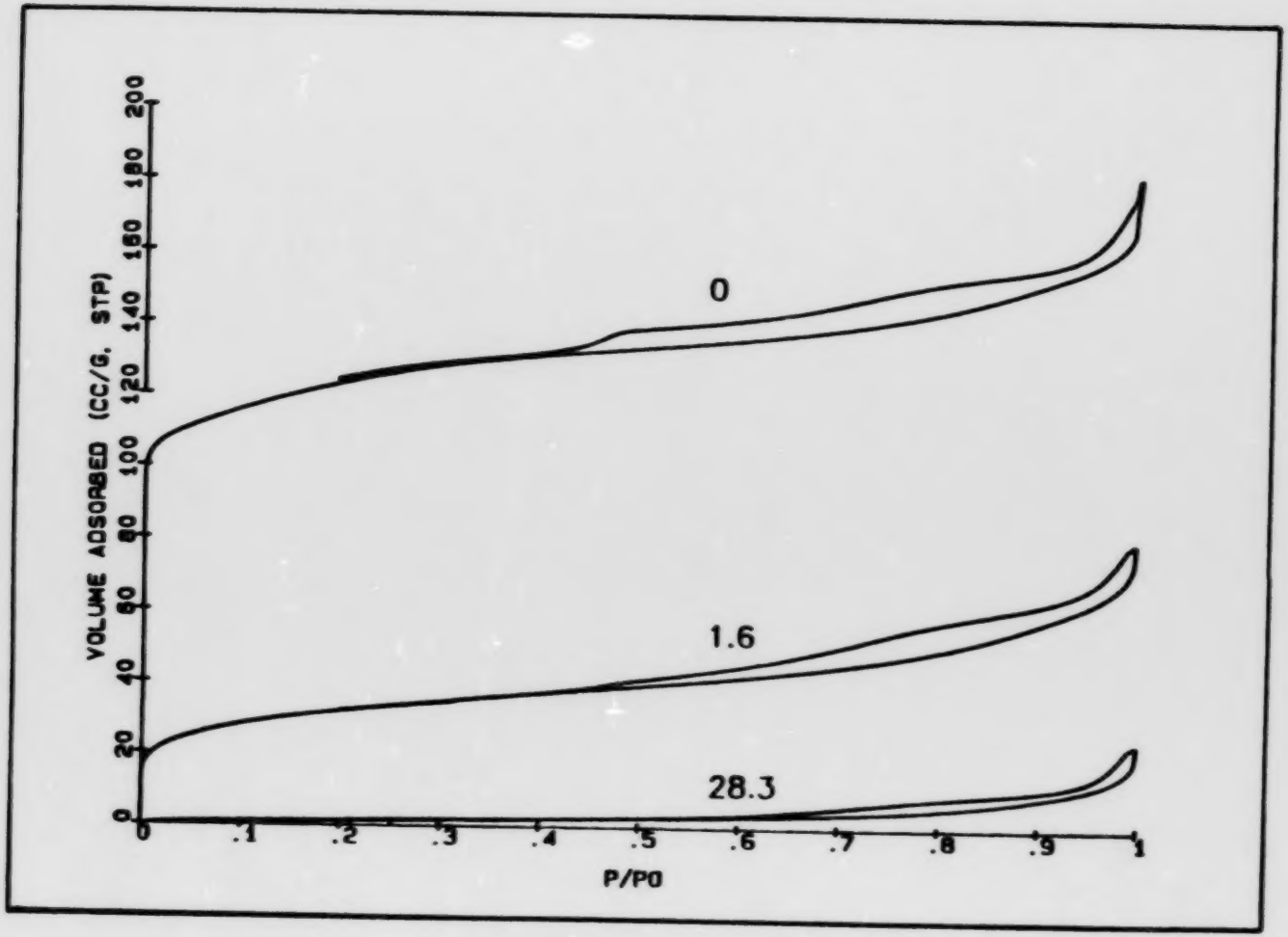

Figure 3. Nitrogen adsorption-desorption isotherm for sample A before and after benzene preadsorption. The figures indicate the residual benzene pressures, P_B (torr).

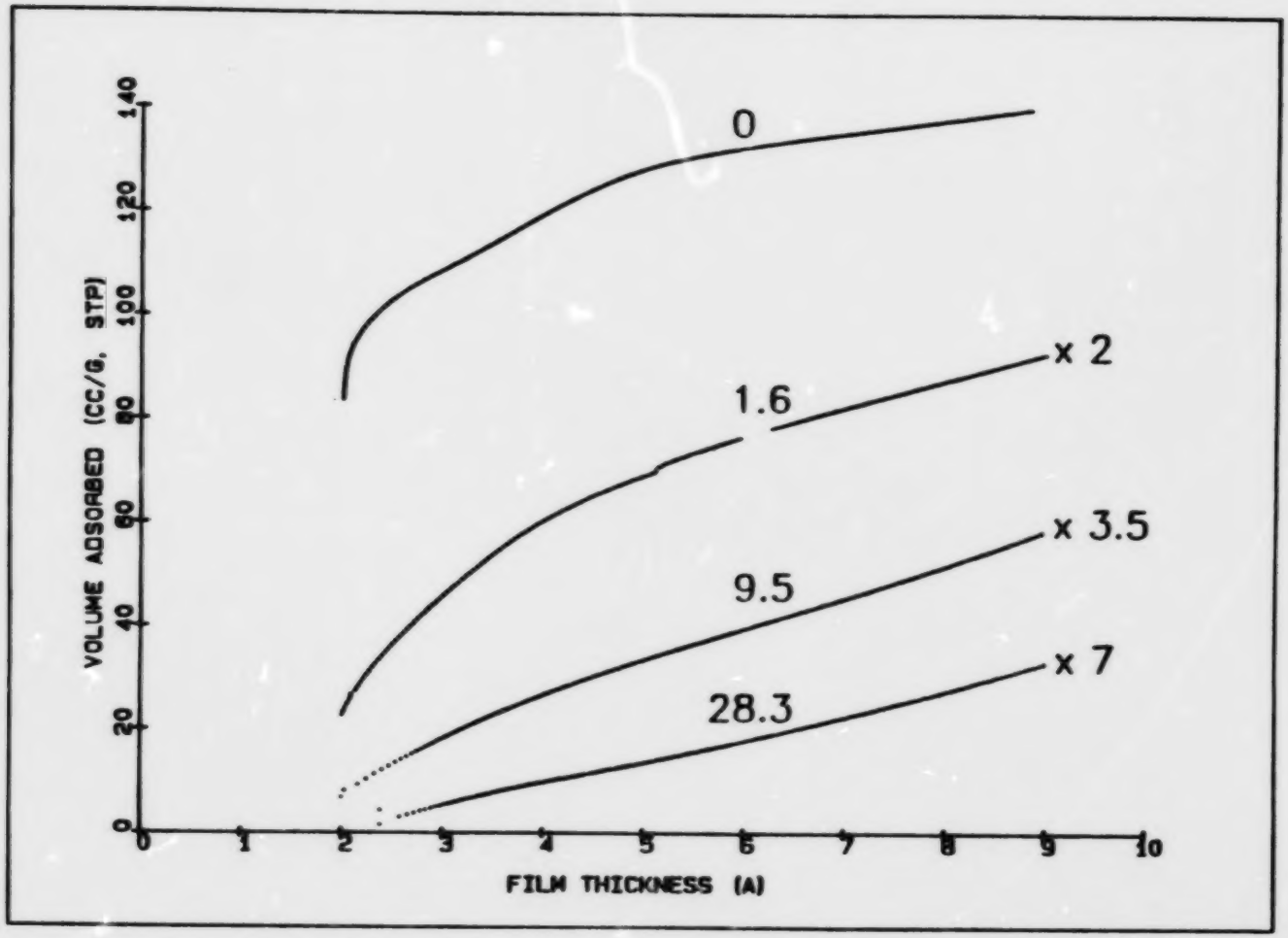

Figure 4. t-plots for sample A before and after benzene preadsorption. The figures indicate benzene residual pressures, P_B (torr). The numbers on the right-hand side are scaling factors.

TABLE IV. Nitrogen Physisorption Data for Samples A and B

Method	BET	t-plot			Benzene preads.			n-Nonane preads.		
Sample	S^a	S_e^b	V_μ^c	V_m^d	S_e^b	V_μ^c	V_m^d	S_e^b	V_μ^c	V_m^d
HZSM-5 A	456	35.5	0.18	0.14	40.0[e]	0	0.09	39.0[g]	0	0.08
HZSM-5 B	346	10.7	0.14	0.02	4.3[f]	0	-	3.5	0	-

a: BET surface area in m^2g^{-1}; *b*: external surface area in m^2g^{-1}; *c*: micropore volume in cm^3g^{-1}; *d*: mesopore volume in cm^3g^{-1}; *e*: ± 2 m^2g^{-1}, P_B = 3 - 10 torr; *f*: ±0.8 m^2g^{-1} P_B = 3 - 45 torr; *g*: ± 1 m^2g^{-1}.

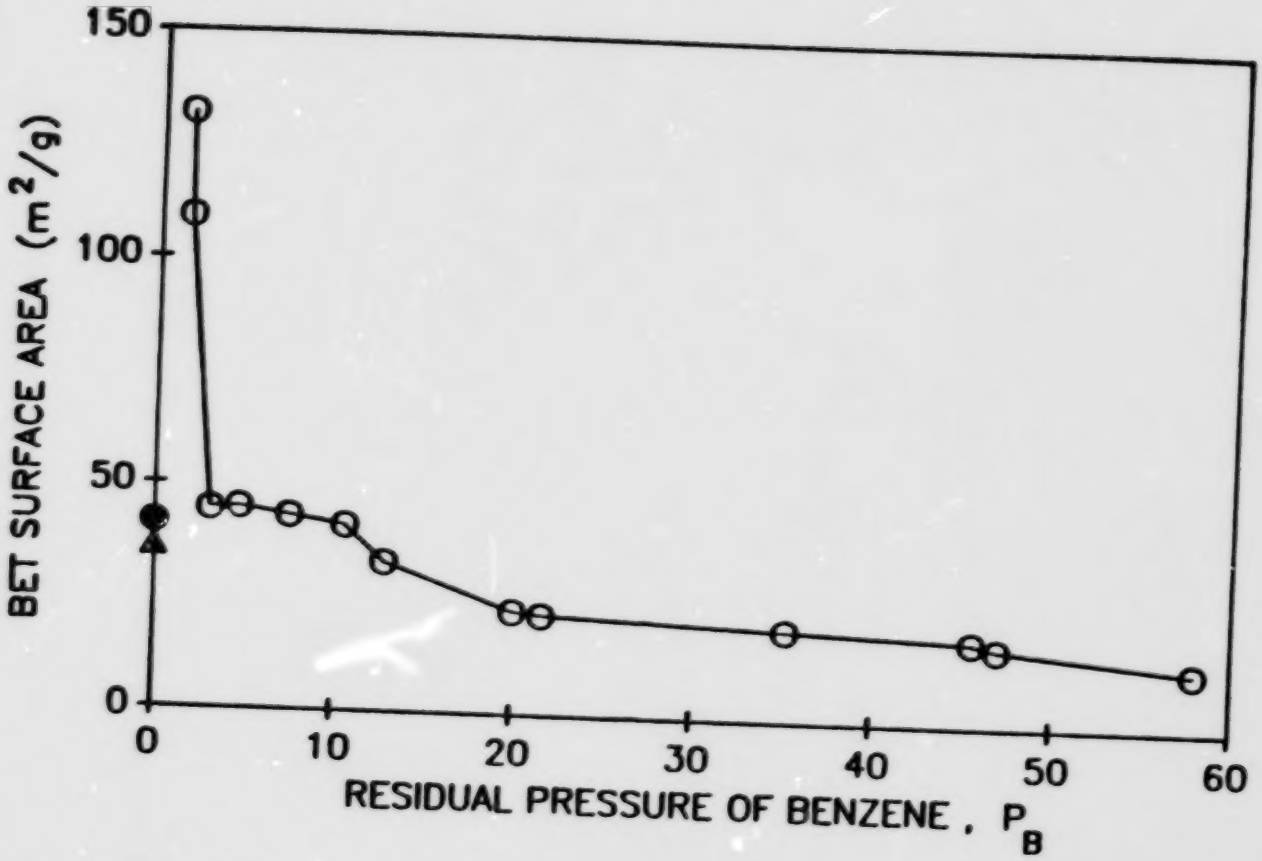

Figure 5. BET surface areas of sample A as a function of the benzene residual pressure, P_B (torr). The external surface areas obtained by the n-nonane plugging technique (●) and the t-plot method (▲) are also indicated.

value (Table IV). Analysis of the mesopore distribution shows that this was due mainly to the benzene plugging of the smallest mesopores having 10 to 20 A radii. At higher P_B values, the remaining mesopore volume decreased further leading to smoother particles with lower apparent external surface areas.

Ideally, P_B should be adjusted within a pressure range for which the micropores would be effectively filled while all larger pores remain completely free. However, in our case even at the lowest pressures required, i.e., 3 torr, almost half of the mesopore volume was already filled with benzene. It is well known that physical adsorption on large pores and flat surfaces occurs layer by layer, while for micropores, it follows a pore filling mechanism. Therefore, such an overlap should not be expected unless it is an indication that the lower end of the mesopore distribution is comprised of pores that behave rather like micropores. This seems to be the case for our ZSM-5 samples.

The adsorption-desorption isotherm of benzene for sample A at 301 K is shown in Figure 6. In contrast to the nitrogen isotherm shown in Figure 1, the hysteresis loop extends over almost the entire range of relative pressures. It is believed that the low pressure hysteresis is due to the fact that the benzene adsorption is a slightly activated process (47). By choosing appropriate relative pressures on each branch of the hysteresis loop, two different conditions for the adsorption of the same amount of benzene may be identified, e.g. N and M in Figure 6. However, BET analysis after benzene preadsorption under conditions M gave a specific surface area of 67 m^2g^{-1}, a much higher value than the 40 m^2g^{-1} determined after benzene preadsorption under conditions N.

Earlier work on the determination of external surface areas of zeolites (34) suggested that the sample be exposed to the saturated vapor pressure of benzene with no further adjustment of P_B. Our study shows that such

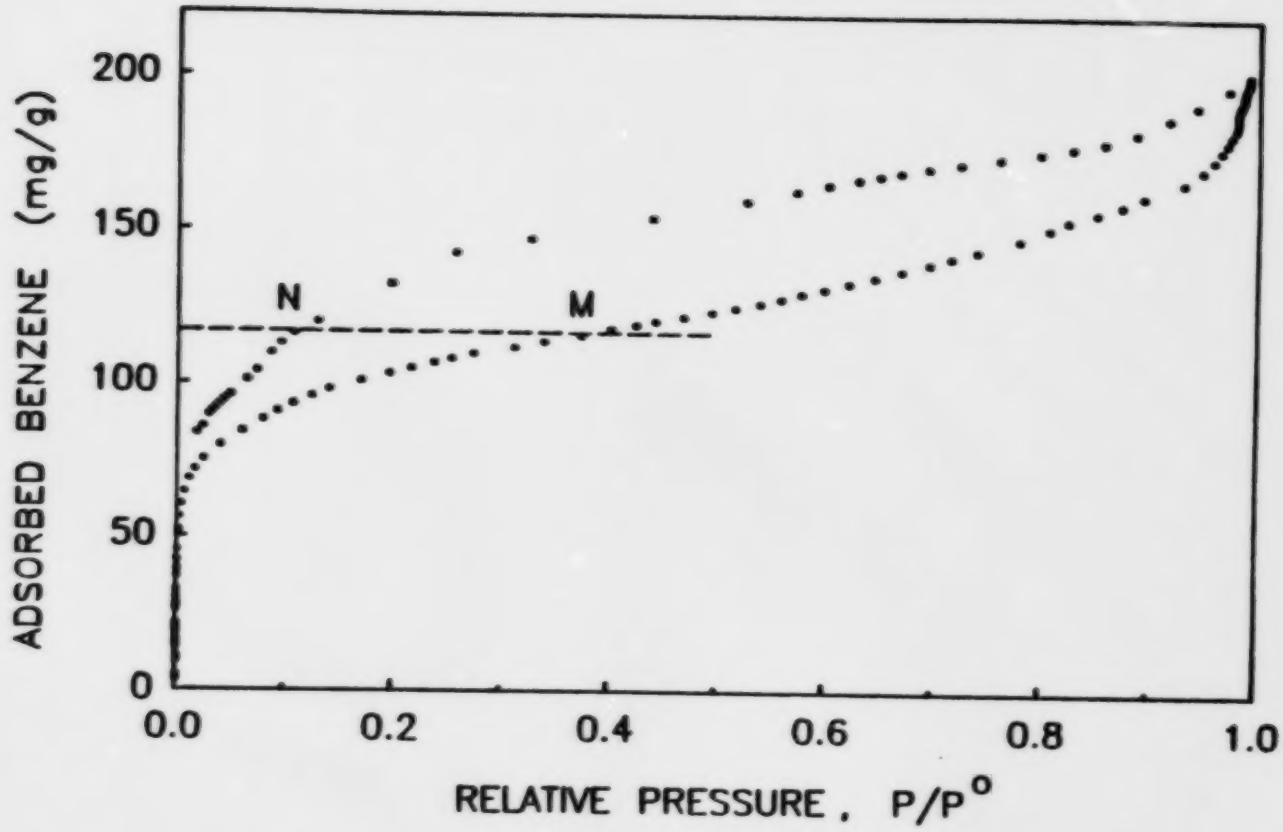

Figure 6. Adsorption-desorption isotherm of benzene for sample A at 301 K.

a procedure may lead to underestimated values. Our data indicate that the sample should be first equilibrated with benzene at its saturated vapor pressure, then this pressure should be adjusted between 3 and 10 torr before carrying out the nitrogen adsorption. For samples that exhibit micropores only, it is anticipated that the residual pressure of benzene would not be critical as long as it is high enough to allow effective plugging of the micropores, i.e. higher than about 3 torr.

In order to further verify these conclusions, a controlled pore glass designated as CPG 120 was studied. This material was chosen to demonstrate that even for a non microporous solid with mesopores larger than those usually found in zeolites (Figures 7 and 8a), the use of a high benzene pressure is likely to block a significant fraction of the external surface area. Indeed, benzene preadsorption with final adjustment at 85 torr led to a decrease in both the surface area and the mesopore volume from 169 to 71 m^2g^{-1} and from 1.12 cm^3g^{-1} to 0.65 cm^3g^{-1} (Figures 8a and 8b) respectively.

n-Nonane is another pore filling sorbent that had been used successfully for microporous carbon (48), titania (49) and other materials (50) but has never been tested for zeolites. Application of the n-nonane plugging technique to three separate batches of sample A led to a mean S_e value of 39 ± 1 m^2g^{-1} (Table IV). As in the case of benzene preadsorption, all micropores were effectively plugged and the remaining mesopore volume was again about 55 % of its original value. These results indicate that both hydrocarbons are equally effective pore fillers for zeolites. The use of n-nonane offers even a slight advantage over benzene as the excess hydrocarbon has simply to be pumped off instead of adjusting its pressure to a suitable value.

The external surface area obtained by the t-plot method as applied without hydrocarbon preadsorption was of 35.5 m^2g^{-1}, in good agreement with

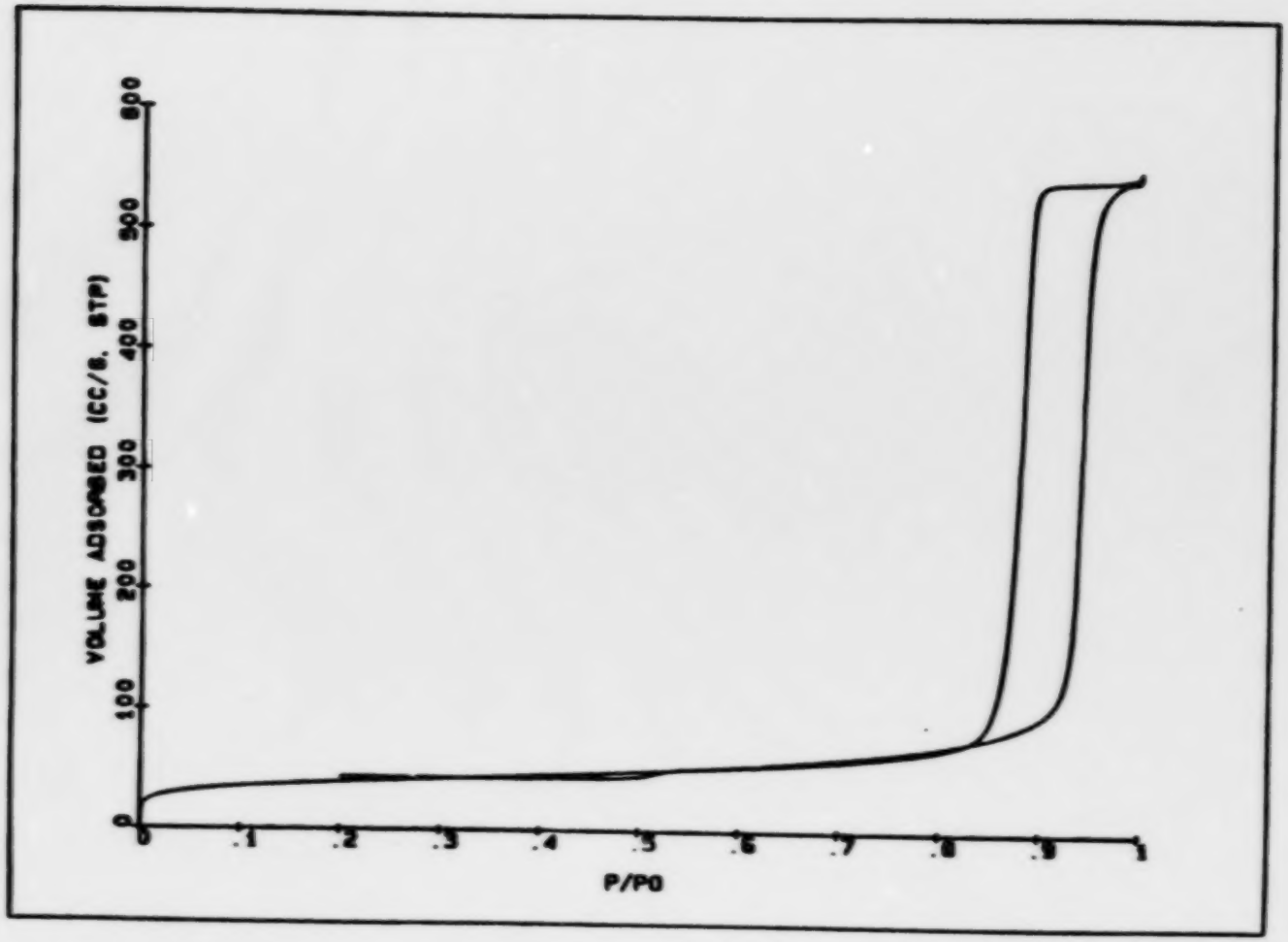

Figure 7. Nitrogen adsorption-desorption isotherm for CPG 120.

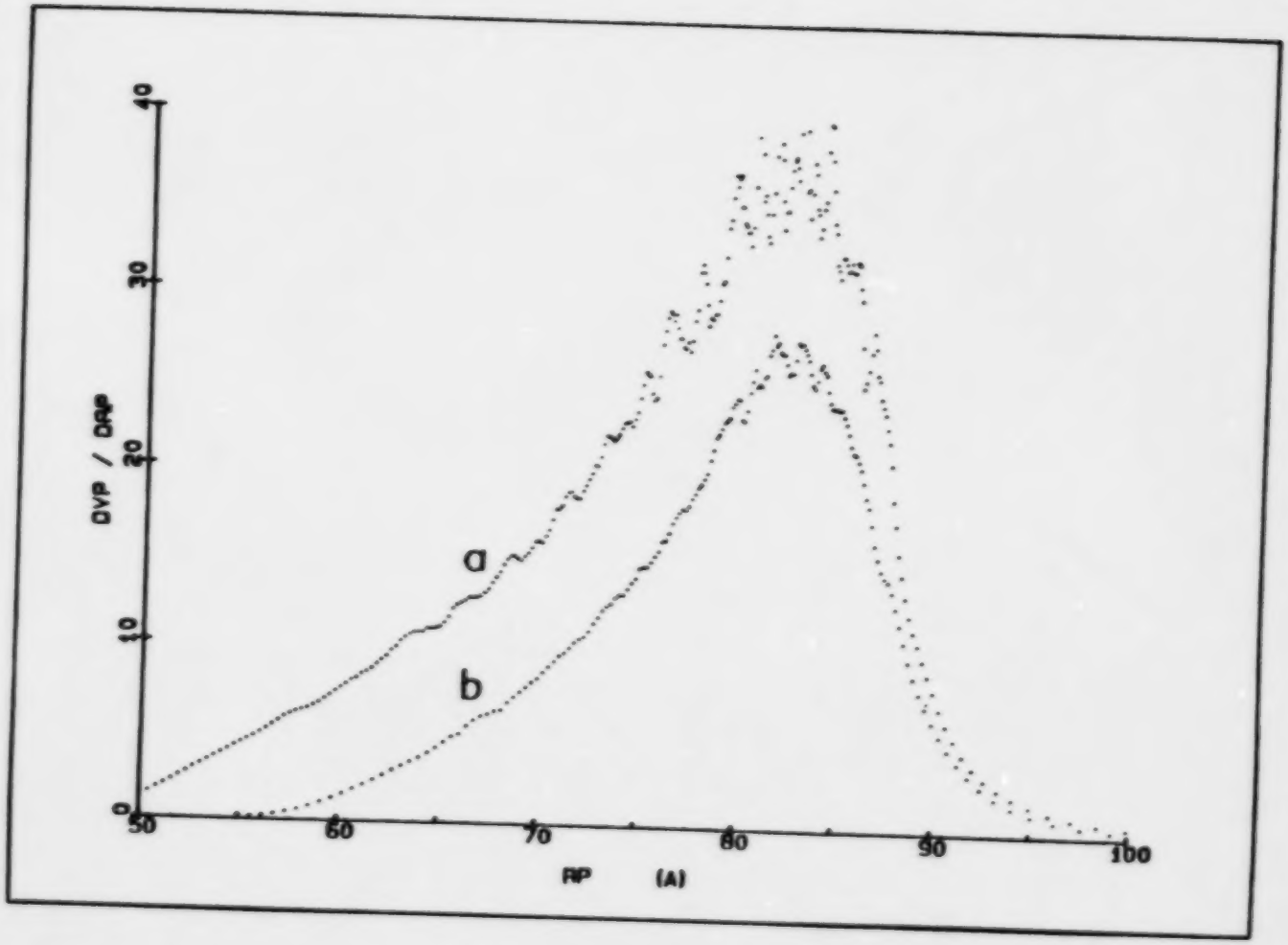

Figure 8. Pore size distributions for CPG 120, (a) before benzene adsorption, (b) after benzene preadsorption (P_B = 85 torr).

those provided by the pore plugging technique. However, as the reliability of the t-plot method rests among other factors on the extent of the linear portion of the t-plot, it is not expected that this method would work properly with zeolites of low external surface areas.

In order to verify this contention, sample B was prepared using the same procedure as for sample A except that NaCl was replaced by CsCl and the autoclavation time was of 11 days instead of 5. Gabelica et al. (24) reported that such a synthesis procedure yields quite large crystals. As expected, sample B was found to have a very small mesopore volume (Table IV) and a micropore volume (0.14 cm^3g^{-1}) comparable to literature data for large crystals of ZSM-5 and silicalite (46).

Using the n-nonane plugging technique, a S_e of 3.5 m^2g^{-1} was determined. Preadsorption of benzene at a P_B ranging from 3 to 45 torr followed by nitrogen adsorption gave an external surface area of 4.3 ± 0.8 m^2g^{-1}. These values seem reasonable in light of the almost complete lack of mesopores. As shown in Table IV, the external surface area obtained by the t-plot method was significantly higher suggesting that this method should be avoided when dealing with large zeolite crystals.

For zeolite samples with a fairly large mesopore volume, the external surface area may be measured properly by the t- or the α_s-plot method. The pore plugging technique using n-nonane or benzene is equally effective even though in the case of benzene, the experimental procedure and in particular the residual pressure range should be considered carefully.

For samples with low external surface areas, the pore plugging method remains quite effective. However, the t-plot technique did not seem to be fully satisfactory. Since the external surface area is proportional to the slope of the extrapolated linear branch of the t-plot, it is not surprising

that the accuracy of the measurements decreases as the slope of the t-plot approaches zero.

IV.2. EXPERIMENTAL RESULTS AND DISCUSSION

IV.2.1. Pd/HZSM-5 Catalysts

IV.2.1.1. Experimental data

A typical XPS spectrum of Pd (3d) emission is shown in Figure 9. XPS data for all zeolite-supported Palladium samples are summarized in Table V. In calcined samples, the results indicate that Pd is sited mostly as PdO ($Pd(3d_{5/2})$ = 336.4 eV), while in reduced samples, Pd is sited as metal ($Pd(3d_{5/2})$ = 335.4 eV) (51). As our major concern was the determination of the intensity of XPS peaks, the experimental procedure was not optimized to yield a high accuracy with regards to peaks positions. Consequently, small (apparent) variations in the binding energies of Pd(3d) electrons do occur.

Textural properties including the BET and external surface areas as well as micro (V_μ) and mesopore (V_M) volumes of Pd/HZSM-5 after various treatments are shown in Table VI. It is seen that in comparison with calcined catalysts, reduced samples have similar textural properties. However, grinding brings about a significant decrease in the micropore volume , thus a decrease in the surface area. Usually, the external surface area increases slightly upon grinding.

In order to solve equation [5], several additional data are needed. These are described below and the procedures for their determination are given.

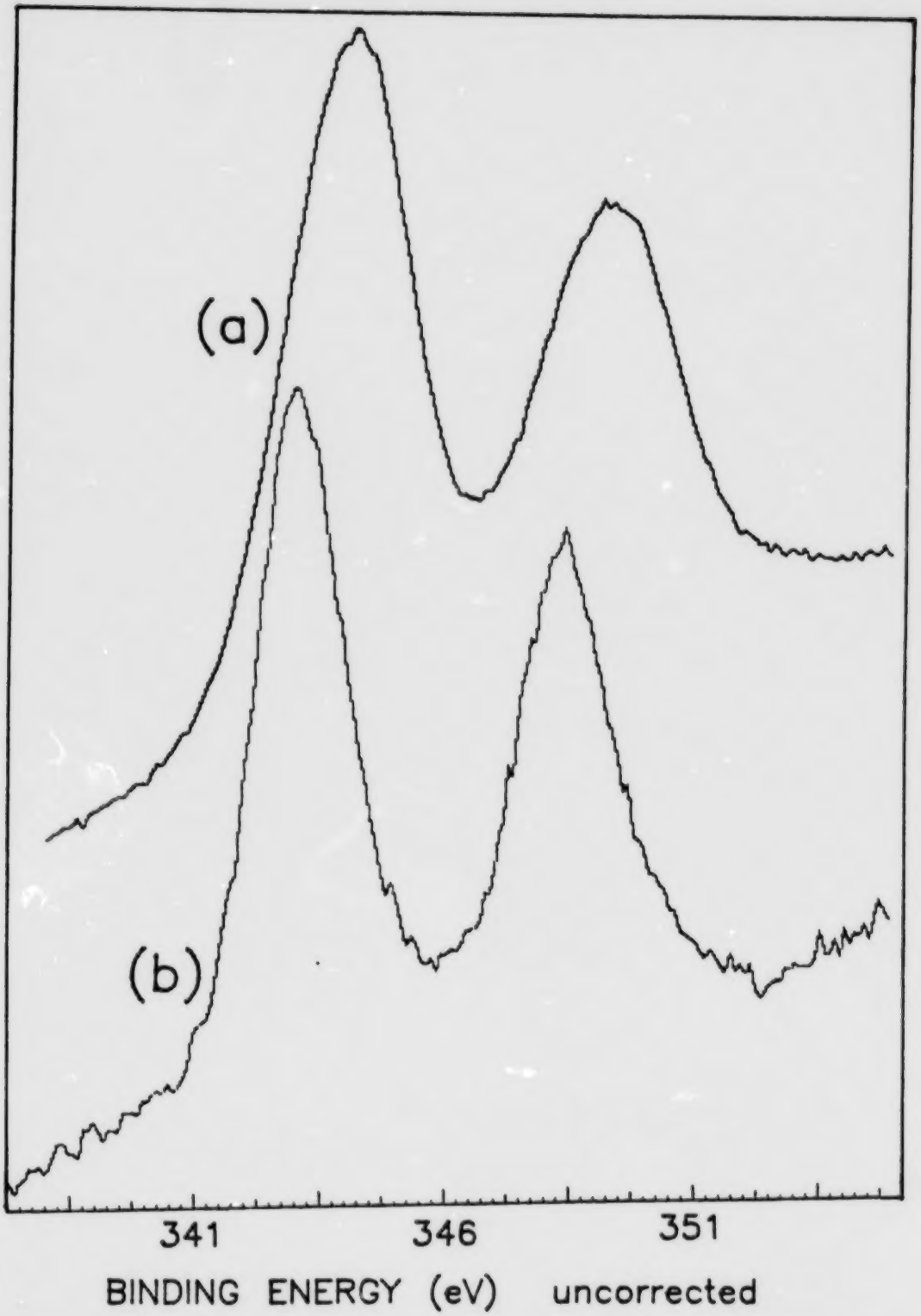

Figure 9. XPS spectra of Pd(3d) in sample 142B (2.43% Pd/HZSM-5) (a) oxidized, (b) reduced.

TABLE V. XPS Data for Pd/HZSM-5 Catalysts

Sample	Binding Energy (eV)			I[Pd(3d)]	I[Si(2p)]	I(Pd)/I(Si)
	$Pd(3d_{5/2})$	$Pd(3d_{3/2})$	O(1s)			
142A 3% Pd/HZSM-5						
Calcined	336.1	341.4	532.7	1.329	13.172	0.101
Reduced	335.6	340.9	532.6	1.471	17.547	0.084
Red.Grnd.[a]	335.3	340.7	532.8	2.076	13.321	0.156
142B 2.43% Pd/HZSM-5						
Calcined	336.6	341.7	532.7	4.703	8.814	0.534
Reduced	335.2	340.6	532.7	3.061	10.145	0.302
Red.Grnd.[a]	335.4	340.6	532.9	2.685	10.137	0.265
180A 3% Pd/HSZM-5						
Calcined	336.1	341.3	532.9	5.850	4.898	1.194
Calc.Grnd.[b]	336.5	341.5	533.0	5.478	8.045	0.681
Reduced	335.3	340.5	532.6	24.638	25.946	0.950
Red.Grnd.[a]	335.3	340.6	533.1	12.161	22.431	0.542
151B 2.93% Pd/HZSM-5						
Calcined	336.6	341.7	532.6	14.149	4.864	2.909
Reduced	335.2	340.5	532.8	11.894	7.391	1.609
Red.Grnd.[a]	335.5	340.8	532.9	5.029	8.416	0.598

(*a*) Reduced under flowing hydrogen at 300 °C, then ground for 5 min., (*b*) calcined at 500 °C overnight, then ground for 5 min.

TABLE VI. Textural Properties of Pd/HZSM-5 Catalysts

Sample	$S_{BET}(m^2g^{-1})$	$S_e(m^2g^{-1})$	$V_M(cm^3g^{-1})$	$V_m(cm^3g^{-1})$
142A 3% Pd/HZSM-5				
- Calcined	408	58.0	0.21	0.150
- Reduced	406	54.3	0.22	0.150
- Red.Grnd.[a]	323	60.0	0.23	0.111
142B 2.43% Pd/HZSM-5				
- Calcined	368	20.2	0.06	0.154
- Reduced	364	19.1	0.09	0.151
- Red.Grnd.[a]	301	23.8	0.08	0.122
180A 3% Pd/HZSM-5				
- Reduced	367	35.0	0.18	0.142
- Red.Grnd.[a]	269	42.3	0.15	0.096
151B 2.93% Pd/HZSM-5				
- Calcined	349	13.3	0.08	0.150
- Reduced	358	27.0	0.11	0.150
- Red.Grnd.[a]	279	20.4	0.09	0.114

(*a*) Reduced under flowing hydrogen at 300 °C, then ground for 5 min.

* *The photoelectron mean free paths* were calculated according to the formula proposed by Vulli and Stark (52):

$$Ln\lambda(E_k) = 3.648 - 0.9318LnE_k + 0.1196(LnE_k)^2 \qquad [26]$$

This equation is very practical because it may be applied to any photoelectron regardless of the nature of the material it originates from. However, as shown by several studies, the dependence of $\lambda(E_k)$ on material may be quiet strong (53-55). Experimental correlations that allow to various degrees for such considerations to be taken into account have been proposed by Penn (56) and others (57,58). A recent review of this topic is available (59). Among the most used correlations are those of Seah and Dench (58) who found three types of empirical correlations depending on the nature of materials:

(a) for elements

$$\lambda(E_k) = 538aE^{-2} + 0.41a^{3/2}E^{1/2} \text{ (nm)}.$$

(b) for inorganic compounds

$$\lambda(E_k) = 2170aE^{-2} + 0.72a^{3/2}E^{1/2} \text{ (nm)}.$$

(c) for organic elements

$$\lambda(E_k) = (10^3/\rho)(49E^{-2} + 0.11E^{1/2} \text{ (nm)}.$$

where a is the monolayer thickness (nm) defined as

$$a^3 = 10^{27}A/\rho nN$$

In these equations, ρ is the bulk density (g cm^{-3}), A is the atomic or molecular weight, n is the number of atoms in the molecule, N is Avogadro's number. The kinetic energies are in eV. For $E_k > 100$ eV, the first terms of these correlations are very small and may be ignored.

A much more recent investigation of this topic was published by Tanuma *et al.* (55,60). They proposed formula for electron inelastic mean free paths for 31 materials from 50 to 2000 eV.

* *The cross sections of photoelectrons* were taken from Scofield's calculated data (61).

* *The atomic density of the promoter*, n_p was calculated as follows. Assuming that the analysed element of the promoter P is actually present in a compound P_xA_y having a density ρ_{pp} and a molar weight M_{pp}. The subscript pp refers to the actual phase of the promoter. Under these conditions, we have $n_p = x\rho_{pp}/M_{pp}$). A similar reasoning was used to calculate n_s, the atomic density of the support. For example for a calcined Pd/HZSM-5 the atomic density ratio n_p/n_s can be calculated as 1.695 using the following data: density of PdO = 8.3 g/cm^3, density of SiO_2 = 2.4 g/cm^3, molecular weight of PdO = 122.4 g/mol, molecular weight of SiO_2 = 60 g/mol. If the same sample is reduced, a n_p/n_s ratio of 2.678 can be calculated using the density of metallic Pd (11.4 g/cm^3) and its atomic weight (106.4 g/mol).

* *The detection efficiency* for a photoelectron with a kinetic energy E_k was considered as proportional to $(E_k)^{-1/2}$.

IV.2.1.2. Application

The following is a comparison between data obtained on the same catalyst using three different techniques. The sample was a 2.43% Pd/HZSM-5 (designated as 142B) prepared by ion-exchange and reduced under flowing hydrogen at 300 °C.

a) X-ray photoelectron spectroscopy

The model described above for the quantitation of XPS data was applied using the photolines Pd(3d) and Si(2p), the following data were introduced into the computer program described in the Appendix:

λ_p = 17.4 Å	λ_s = 20.5 Å.	ρ_{pp} = 11.4 cm^3g^{-1}
ρ_s = 2.4 cm^3g^{-1}	S_u = 364 m^2g^{-1}	S_g = 301 m^2g^{-1}
A_u = 19.1 m^2g^{-1}	A_g = 23.8 m^2g^{-1}	σ_s = .865
σ_p = 15.12	n_p/n_s = 2.678	D_p/D_s = 1.121
C_1 = 3 Å	x_s = 2.43%	M_{pp} = 106.4 g/mol
M_p = 106.4 g/mol	$(I_p/I_s)_u$ = .3017	$(I_p/I_s)_g$ = .2648
Initial guess for C_2 = 100 Å	Number of iterations = 20	

The solutions of equation [22] were as follows: sol.(1): P_2 = .9989 and sol.(2): P_2 = -2.9139. Using P_2 = .9989 as the only acceptable solution the fraction of well dispersed palladium and that of segregated palladium were found to be .83% and 1.60%, respectively. For a C_1 value arbitrarily fixed as 3 Å, an average crystallite size of the segregated palladium (C_2) of 164 Å was calculated.

Assuming that (i) there are $1.27*10^{19}$ atoms per square meter of pure metallic palladium (1), (ii) all Pd is in the form of cubic particles of dimension d(Å), (iii) five faces only of the particles are available for chemisorption, then the following relationship between the mean particle size and the dispersion can be established: d(Å) = 984/D(%). Using this relation an average dispersion of 38.1% was calculated for our supported Pd sample 142B.

b) Hydrogen chemisorption

The metallic dipersion of sample 142B was also determined directly by hydrogen chemisorption. Figure 10 shows the total and reversible hydrogen isotherms for a sample containing 118 µatom.gr of Pd. The amount of irreversibly held hydrogen as obtained by extrapolation to zero pressure was 38 µatom.gr corresponding to a metallic dispersion of 35.2%. This value is in reasonable agreement with the dispersion of 38.1% found using XPS data along with the sheet stacking model as modified to include surface segregation.

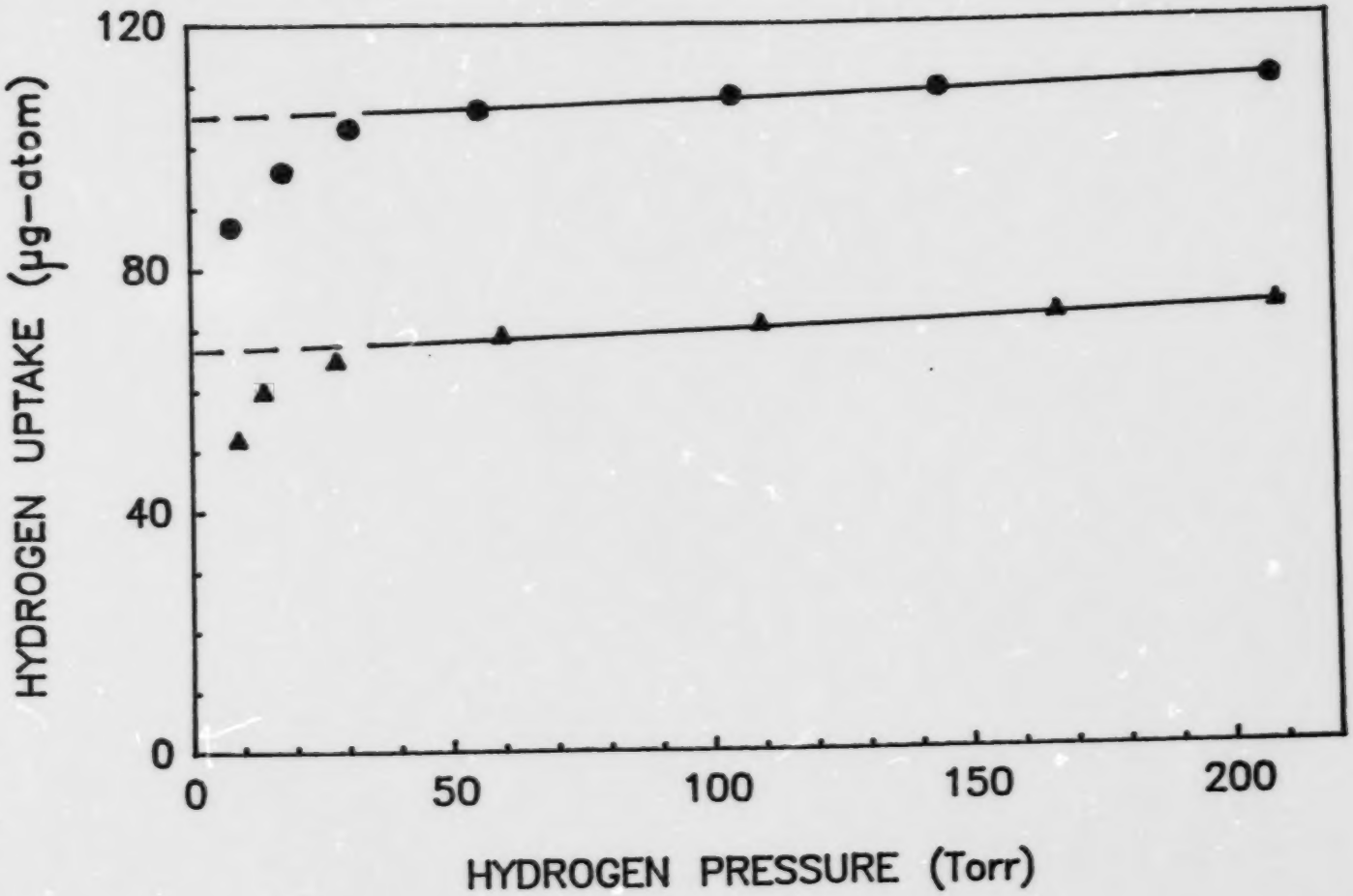

Figure 10. Hydrogen chemisorption isotherms for sample 142B (2.43% Pd/HZSM-5). (●) total uptake, (▲) reversible uptake.

c) Transmission electron microscopy

Transmission electron micrograph of this sample is shown in Figure 11. Since we used the extractive replica technique, this micrograph is representative of the metallic particles located on the external surface of the support. As indicated in Figure 12, particle size analysis gave a mean particle diameter of 129 Å. This value is only 20% off the value of 164 Å found by XPS.

IV.2.1.3. Effects of various parameters on C_2 and x_1

At this stage, it is worthwhile to use the data of the same sample 142B to check the effect of various parameters on the calculated variables, i.e. the particle size of the segregated material, C_2 and the amount of dispersed material, x_1. The results obtained are expected to be helful in assessing the influence of various uncertainties related to either experimental data or to arbitrarily chosen parameters. Included in this study are the effect of the arbitrary value chosen for C_1, the effect of the external surface areas either at a contant A_g or at a constant A_u/A_g, the effect of the XPS intensity ratio of the ground catalyst, either at a constant $(I_p/I_s)_u$ or at a constant $[(I_p/I_s)_u/(I_p/I_s)_g]$ ratio.

a) Effect of C_1

Figure 13 shows that for a fivefold increase in C_1 within reasonable limits (from 3 to 15 Å), both the weight percent (x_2) and the size (C_2) of the segregated fraction decrease by about 30 % only. These findings are in good agreement with previously published data (22).

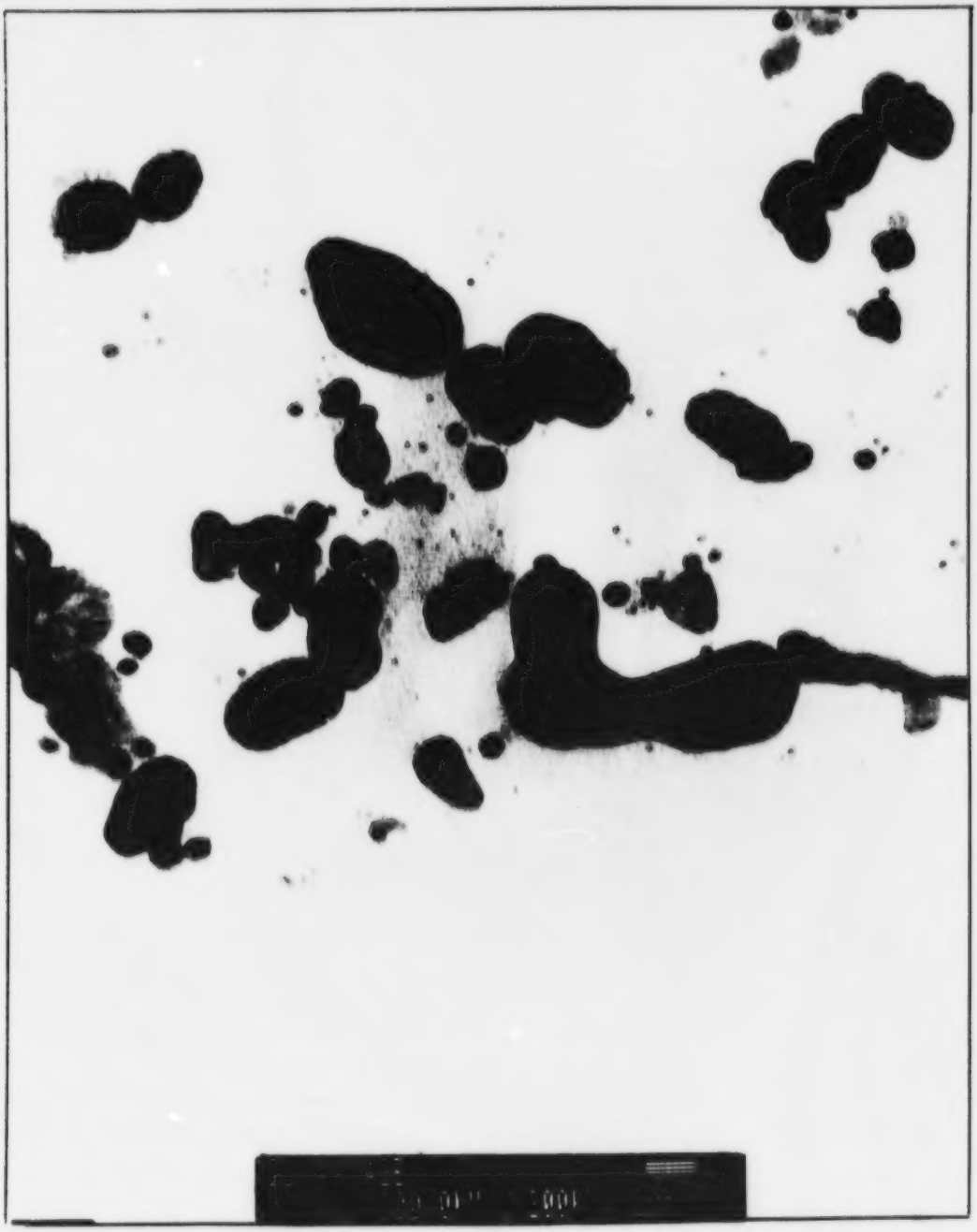

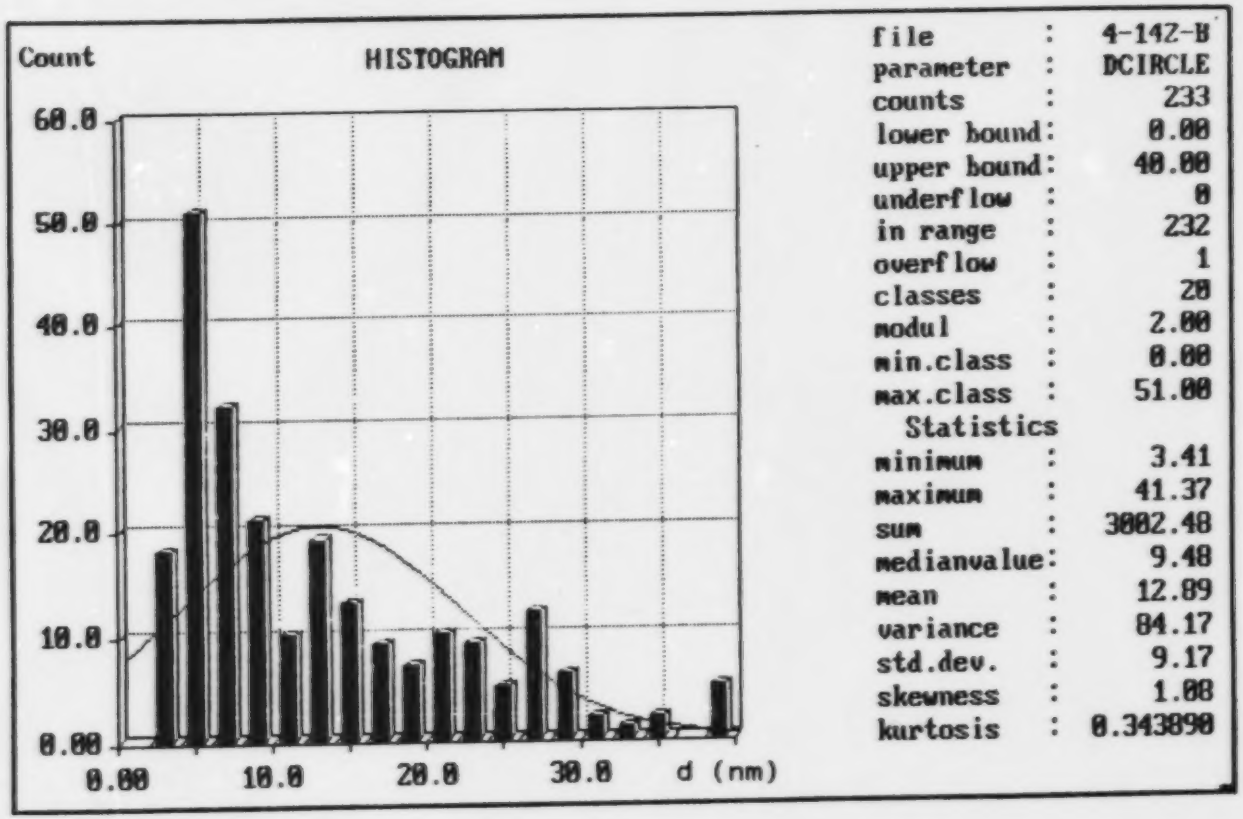

Figure 12. Particle size distribution from TEM micrograph of sample 142B (2.43% Pd/HZSM-5).

counts: number of particles counted to build the histogram;
mean: average particle size in nm.

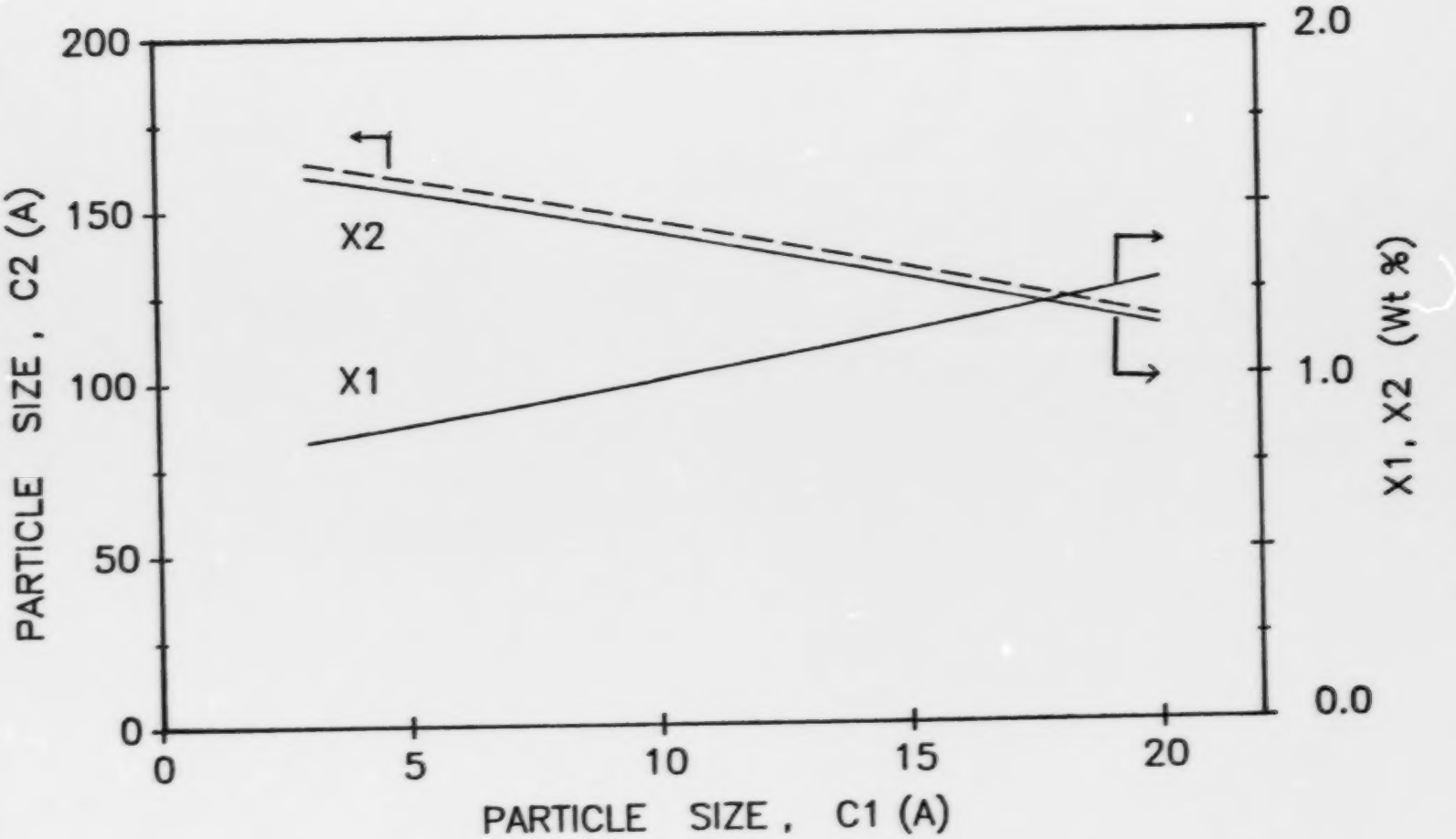

Figure 13. Effect of the size of dispersed particles (C_1) on: (dashed line) the size of segregated particles (C_2), (solid lines) the particles distribution (x_1 and x_2). SAMPLE 142B (2.43% Pd/HZSM-5).

b) Effect of the external surface area A_u

The effect of the external surface areas on C_2 and x_1 is however, much more pronounced than the effect of C_1. At a constant ratio between the external surface areas of the sample before and after grinding, the effect of A_u (or A_g) on x_2 (thus on x_1) is practically nil (Figure 14) while the particle size of the segregated fraction of the promoter is dramatically affected. Note that for Figure 14, all calculations were carried out based on a value of 3 Å for C_1. Therefore, to generate meaningful results, not only has the ratio A_u/A_g to be determined with the highest possible accuracy, but the actual external surface areas, A_u and A_g, also have to be measured with a high precision.

As summarized in Figure 15, such a conclusion is better illustrated through the effects of A_u at a constant value of A_g. Here the calculations were carried out using the A_g value (23.8 m^2g^{-1}) found for sample 142B in its ground form. Under these conditions, it is seen that the effect of A_u on both the particle size of the segregated fraction and the particles distribution of the promoter is quite strong. Note that for this particular example, equation [22] has no solutions in the 0 to 1 range, for A_u values higher than 20.9 m^2g^{-1}; therefore, the problem can no longer be solved. Attention has to be drawn to the fact that the limiting value of 21 m^2g^{-1} is only 10 % higher than the measured 19.1 m^2g^{-1} which generate quite reasonable results!!

Effect of the XPS intensity ratio $(I_p/I_s)_g$

Here also, the effect of the XPS intensity ratio $(I_p/I_s)_g$ on the calculated value of C_2 and x_1, depends on whether $(I_p/I_s)_u$ is considered as constant, or is actually changing in the same way as $(I_p/I_s)_g$. To address this problem, two limiting situations were considered, (i) the effect of $(I_p/I_s)_g$ at a constant $(I_p/I_s)_u$, (ii) the effect of $(I_p/I_s)_g$ at a constant

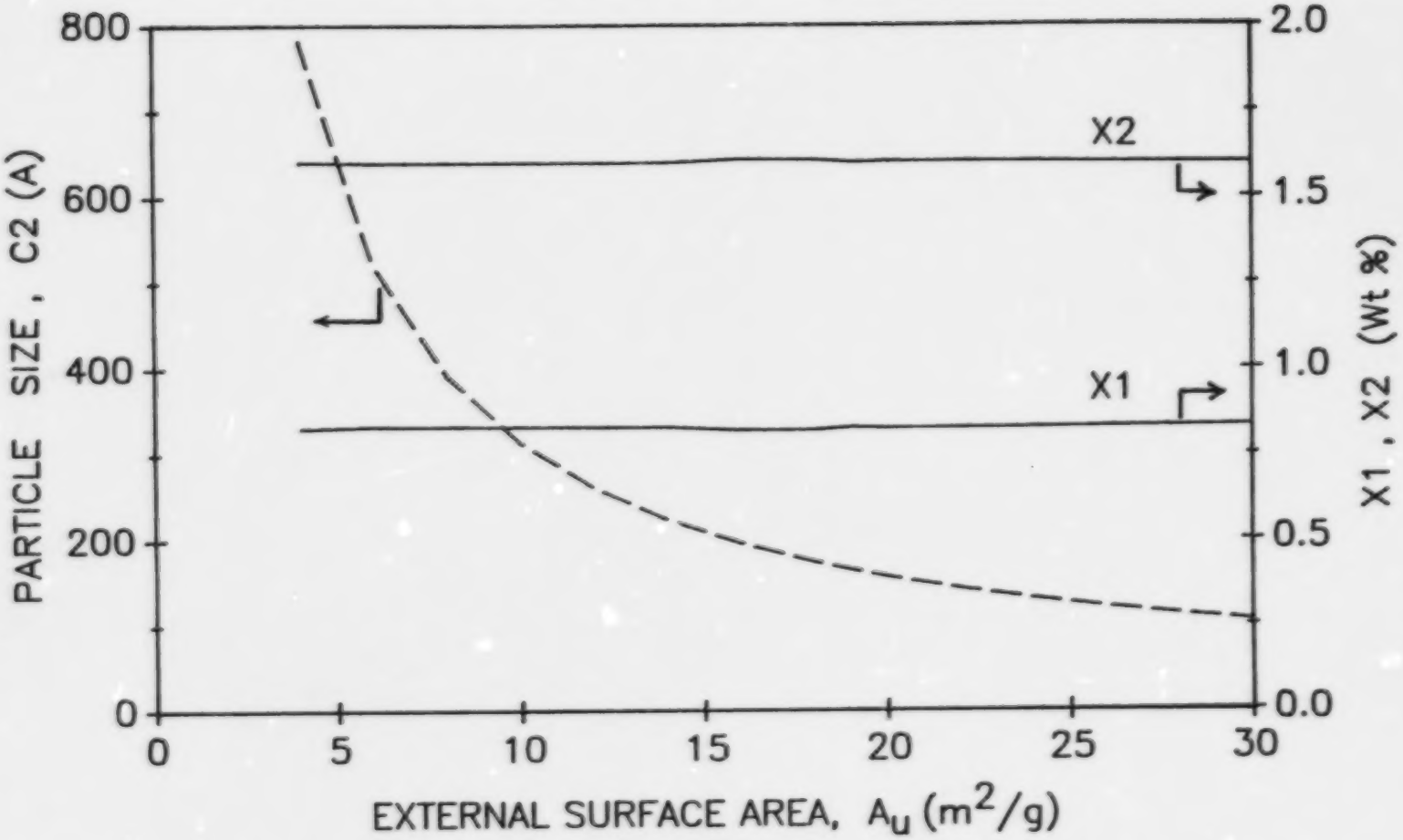

Figure 14. Effect of the external surface area A_u at a constant A_u/A_g (A_u/A_g = .8025) on:
(dashed line) the size of segregated particles (C_2),
(solid lines) the particles distribution (x_1 and x_2).
SAMPLE 142B (2.43% Pd/HZSM-5).

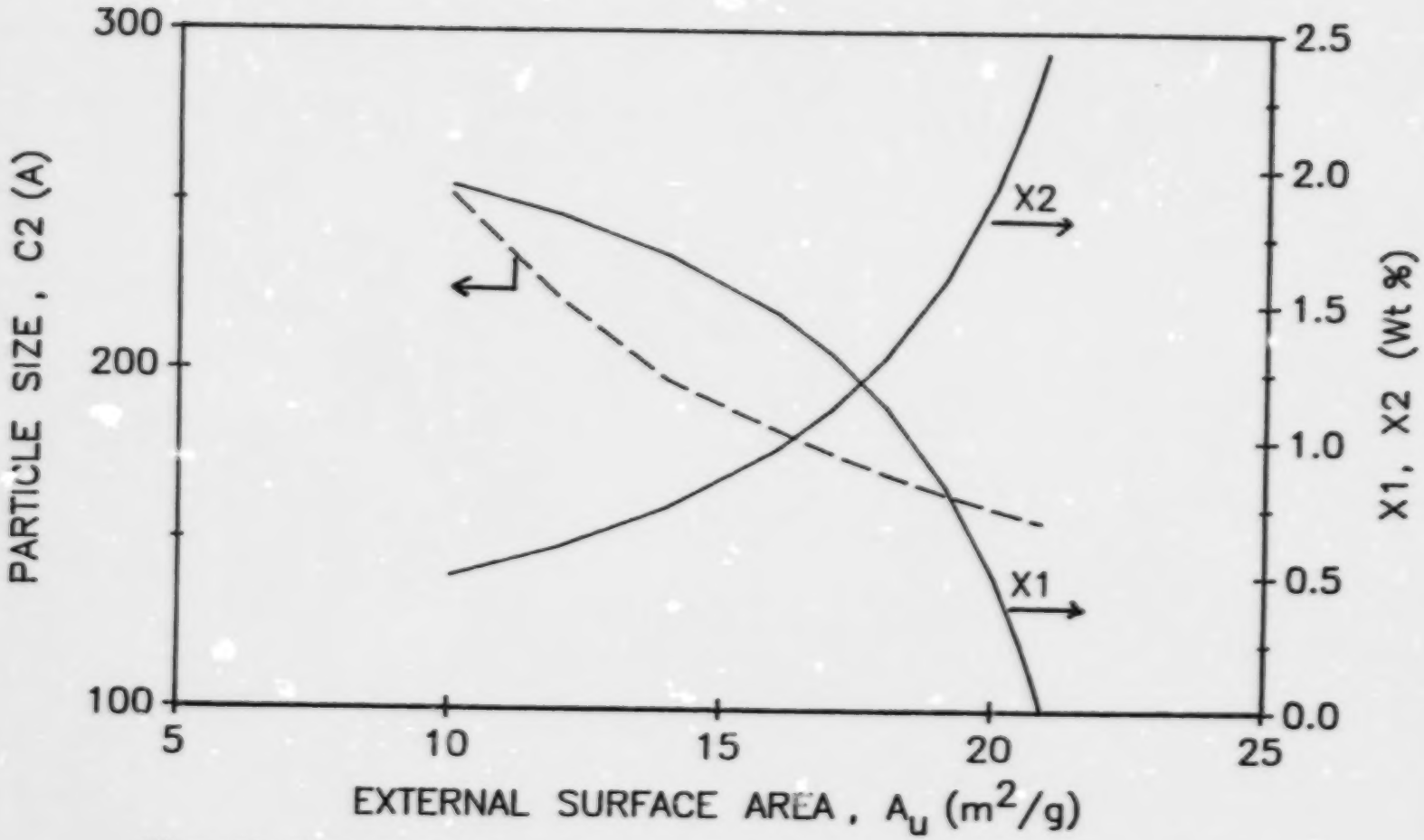

Figure 15. Effect of the external surface area A_u at a constant A_s (A_s = 23.8 m^2g^{-1}) on:
(dashed line) the size of segregated particles (C_2),
(solid lines) the particles distribution (x_1 and x_2).
SAMPLE 1428 (2.43% Pd/HZSM-5).

$[(I_p/I_s)_u]/[(I_p/I_s)_g]$ ratio.

Figure 16 shows that as long as the ratio $[(I_p/I_s)_u]/[(I_p/I_s)_g]$ is constant, the effect of $(I_p/I_s)_g$ on C_2 and x_1 is not dramatic, though important. Note that in Figure 16, the overall variations of C_2 and x_1 may seem, in relative terms, extremely large. These variations are however the result of a fivefold increase of the $(I_p/I_s)_g$ ratio. If a more realistic change of the $(I_p/I_s)_g$ ratio as a result of experimental incertainties is considered, say 10 to 20%, the effect of such a change would be quite small provided that the XPS intensity ratio of the unground catalyst changes accordingly.

In contrast, the effect of $(I_p/I_s)_g$ at a constant $(I_p/I_s)_u$ ratio is very strong (Figure 17). As seen, the distribution of the supported material changes from a completly homogeneous one ($x_1 = x_B$, i.e., 2.43% in our case) to a completely segregated distribution ($x_1 = 0$) when the XPS intensity ratio decreases by less than 20%. The effect of $(I_p/I_s)_g$ on C_2 is less drastic except when x_2 approaches zero.

IV.2.1.4. Conclusions

Three main conclusions may be drawn,

(i) The C_1 value which is usually fixed arbitrarily in the 3 to 10 Å range has little effect on the calculated distribution of supported materials.

(ii) The effect of the external surface area of the unground catalyst (A_u) depends strongly on whether the external surface area of the ground catalyst (A_g) is changing to the same extent as A_u, or it is eventually constant. The two limiting cases discussed above show that the effect of A_u on the calculated characteristics of the distribution (C_2 and x_1) is very strong

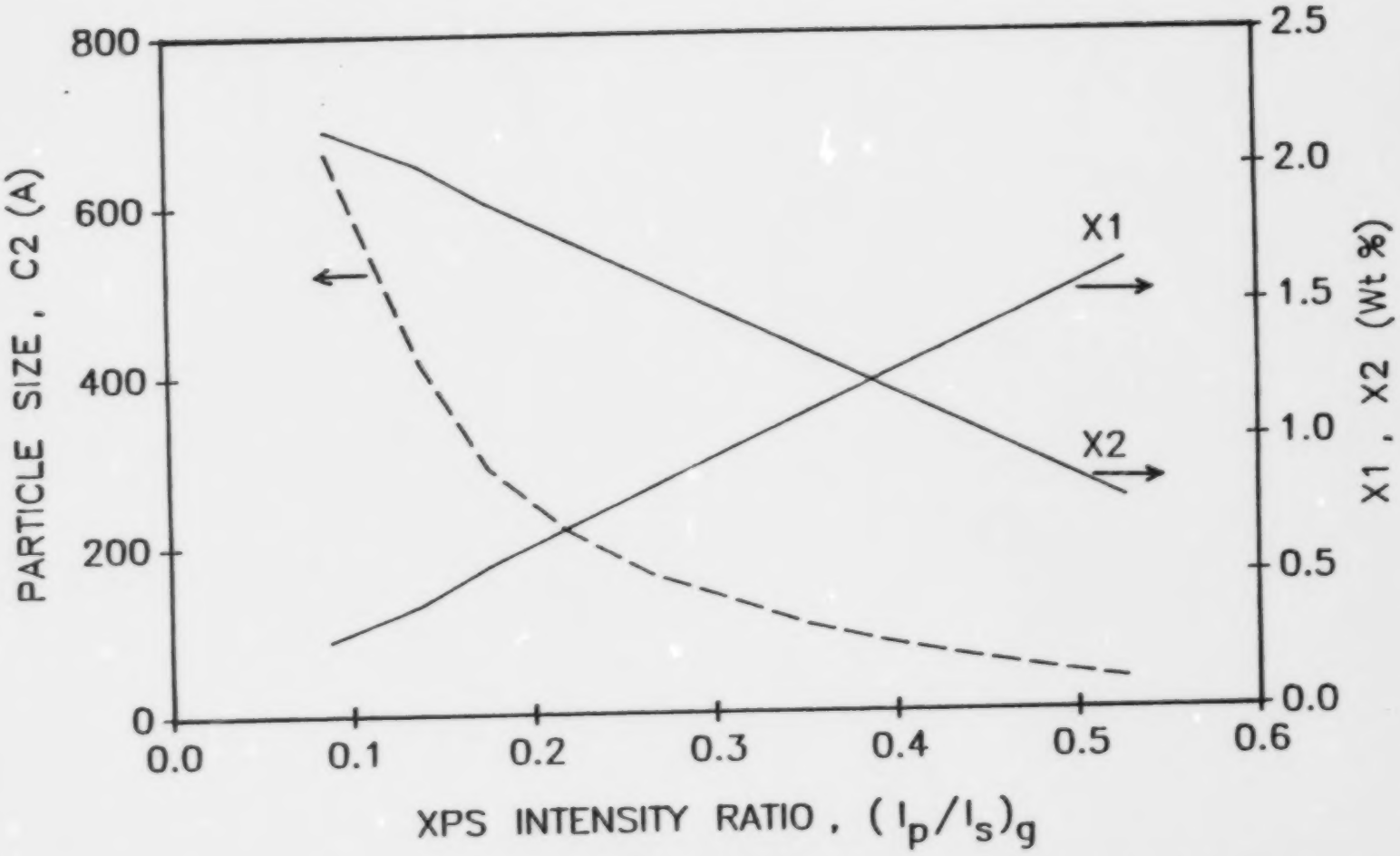

Figure 16. Effect of the XPS intensity ratio $(I_p/I_s)_g$ at a constant $(I_p/I_s)_u/(I_p/I_s)_s$ on:
(dashed line) the size of segregated particles (C_2),
(solid lines) the particles distribution (x_1 and x_2).
SAMPLE 142B (2.43% Pd/HZSM-5).

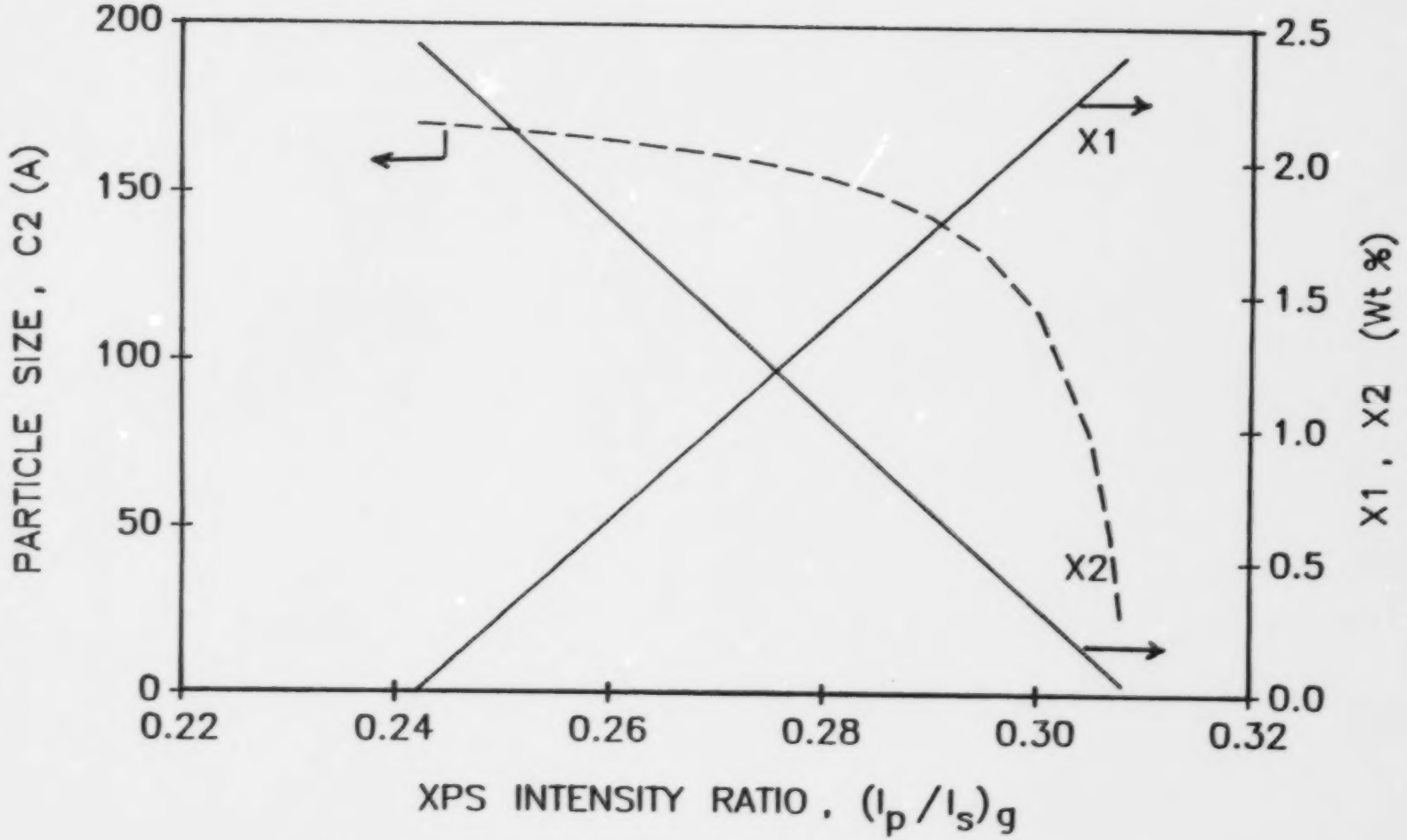

Figure 17. Effect of the XPS intensity ratio $(I_p/I_s)_g$ at a constant $(I_p/I_s)_u$ ratio $[(I_p/I_s)_u = .3017]$ on:
(dashed line) the size of segregated particles (C_2),
(solid lines) the particles distribution (x_1 and x_2).
SAMPLE 142B (2.43% Pd/HZSM-5).

when A_g is kept constant. However, if A_g changes in such a way that the A_u/A_g is kept constant, then the external surface area of the catalyst has no effect on x_1 and little effect on C_2 except at low values of A_u.

(iii) There is a strong analogy between the effect of A_u and the effect of the XPS intensity ratio of, say the unground catalyst $(I_p/I_s)_u$. If the ratio $[(I_p/I_s)_g/(I_p/I_s)_u]$ is kept constant, the effect of $(I_p/I_s)_u$ will not be as strong as in the case of a constant $(I_p/I_s)_g$ ratio.

The foregoing discussion has revealed the extreme sensitivity of the model to some of the parameters involved. In particular, one important area where progress can be made is the adjustment of the external surface area to better fit the overall analysis. It is suggested that samples, the distributions of which have been determined by independent methods, be fitted with calculated external surface areas. These values would then be used to fine tune the definition of the external surface area and find the most suitable experimental conditions for its determination.

Using the available data for the three other Pd containing catalysts, the model did not lead to satisfactory results (Figures 18 and 19). The reason is most probably linked to an unfavorable accumulation of uncertainties, in particular in relation with the XPS intensity ratios and the external surface areas. Possible manipulations of the data that clearly illustrate the effect of the two parameters on the calculated values of C_2 and x_1 are given below for a Pt containing sample. Since the aim of such a manipulation is only to demonstrate that a physically meaningful solution may be found by using external surface areas and/or XPS intensity ratios within the uncertainties limits of the actual experimental data, there is no need to apply it to all catalysts.

SOLN= .993965 SOLP= -1.958775

RESULTS

Dispersed fraction: 5.132544
(Distribution NOT ACCEPTABLE)!!!
Segregated fraction:-2.132544

CALCULATION OF PARTICLE SIZE (ITERATION)

C0	C2	ABS(C2 - C0)
100	31.4092	68.59081
31.4092	24.6153	6.793898
24.6153	23.78973	.8255692
23.78973	23.77308	1.664925E-02
23.77308	23.77308	7.629395E-06
23.77308	23.77308	0

Particle size: 23.77308

SOLN= 1.01047 SOLP= -3.149154 (Solutions NOT ACCEPTABLE)!!!

RESULTS

Dispersed fraction: 768.7644
(Distribution NOT ACCEPTABLE)!!!
Segregated fraction:-765.7644

CALCULATION OF PARTICLE SIZE (ITERATION)

C0	C2	ABS(C2 - C0)
100	135.7795	35.77948
135.7795	135.2663	.5131378
135.2663	135.2663	3.051758E-05
135.2663	135.2663	0

Particle size: 135.2663

Figure 18. XPS quantification results for (upper figure) sample 142A (3% Pd/HZSM-5), and (lower figure) sample 180A (3% Pd/HZSM-5)

```
SOLN= -3.480883   SOLP=  .9310855


                          RESULTS
                          ---------
                  Dispersed fraction: 47.38324
(Distribution NOT ACCEPTABLE)!!!
                  Segregated fraction:-44.45324

              CALCULATION OF PARTICLE SIZE (ITERATION)
-------------------------------------------------------------------------------
              C0                  C2                  ABS(C2 - C0)
-------------------------------------------------------------------------------
              100                 173.9846            73.98462
              173.9846            172.1886            1.796066
              172.1886            172.1885            4.577637E-05
              172.1885            172.1885            0
                    Particle size: 172.1885
-------------------------------------------------------------------------------
```

Figure 19. XPS quantification results for sample 151B (2.93% Pd/HZSM-5).

IV.2.2. Pt/HZSM-5 catalysts.

The Pt(4d) XPS bands of sample 140A (1.85% Pt/HZSM-5) after various treatments are shown in Figure 20. Binding energies corrected for charging are gathered in Table VII along with the intensity of the XPS bands of Pt(4d) and Si(2p). It is important to notice that the binding energy of the Pt(4d) electrons remain the same regardless of the nature of the pretreatment the catalyst had undergone, i.e., oxidation, reduction or reduction followed by grinding. The binding energies of 315.2 and 332.3 eV for $Pt(4d_{5/2})$ and $Pt(4d_{3/2})$, respectively correspond to the presence of metallic platinum.

The state of Pt in zeolites after the calcination step is a matter of dispute. In one of the earlier detailed study on Pt/Y catalysts, Gallezot *et al.* (62) reported that upon decomposition of the platinum tetrammine complex in flowing oxygen, platinum atoms are in the form Pt^{2+} located in cationic positions (63). In contrast, Sachtler and coworkers (64) reported that after calcination at 300 °C, Pt is oxidized into PtO or PtO_2 depending on whether the zeolite is neutral (NaY) or acidic (HY). A third type of conclusions which seems to be in agreement with our findings was reported by Chester *et al.* (65,66). Based on the stoichiometry of the evolved gases, these authors concluded that Pt is auto-reduced to the metallic state by the ammine ligands during the calcination, in air as well as in inert atmospheres.

Textural properties including external surface areas as well as meso- and micropore volumes of Pt/HZSM-5 catalysts after different pretreatments are summarized in Table VIII. As in the case of Pd/HZSM-5 samples (see Table VI), grinding brings about a significant decrease in the micropore volume, and consequently a decrease in BET surface area.

For Pt/HZSM-5 catalysts containing metallic platinum, the data needed to calculate the platinum distribution and which are sample-independent

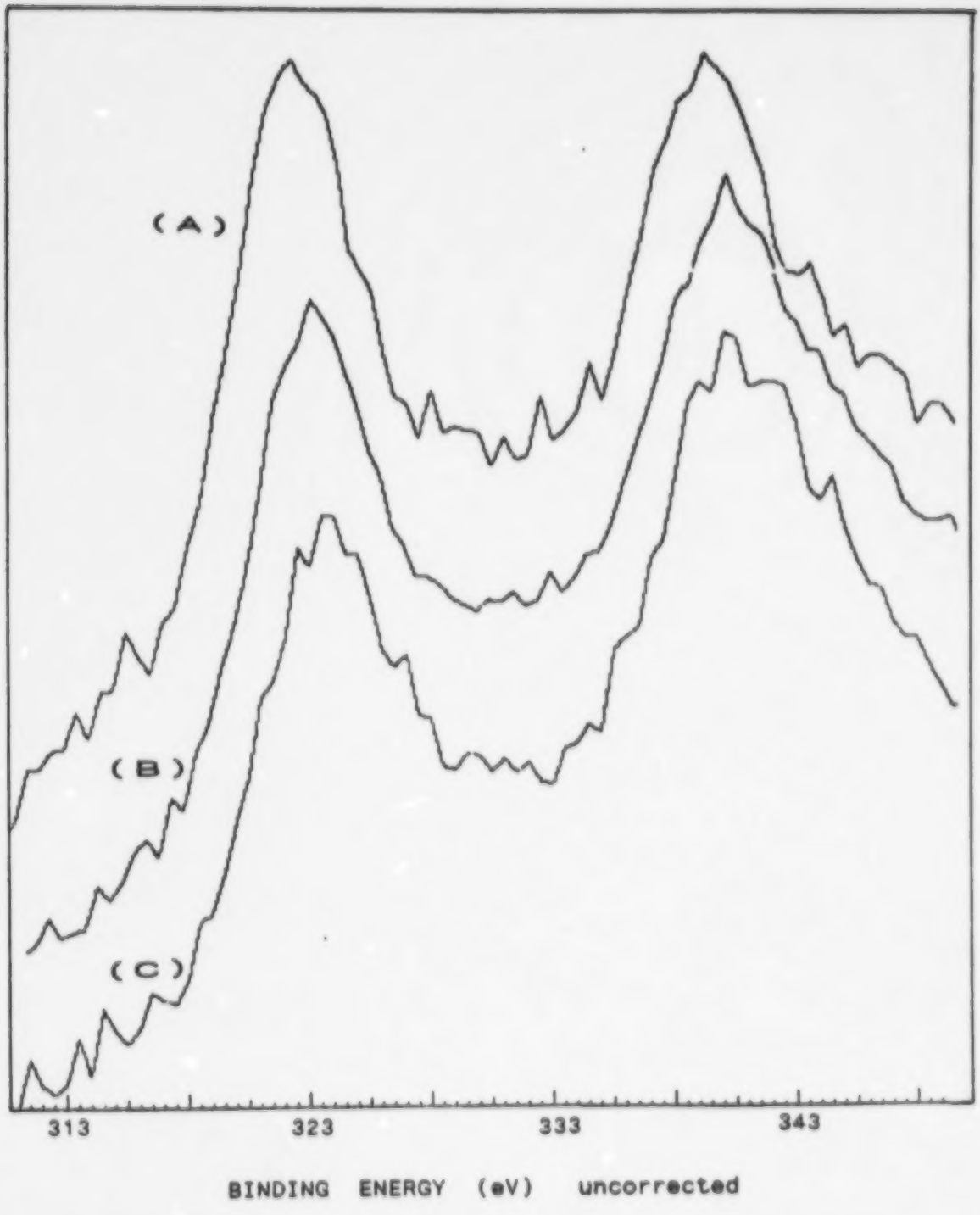

Figure 20. XPS spectra of Pt(4d) in sample 140A (1.85% Pt/HZSM-5) (a) oxidized, (b) reduced, (c) reduced and ground.

TABLE VII. XPS Data for Pt/HZSM-5 Catalysts

Sample	Binding Energy (eV)			I[Pt(4d)]	I[Si(2p)]	I(Pt)/I(Si)
	$Pt(4d_{5/2})$	$Pt(4d_{3/2})$	O(1s)			
140A 1.85% Pt/HZSM-5						
Calcined	315.3	332.3	532.8	1.329	9.085	0.232
Reduced	315.3	332.3	532.8	1.471	9.055	0.247
Red.Grnd.[a]	315.2	332.2	532.8	2.076	10.736	0.212
140B 2.53% Pt/HZSM-5						
Calcined	315.5	332.3	532.5	4.703	5.521	0.871
Reduced	315.2	332.2	532.8	3.061	7.201	0.460
Red.Grnd.[a]	315.3	332.3	533.1	2.685	6.658	0.269

(*a*) Reduced under flowing hydrogen at 300 °C, then ground for 5 min.

TABLE VIII. Textural Properties of Pt/HZSM-5 Catalysts

Sample	$S_{BET}(m^2g^{-1})$	$S_e(m^2g^{-1})$	$V_H(cm^3g^{-1})$	$V_m(cm^3g^{-1})$
140A 1.85% Pt/HZSM-5				
- Calcined	403	49.2	0.18	0.151
- Reduced	400	58.5	0.22	0.146
- Red.Grnd.[a]	272	51.8	0.20	0.093
140B 2.53% Pt/HZSM-5				
- Calcined	367	16.8	0.06	0.154
- Reduced	365	25.3	0.09	0.149
- Red.Grnd.[a]	249	22.0	0.04	0.085

(a) Reduced under flowing hydrogen at 300 °C, then ground for 5 min.

are gathered in Table IX. The missing data fall into two categories, those which depend on the particular sample under investigation, and those which are usually fixed arbitrarily, i.e., the initial guess for C_2, and the number of iterations.

Unfortunately, as shown in Figure 21, using data of Table IX in addition to experimental data regarding the textural properties of the ground and unground samples and their XPS intensity ratios did not lead to satisfactory results for both Pt/HZSM-5 samples. As mentioned earlier, more work in the following areas is still needed, (i) the most suitable definition of the external surface area, (ii) the best experimental procedure to measure such an area, (iii) the reproducibility of the XPS intensity ratios.

The average size of the segregated platinum particles in sample 140A (1.85% Pt/HZSM-5) as determined by transmission electron microscopy was 89 Å (Appendix 2). Figure 22 shows possible solutions of the XPS model for sample 140A using the experimental value of A_g (51.8 m^2g^{-1}) while A_u is varied within reasonable limits. For A_u values that lead to physically acceptable solutions, C_2 would be within the 15 - 35 Å range, significantly below the average value obtained by TEM.

Higher C_2 values may be obtained by using XPS intensity ratios for both the ground and unground catalysts lower, say within 20%, than their experimental counterparts, while keeping the ratio $[(I_p/I_s)_u/(I_p/I_s)_g]$ constant and equal to the value determined experimentally. This is illustrated in Figure 23 for which the results corresponding to A_u = 43 m^2g^{-1} and A_g = 51.8 m^2g^{-1} were taken as an arbitrary solution for the model. The solid line in Figure 23 gives C_2 as a function of A_g at a constant A_u/A_g (A_u/A_g = 43/51.8 = .8301) using the experimental values of the XPS intensity ratios. The upper curve (a) and the lower curve (c) were calculated using XPS intensity ratios 20% below and 20% above the experimental ratios, respectively. It is seen that

TABLE IX. Data for XPS quantification for reduced Pt/ZSM-5 catalysts

Mean Free Path of Photoelectron from Promoter	17.6
Mean Free Path of Photoelectron from Support	20.5
Density of Support	2.4
Density of Promoter	21.45
BET Surface Area of Unground Catalyst	
BET Surface Area of Ground Catalyst	
External Surface Area on Unground Catalyst	
External Surface Area of Ground Catalyst	
Cross Section of Photoelectron from Support	.865
Cross Section of Photoelectron from Promoter	15.48
Atomic Density Ratio np/ns	2.749
Detection Efficiency Ratio Dp/Ds	1.112
Size of the Small Particles	3
Promotor Loading in wt%	
Molecular Weight of the Promoter Phase	195.09
Molecular Weight of Promoter	195.09
XPS Intensity Ratio for Unground Catalyst	
XPS Intensity Ratio for Ground Catalyst	
Initial Guess for the Particle Size in A	
The Number of Iterations	

SOLN= -4.912962 SOLP= .9834195

RESULTS

Dispersed fraction: 26.73521
(Distribution NOT ACCEPTABLE)!!!
Segregated fraction:-24.88521

CALCULATION OF PARTICLE SIZE (ITERATION)

C0	C2	ABS(C2 - C0)
100	66.88201	33.11799
66.88201	65.95477	.9272385
65.95477	65.95242	2.349854E-03
65.95242	65.95242	0

Particle size: 65.95242

SOLN= -1.308137 SOLP= .9373559

RESULTS

Dispersed fraction: 91.51078
(Distribution NOT ACCEPTABLE)!!!
Segregated fraction:-88.98077

CALCULATION OF PARTICLE SIZE (ITERATION)

C0	C2	ABS(C2 - C0)
100	151.5939	51.59387
151.5939	150.5738	1.020096
150.5738	150.5737	4.577637E-05
150.5737	150.5737	0

Particle size: 150.5737

Figure 21. XPS quantification results for (upper figure) sample 140A (1.85% Pt/HZSM-5), and (lower figure) sample 140B (2.53% Pt/HZSM-5)

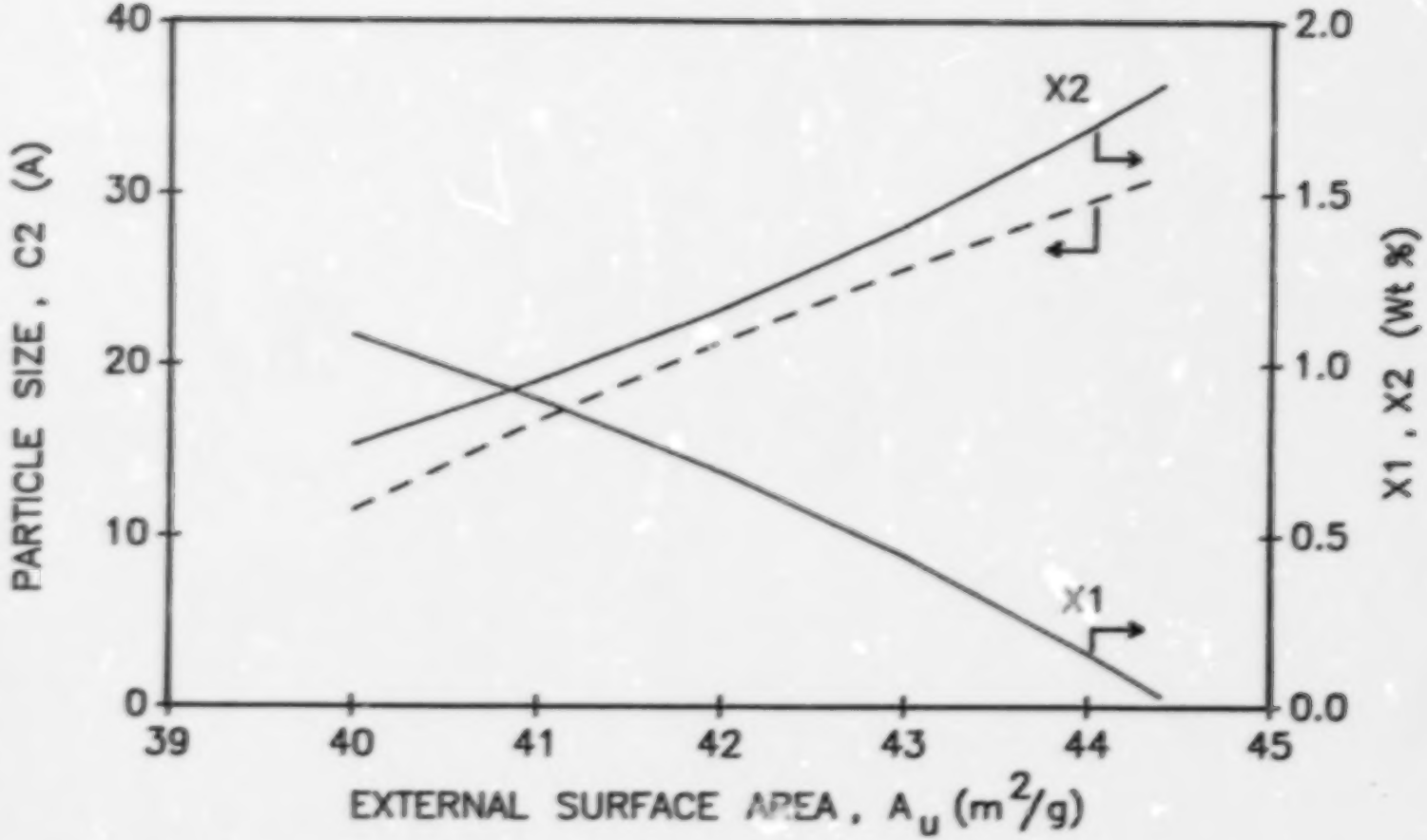

Figure 22. Effect of the external surface area A_u at a constant A_s (A_s = 51.8 m^2g^{-1}) on:
(dashed line) the size of segregated particles (C_2),
(solid lines) the particles distribution (x_1 and x_2).
SAMPLE 140A (1.85% Pt/HZSM-5).

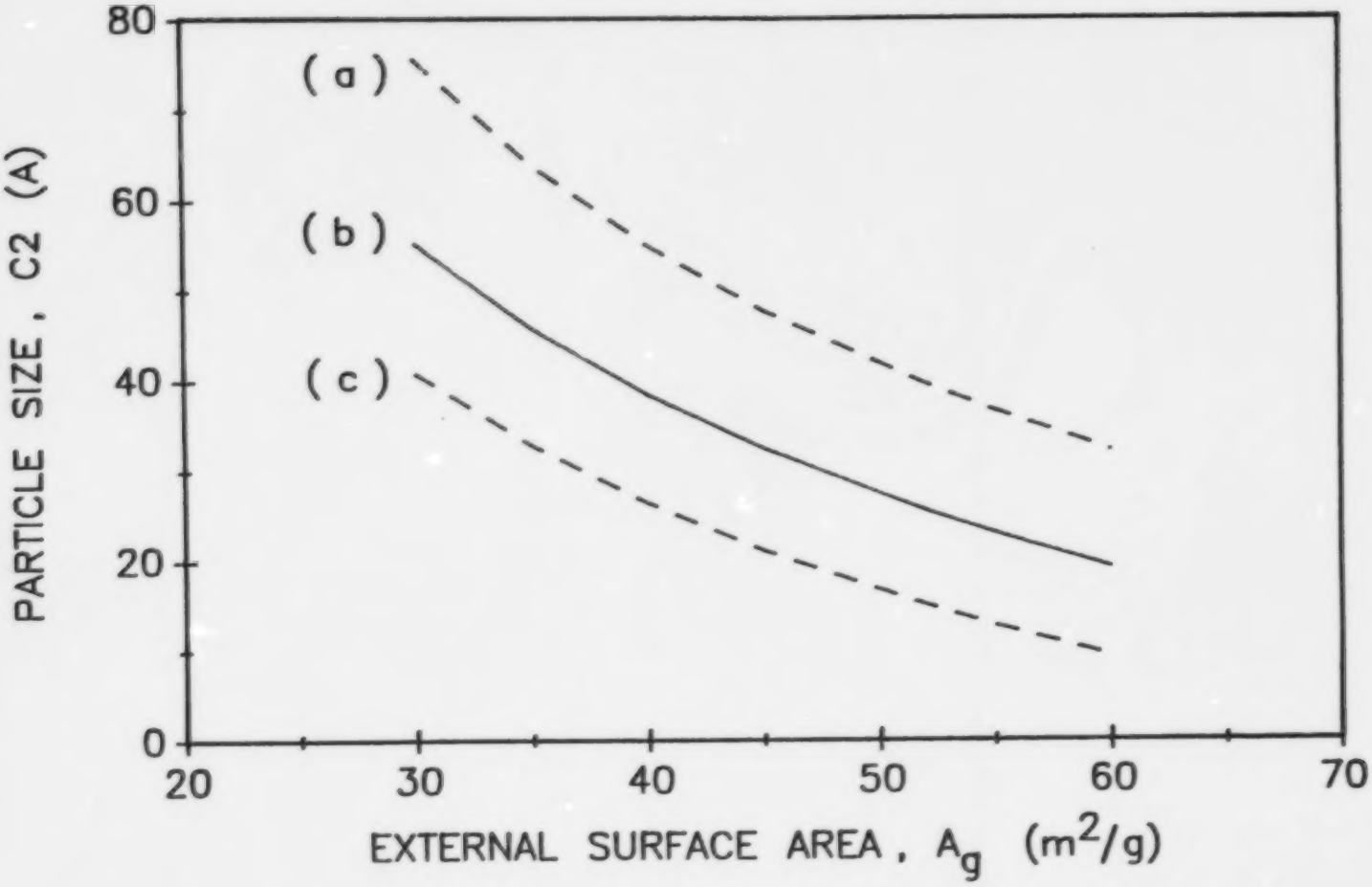

Figure 23. Effect of the external surface area A_u at a constant A_u/A_g (A_u/A_g = .8301) on the size of segregated particles (C_2). The XPS intensity ratios $(I_p/I_s)_u$ and $(I_p/I_s)_g$ were (a) decreased by 20%, (b) unchanged, (c) increased by 20%. SAMPLE 140A (1.85% Pt/HZSM-5).

the calculated value of C_2 can eventually be adjusted to the value obtained by electron microscopy. Further work will be carried out toward this objective.

IV.2.3. Pt/SiO_2 and Pt/Al_2O_3 catalyst.

XPS data for all Pt/SiO_2 and Pt/Al_2O_3 samples are given in Table X. The binding energies of Si(2p) = 103.3 eV and Al(2p) 74.5 eV were used as references for Pt/SiO_2 and Pt/Al_2O_3 catalysts, respectively. It is worth mentioning that for calcined samples, the binding energies for $Pt(4d_{5/2})$ in Pt/Al_2O_3 and Pt/SiO_2 were *ca.* 319.0 and 316.5 eV. This indicates that Pt is sited mostly as oxide in Pt/Al_2O_3, and as metal in Pt/SiO_2.

For the XPS intensity ratios, we used I(Pt4d)/I(Al2p) for Pt/Al_2O_3 samples because the Pt(4f) and the Al(2p) XPS photolines overlap. For Pt/SiO_2 samples, we used the I(Pt4f)/I(Si2p) ratio. It is seen in Table X that upon grinding, the XPS intensity ratios for Pt/Al_2O_3 samples, [I(Pt4d)/I(Al2p)], do change to some extent. In contrast, for Pt/SiO_2, the ratio I(Pt4f)/I(Si2p) hardly change regardless of the nature of the pretreatment.

Data concerning the textural properties of Pt/SiO_2 and Pt/Al_2O_3 samples are gathered in Table XI. Two remarks can be made. First, the BET surface area of alumina does not change upon grinding, while the BET surface area of the softer silica, decreases significantly. Second, the values of external surface areas, particularly for alumina-supported catalysts are somewhat erratic most probably because of lack of suitability of the standard adsorbent used to calculate the t-plot. Note that all these samples exhibit hardly any microporosity and therefore are supposed to have external surface areas close to their actual BET surface areas.

Using appropriate data from Tables III (metal contents), IX (various data), X (XPS intensity ratios) and XI (surface areas), the XPS

TABLE X. XPS Data for Pt/SiO_2 and Pt/Al_2O_3 Catalysts

Sample	Binding Energy (eV)			XPS intensity			I(Pt)/I(Si)	I(Pt)/I(Al)
	$Pt(4d_{5/2})$	$Pt(4d_{3/2})$	O(1s)	Pt(4d)	Si(2p)	Al(2p)		
185A 1.85% Pt/Al_2O_3[a]								
Calcined	318.9	335.7	531.4	3.280		19.427		0.169
Calc.Grnd.	318.1	334.9	531.4	3.767		28.496		0.132
Reduced	316.5	333.3	531.4	2.652		32.566		0.081
Red.Grnd.	316.6	333.3	531.5	3.957		34.624		0.114
185B 0.96% Pt/Al_2O_3[a]								
Calcined	319.1	335.5	531.5	1.491		19.994		0.075
Calc.Grnd.	319.0	335.1	531.6	1.264		20.747		0.061
Reduced	-	-	531.5	2.041		30.229		0.067
Red.Grnd	-	-	531.7	1.682		35.084		0.048
186A 2.97% Pt/SiO_2[b,c]								
Calcined	316.3	333.3	532.9	4.355	9.860		0.442	
Calc.Grnd.	316.3	333.3	533.0	11.180	26.767		0.418	
Reduced	-	-	533.1	-	27.010		-	
Red.Grnd	-	-	533.0	-	26.999		-	
186B 1.10% Pt/SiO_2[b,d]								
Calcined	316.5	333.1	533.0	3.814	20.240		0.188	
Calc.Grnd	316.6	333.1	533.1	4.573	23.312		0.196	
Reduced	-	-	532.9	-	32.434		-	
Red.Grnd	-	-	533.0	-	30.169		-	

(a) BE reference Al(2p) = 74.5 eV, *(b)* BE reference Si(2p) = 103.3, *(c)* The [I(Pt4f)/I(Si2p)] ratios were found to be constant for all samples (0.1011, 0.1019, 0.1019 and 0.099 in the same order), *(d)* The [I(Pt4f)/I(Si2p)] ratios were found to be 0.0420, 0.0352, 0.0390 and 0.0376, respectively.

TABLE XI. Textural Properties of Pt/SiO_2 and Pt/Al_2O_3 Catalysts.

Sample		$S_{BET}(m^2g^{-1})$	$S_e(m^2g^{-1})$	$V_H(cm^3g^{-1})$	$V_m(cm^3g^{-1})$
185A	1.85% Pt/alumina				
	Reduced	187	192	0.503	-
	Red. Grnd.	163	179	0.280	-
185B	0.96% Pt/alumina				
	Calcined	178	214	0.490	-
	Calc. Grnd.	168	191	0.351	-
	Reduced	181	197	0.473	-
	Red. Grnd.	167	173	0.305	-
186A	2.97% Pt/silica				
	Reduced	499	611	0.959	0
	Red. Grnd.	474	387	0.485	0.040
186B	1.10% Pt/silica				
	Calcined	625	572	0.973	0.028
	Calc. Grnd.	543	470	0.705	0.036
	Reduced	628	565	0.939	0.034
	Red. Grnd.	465	374	0.476	0.042

equations could not be solved properly. The following is a list of possible reasons the model is not working for these catalysts, along with the necessary measures to be taken to check and eventually correct the problem:

(a) The definition and determination of the external surface areas are not yet satisfactory. Calculations have to be made backward using mean particle sizes determined by an independent technique. These calculations are expected to lead to what ought to be the external surface area. Then, appropriate means to measure such an area should be developed.

(b) The model as it stands now is inherently less suitable for catalysts with widely open structures with no internal surface than for zeolite-supported catalysts. The model must then be adapted to such catalysts.

(c) Contrary to our assumptions, the sizes of the supported particles change during grinding. This could be easily checked on selected samples using TEM before and after grinding.

IV.2.4. Other catalysts: Ni/Al_2O_3 and Mo/Al_2O_3.

XPS data for calcined Ni/Al_2O_3 and Mo/Al_2O_3 are gathered in Tables XII and XIII. Typical spectra are shown in Figures 24 and 25. The binding energy for $Ni(2p_{3/2})$ was found to be 855.8 eV indicative of the presence of NiO. Likewise, the binding energies of 233.0 and 236.1 eV for $Mo(3d_{5/2})$ and $Mo(3d_{3/2})$, respectively indicate also that Mo is present as MoO_3.

Textural properties of Ni/Al_2O_3 and Mo/Al_2O_3 samples after various pretreatments are shown in Table XIV. It is seen that the BET surface area is insensitive to the metal nature and loading as well as to the grinding. The external surface area however, suffers the same problems as Pt/Al_2O_3 catalysts probably, as it was put forward earlier, because of lack of suitability of the

TABLE XII. XPS Data for Ni/Al_2O_3[a] (Sample 182).

Sample	Binding Energy (eV)	XPS intensity		I(Ni)
	$Ni(3p_{3/2})$	Ni(3p)	Al(2p)	I(Al)
Calcined	855.8	11.205	7.438	1.506
Calc. Grnd.	855.9	12.212	10.017	1.219

(a) BE reference Al(2p) = 74.5 eV

TABLE XIII. XPS Data for Mo/Al_2O_3[a] (Sample 183).

Sample	Binding Energy (eV)		XPS intensity		I(Mo)
	$Mo(3d_{5/2})$	$Mo(3d_{3/2})$	Mo(3d)	Al(2p)	I(Al)
Calcined	233.0	236.1	14.761	6.836	2.159
Calc. Grnd.	233.1	236.0	12.001	9.488	1.265

(a) BE reference Al(2p) = 74.5 eV

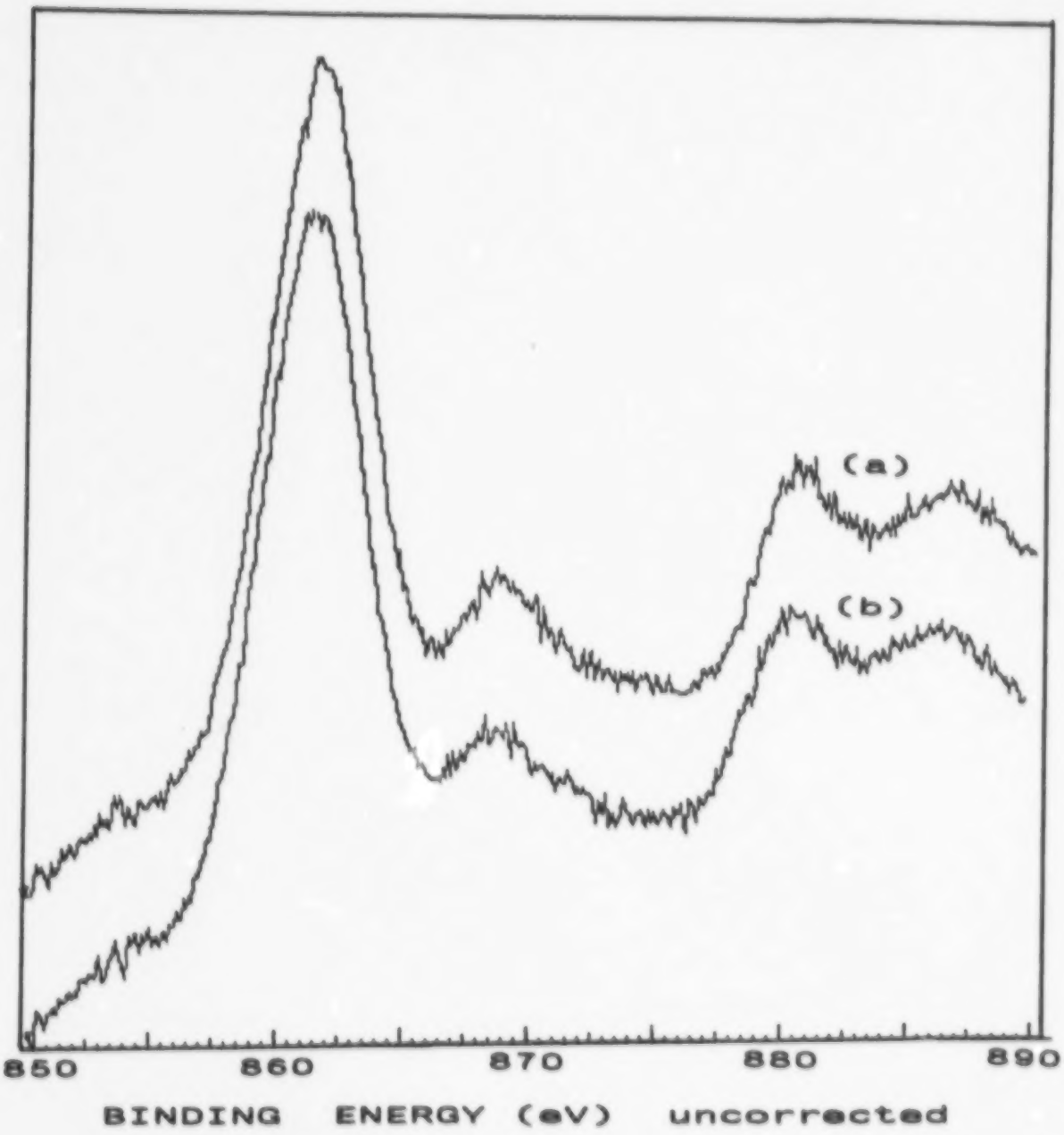

Figure 24. XPS spectra of Ni(3p) in sample 182 (3.36% Ni/Al_2O_3)
(a) oxidized, (b) oxidized and ground

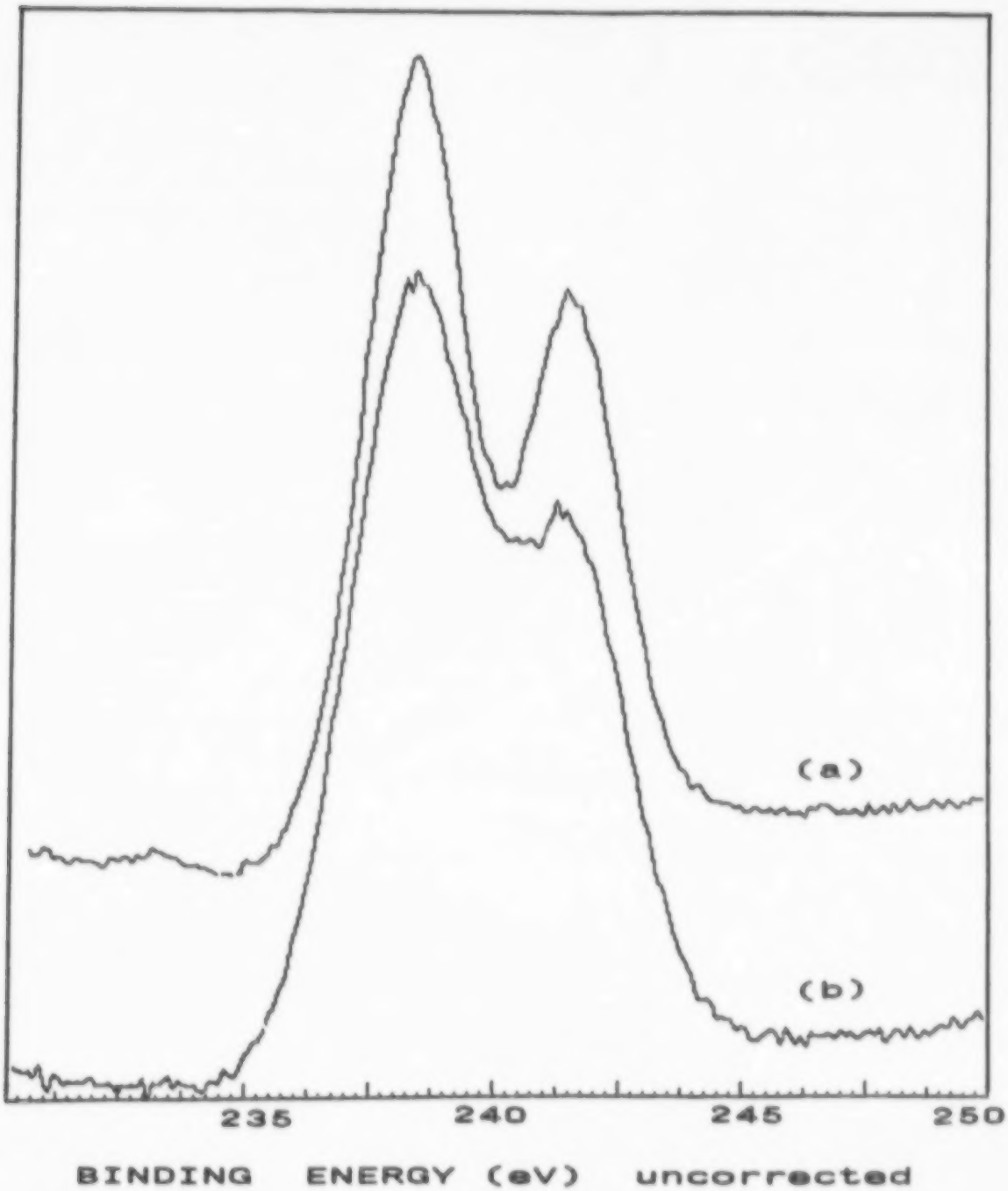

Figure 25. XPS spectra of Mo(3d) in sample 183 (9.30% Mo/Al_2O_3)
(a) oxidized, (b) oxidized and ground

TABLE XIV. Textural Properties of Ni/Al_2O_3 and Mo/Al_2O_3.

Sample		$S_{BET}(m^2g^{-1})$	$S_e(m^2g^{-1})$	$V_M(cm^3g^{-1})$	$V_m(cm^3g^{-1})$
182	3.36% Ni/alumina				
	Calcined	181	177	0.510	-
	Calc. Grnd.	166	206	0.354	-
183	9.30% Mo/alumina				
	Calcined	161	132	0.432	-
	Calc. Grnd.	166	189	0.0352	-

standard material used to calculate the t-plot.

Additional data needed for XPS calculations for Ni/Al_2O_3 and Mo/Al_2O_3 catalysts are summarized in Tables XV and XVI, respectively. As in the case of Pt/Al_2O_3 catalysts, application of the XPS model was not successful and the reasons mentioned above are suspected to be responsable for this.

CONCLUSIONS AND RECOMMENDATIONS

Even though X-ray photoelectron spectroscopy has become a routine technique to measure surface concentrations of catalysts, relatively little has been done to widen the analysis of XPS spectra to encompass the determination of the dispersion of supported species in heterogeneous catalysts. This work which is a natural extention of previous investigations carried out at the Catalyst Laboratory of Laval University is indeed a contribution to the development of this potentially rewarding application of XPS techniques.

The model used here is an improved version, developed by Kaliaguine *et al.* (22), of the so-called sheet-stacking model. This version was designed so that phenomena such as surface segregation and bimodal distributions of supported materials can be accounted for. The method we developed to characterize such bimodal distributions is based on the simultaneous resolution of two independent equations corresponding to two forms of the same catalyst. The first one is an expression of the XPS intensity ratio for the catalyst as synthesized, whereas the second equation is an analogous expression for a ground form of the same catalyst. Moreover, in addition to the two XPS intensity ratios, the BET and the external surface areas of both forms of the catalyst were also needed. The most significant novelty of the present study lies within the approach we used to solve the mathematical equations derived from the model. By limiting the number of

TABLE XV. Data for XPS quantification for NiO-Alumina catalysts

Mean Free Path of Photoelectron from Promoter	10.56
Mean Free Path of Photoelectron from Support	20.9
Density of Support	3.8
Density of Promoter	6.67
BET Surface Area of Unground Catalyst	
BET Surface Area of Ground Catalyst	
External Surface Area on Unground Catalyst	
External Surface Area of Ground Catalyst	
Cross Section of Photoelectron from Support	.5735
Cross Section of Photoelectron from Promoter	1.36
Atomic Density Ratio np/ns	1.1977
Detection Efficiency Ratio Dp/Ds	1.719
Size of the Small Particles	3
Promotor Loading in wt%	
Molecular Weight of the Promoter Phase	74.71
Molecular Weight of Promoter	58.71
XPS Intensity Ratio for Unground Catalyst	
XPS Intensity Ratio for Ground Catalyst	
Initial Guess for the Particle Size in A	
The Number of Iterations	

TABLE XVI. Data for XPS quantification for Molybdena-Alumina catalysts

Mean Free Path of Photoelectron from Promoter	18.8
Mean Free Path of Photoelectron from Support	20.9
Density of Support	3.8
Density of Promoter	4.69
BET Surface Area of Unground Catalyst	
BET Surface Area of Ground Catalyst	
External Surface Area on Unground Catalyst	
External Surface Area of Ground Catalyst	
Cross Section of Photoelectron from Support	.5735
Cross Section of Photoelectron from Promoter	9.74
Atomic Density Ratio np/ns	.437
Detection Efficiency Ratio Dp/Ds	1.075
Size of the Small Particles	3
Promotor Loading in wt%	
Molecular Weight of the Promoter Phase	143.94
Molecular Weight of Promoter	95.94
XPS Intensity Ratio for Unground Catalyst	
XPS Intensity Ratio for Ground Catalyst	
Initial Guess for the Particle Size in A	
The Number of Iterations	

constraints to a minimum, the method developed here was designed to apply under a wide range of circumstances.

At this stage of development, the model was found to be better suited for zeolite-supported catalysts than for catalysts based on more conventional supports. For example, some zeolite-supported catalyst showed excellent agreement between dispersions as measured by our XPS method and by other techniques such as hydrogen chemisorption or TEM. The higher rate of success scored with zeolite-based catalysts as compared to other solids is due to the following reasons (a) owing to the well defined pore structure of zeolites, a bimodal distribution fits more closely the distribution of a zeolite-supported material than a material dispersed on a conventional oxide. For catalysts supported on non zeolitic materials, a smoother distribution may be required; (b) it is also easier to distinguish between external and BET surface areas for zeolite based catalysts than for catalysts supported on silica or alumina.

Because of the extreme sensitivity of the model to some of the parameters involved, the application of the method developed here was not always successful. This indicates that further refinements of the current method are still needed. In particular progress has to be made with regards to the definition and determination of external surface areas. One way to tackle this problem is to use samples which have already been characterized by independent techniques while considering the external surface area as a parameter that has to be adjusted. The values that fit best the external surface areas will then be used to find appropriate experimental conditions for the determination of such areas.

The ultimate goal of this investigation is to use the XPS intensity ratios for supported catalysts to determine their particle size

distributions. The method developed here is a significant step toward such an objective. However, a critical appraisal of this method reveals some weaknesses that have to be addressed in future studies. For example, because we have only two independent equations, one among the three variables (C_1, C_2, x_1) to be calculated had to be fixed arbitrarily. The value, between 3 and 10 Å, given arbitrarily to C_1 may be suitable for zeolite-supported catalysts because of their well defined pore structure. However, for other types of catalysts, not only such values are much less justifiable but there is no easy way to make a reasonable guess for C_1. One alternative way to circumvent this problem would be to generate a third independent equation.

Another drawback of the current model is that the bimodal distribution was defined by only its mean particle sizes and a weight factor. This was dictated by the need to keep the number of independent variables as low as possible. Therefore, the next step toward a more realistic bimodal distribution would be the introduction of a variance associated with each of the two particle fractions. Obviously, if additional variables are introduced, the number of independent equations has to be increased accordingly.

One distinct possibility to generate additional independent equations is through the use of incident X-rays with different wavelengths. To this end, the use of the Canadian Synchrotron Radiation Facility is being considered. If successful, this would allow even more realistic particle size distributions to be contemplated. Moreover, the use of incident beams with different energies may well offer opportunities to make progress on another front, that is the characterization of conventional catalysts for which our method does not seem up to now to be very successful.

REFERENCES

1) J.R. Anderson and K.C. Pratt, *"Introduction to Characterization and Testing of Catalysts"*, Academic Press, Sydney, 1985, Chapter 1 and references therein.

2. J.V. Sanders, in *"Catalysis, Science and Technology"*, eds. J.R. Anderson and M. Boudart, Springer-Verlag, Berlin, 1985, Vol. 7, p. 51.

3. P. Gallezot, in *"Catalysis, Science and Technology"*, eds. J.R. Anderson and M. Boudart, Springer-Verlag, Berlin, 1984, Vol. 6, p. 221,

4. H. Dexpert, P. Gallezot and C. Leclercq, in *"Les Techniques Physiques d'Etude des Catalyseurs"*, eds. B. Imelik and J.C. Vedrine, Technip Paris, 1988, p. 655.

5. W.J. Carter, G.K. Schweitzer and T.A. Carlson, *J. Electron Spectrosc. Relat. Phenom.* 5 (1974) 827.

6. R.D. Shannon, J.C. Vedrine, C. Naccache and F. Lefebvre, *J. Catal.* 88 (1984) 431.

7. A. Rahman, G. Lemay, A. Adnot and S. Kaliaguine, *J. Catal.* 112 (1988) 453.

8. J.Z. Shyu, E.T. Skopinsky, J.G. Goodwin, Jr. and A. Sayari, *Appl. Surf. Sci.* 21 (1985) 297

9. Th. Gross, U. Lohse, G. Engelhadrt, K.H. Richter and V. Patzelova, *Zeolites* 4 (1984) 25.

10. L. Tebassi, A. Sayari, A. Ghorbel, M. Dufaux, Y. Ben Taarit and C. Naccache, in *Proceedings, 6th International Zeolite Conference*, Butterworth, 1984, p. 368.

11. V. Ponec, *Catal. Rev.-Sci. Eng.* 11 (1975) 41.

12. R.B. Borade, A. Sayari, A. Adnot and S. Kaliaguine, *J. Phys. Chem.* 94 (1990) 5989.

13. R.B. Borade, A. Adnot and S. Kaliaguine, *J. Catal.* 126 (1990) 26.

14. P.J. Angevine, J.C. Vartuli and W.N. Delgass, in *"Proceedings, 6th International Congress on Catalysis"*, The Royal Society, London, 1977, Vol. 2, p. 611.

15. S.C. Fung, *J. Catal* 58 (1979) 454.

16. C. Defosse, *J. Electron Spectrosc. Relat. Phenom.* 23 (1981) 157

17 C. Defosse, P. Canesson, P.G. Rouxhet and B. Delmon, *J. Catal.* 51 (1978) 269.

18. F.P.J.M. Kerkhof and J.A. Moulijn, *J. Phys. Chem.* 83 (1979) 1612.

19. S.M. Davis, *J. Catal.* 117 (1989) 432.

20. S.M. Davis, *J. Catal.* 122 (1990) 240.

21. S.M. Davis, *Langmuir.* 6 (1990) 517.

22. S. Kaliaguine, A. Adnot and G. Lemay, *J. Phys. Chem.* 91 (1987) 2886.

23. S. Kaliaguine, A. Adnot, G. Lemay and L. Rodrigo, *J. Catal.* 118 (1989) 275.

24. Z. Gabelica, E.G. Derouane and N. Blom, *Appl. Catal.* 5 (1983) 227.

25. S.T. Homeyer and W.M.H. Sachtler, *Stud. Surf. Sci. Catal.* 49B (1989) 975.

26. P. Gallezot, in *Metal Clusters*, M. Moskovits, ed., Wiley, New York, 1986, p. 220.

27. S.J. Gregg and K.S.W. Sing, *"Adsorption, Surface Area and Porosity"*, Academic Press, London, 1982.

28. G. Horvath and K. Kawazoe, *J. Chem. Eng. Jpn.* 16 (1983) 470.

29. E.P. Barrett, L.G. Taylor and P.H. Helenda, *J. Amer. Chem. Soc.* 73 (1951) 373.

30. I. Suzuki, S. Namba and T. Yashima, *J. Catal.* 81 (1983) 485.

31. I. Suzuki, S. Oki and S. Namba, *J. Catal.* 100 (1986) 219.

32. D.J. O'Rear, D.G. Loffler and M. Boudart, *J. Catal.* 121 (1990) 131.

33. J.E. Benson, H.S. Hwang and M. Boudart, *J. Catal.* 30 (1973) 146.

34. M. Inomata, M. Yamada, S. Okada, M. Niwa and Y. Murakami, *J.Catal.* 100 (1986) 264.

35. S.W. Addison, S. Cartlidge, D.A. Harding and G. McElhiney, *Appl. Catal.*

45 (1988) 307.

36. R.C. Bansal, J.B. Donnet and F. Stoeckli, *Active Carbon*, Marcel Dekker, New York, 1988.

37. P. Hudec, J. Novanski, S. Silhar, T.N. Trung, M. Zubek and J. Madar, *Adsorption Sci. Tech.* 3 (1986) 159.

38. P.J.M. Carrott and K.S.W. Sing, *Chem. Ind.* 1986, 786.

39. G.P. Hendreck and T.D. Smith, *J. Chem. Soc., Faraday Trans.1* 85 (1989) 645.

40. S.G. Hedge and S.B. Kulkarne, in *Advances in Catalysis*, P. Rao, ed. Wiley, New York, 1985, p. 233.

41. J. Take, H. Yoshioka and M. Misono, in *Proceedings 9th Intenational Congress on Catalysis*, M.J. Phillips and M.Ternan, eds., The Chemical Institute of Canada, Ottawa, 1988, Vol. 1, p. 372.

42. L. Abrams, M. Keane, Jr. and G.C. Sonnichsen, *J. Catal.* 115 (1989) 410.

43. D.R. Corbin, M. Keane, L. Abrams, R.D. Farlee, P.E. Bierstedt and T. Bein, *J. Catal.* 124 (1990) 268.

44. J.H. de Boer, B.C. Lippens, B.G. Linsen, J.C.P. Broekhoff, A. van den Heuvel and Th.V. Osinga, J. Colloid. Interface Sci. 21 (1966) 405.

45. W.K. Hall, J. Engelhardt and G.A. Still, *Stud. Surf. Sci. Catal.* 42 (1989) 1253.

46. P. Voogd, J.J.F. Scholten and H. van Bekkum, in *Zeolites for the Nineties, Recent Research Reports*, J.C. Jansen, L. Moscou and M.F.M. Post, eds., 8th Int. Zeol. Conf., Amsterdam, 1989, p. 349.

47. W. Schirmer, H. Thamm, H. Stach and U. Lohse, in *The Properties and Applications of Zeolites*, R.P. Towsend, ed., The Chemical Society, London, 1980, p. 204.

48. S.J. Gregg and J.F. Langford, *Trans. Faraday Soc.* 65 (1969) 1394.

49. G.D. Parfitt, K.S.W. Sing and D. Urwin, *J. Colloid Interface Sci.* 53 (1975) 187.

50. S.J. Gregg and M.M. Tayyab, *J. Chem. Soc., Faraday Trans.1* 74 (1978) 349.

51. S. Kohichi, *Appl. Surf. Sci.* 25 (1986) 81.

52. M. Vulli and K. Stark, *J.Phys. E.* 10 (1977) 158.

53. C.D. Wagner, L.E. Davis and W.M. Riggs, *Surface Interface Anal.* 2 (1980) 53.

54. C.J. Powell, *Surface Interface Anal.* 7 (1985) 256.

55. S. Tanuma, C.J. Powell and R.D. Penn, *Surf. Sci.* 192 (1987) L849.

56. D.R. Penn, *J. Electron Spectrosc. Relat. Phenom.* 9 (1976) 29.

57. J. Szajman, J.G. Jenkin, R.C.G. Leckey and J. Liesegang, *J. Electron Spectrosc. Relat. Phenom.* 19(1980) 393.

58. M.P. Seah and W.A. Dench, *Surface Interface Anal.* 1 (1979) 2.

59. C.J. Powell, *J. Electron Spectrosc. Relat. Phenom.* 47 (1988) 197.

60. S. Tanuma, C.J. Powell and R.D. Penn, *J. Electron Spectrosc. Relat. Phenom.* 52 (1990) 393.

61. J.H. Scofield, *J. Electron Spectrosc. Relat. Phenom.* 8 (1976) 29.

62. P. Gallezot, A. Alarcon-Diaz, J.A. Dalmon, A.J. Renouprez and B. Imelik, *J. Catal.* 39 (1975) 334.

63. P. Gallezot, *Catal. Rev. SCi. Eng.* 20 (1979) 121.

64. S.H. Park, M.S. Tzou and W.M.H. Sachtler, *Appl. Catal.* 24 (1986) 85.

65. W.J. Reagan, A.W. Chester and G.T. Kerr, *J.Catal.* 69 (1981) 89.

66. A.W. Chester, *J. Catal.* 86 (1984) 16.

APPENDIX 1

SOFTWARE DESCRIPTION AND OPERATIONS

BACKGROUND

The LAVCAN program was developed to numerically solve the equations that describe a model we developed for the quantitation of XPS data of supported catalysts. The model is particularly adapted to the characterization of bimodal distributions that are usually brought about by surface segregation of the active phase which occurs during the preparation or pretreatment of catalysts. Details concerning the basic assumptions involved in building this model, as well as the mathematical derivation and the general approach to solve the problem are described in a companion report.

GENERAL CONSIDERATIONS

1. The LAVCAN program is presented in two different versions, both of them can be used in an IBM or an IBM compatible microcomputer.

*** The first version is written in QUICK BASIC and can be operated only with a QUICK BASIC software. It has however, the advantage to be easily modified or adapted to future sophistications of the model, as the program is readily accessible.

*** The second version is directly "executable" using the MS DOS operating system. This version does not need any particular software. However, it cannot be modified as easily as the first version, because getting access to the program is not an obvious task.

2. Both versions can be used in either of the Official Languages. The results as well as all interactions through the screen will displayed in the chosen language.

3. Both versions are operated following the same procedure except for the first step during which the program is activated.

*** For the QUICK BASIC version, you need to activate your QUICK BASIC

software. You usually have to select the LAVCAN program, then press simultaneously SHIFT and F5.

*** For the "executable" version, verify that you have the MS DOS operating system and that the appropriate disk drive is activated. Type LAVCAN, then press ENTER.

4. In the present version of LAVCAN, twenty different data have to be introduced for the program to run properly. Frequently, for a series of similar catalysts, a number of these data do not change from one sample to another. In order to avoid introducing the same data again and again, the user has the possibility to create data files that can be saved and used as needed. Also, for all the data to not have a default value of zero, they were given default values corresponding to the data of a reduced Pd/ZSM-5 catalyst (this is an arbitrary choice).

DETAILED OPERATING PROCEDURE

STEP 1: Once LAVCAN software is activated, the screen would look like Figure 1. Now you have to indicate your choise of language, by answering the question as displayed on the screen. If you elect to use English, you must answer by pressing E or e, then ENTER. Otherwise, if you press any other key followed by ENTER, or if you just press ENTER, French will be chosen as a default language.

In what follows, it is assumed that the use of English was chosen. For the alternative choice, the procedure is exactly the same, except that all communications will be in French.

STEP 2: the next question as displayed on the screen is

DO YOU WANT TO USE DATA FROM A FILE?

If you answer NO by pressing either N or n, then ENTER, the default values of the data will appear in sequence. The default answer to this question is YES, that is if you press any key but N or n (or no key) followed by ENTER, the following question will appear on the screen:

L A V A L - C A N M E T

```
PARTICLE SIZE FROM XPS DATA

Would you like to use the english version [E]
Voulez-vous utiliser la version francaise [F]

Your choice / Votre choix:
```

Figure 1.

```
Would you like to use the english version [E]
Voulez-vous utiliser la version francaise [F]

Your choice / Votre choix: E
DO YOU WANT TO USE DATA FROM A FILE? Y
DO YOU WANT FILES DIRECTORY? Y

A:\
MO-1    .DAT    NI-1    .DAT    PD-1    .DAT    PD-2    .DAT
PD-4    .DAT    PD-T1   .DAT    PDMET   .DAT    PT-1    .DAT
PT-10   .DAT    PT-2    .DAT    PT-3    .DAT    TEST    .DAT

 448512 Bytes free

FILE NAME= A:
```

Figure 2.

DO YOU WANT FILES DIRECTORY?

If you are absolutely positive about the name of the file you want to use, answer NO by pressing N or n, then ENTER. If not, or if you want to look at the list of data files that are available, you may want to press any key, but N or n, then ENTER. You may also just press ENTER, as once again the default answer to the question is YES. Under these circumstances, the list of all data files will be displayed on the screen followed by (Figure 2).

FILE NAME= A:

At this point you must provide the name of the data file you want to use.

STEP 3: Using as an example the default data, Figure 3 shows the the sequence of questions that need to be answered to carry out the calculations. The first question is about the mean free path of the chosen photoelectron that originat from thr promoter. The default value is 17.4 Å. You can either type the new data and press ENTER, or simply press ENTER to keep the same value. At this point, the next question appears on the screen and has to be treated in a similar way. The last question concerns the number of iterations you wish to use for the determination of the particle size (C_1) of segregated fraction of the active material.

STEP 4: The results will appear on the screen as shown in Figure 4. As seen, in the upper section, apart from the date and time, the name of the data file you used (if you have used one) is displayed regardless of the whether you have altered the data or not. Next, both solutions of equation [22] are shown, but as described in the main report, only the solution that belongs to the range 0 - 1 is considerd for further calculations. In the results section, the dispersed and segregated fractions are given. In addition, the iterative calculations of C_1 are displayed in a Table. In each line, the numbers are shown in the following order, the starting value of C_1 for a given iteration, the C_1 value as calculated by such an iteration and the difference between these two values. When this difference becomes lower than $1x10^{-6}$, the iteration stops and the last calculated value of C_1 is suggested as the particle size.

As the model is extremely sensitive to some parameters, particularly the external surface areas of the catalyst, it happens that the problem cannot be

```
Mean Free Path of Photoelectron from Promoter [ 17.4    ]?
Mean Free Path of Photoelectron from Support [ 20.5    ]?
                              Density of Support [ 2.4    ]?
                              Density of Promoter [ 11.4    ]?
                BET Surface Area of Unground Catalyst [ 364    ]?
                  BET Surface Area of Ground Catalyst [ 301    ]?
External Surface Area on Unground Catalyst [ 19.1    ]?
  External Surface Area of Ground Catalyst [ 23.8    ]?
Cross Section of Photoelectron from Support [ .865    ]?
Cross Section of Photoelectron from Promoter [ 15.12    ]?
                     Atomic Density Ratio np/ns [ 2.678    ]?
          Detection Efficiency Ratio Dp/Ds [ 1.121    ]?
                     Size of the Small Particles [ 3    ]?
                        Promotor Loading in wt% [ 2.43    ]?
     Molecular Weight of the Promoter Phase [ 106.4    ]?
                  Molecular Weight of Promoter [ 106.4    ]?
XPS Intensity Ratio for Unground Catalyst [ .3017    ]?
            XPS Intensity for Ground Catalyst [ .2648    ]?
Initial Guess for the Particle Size in A [ 100    ]?
                  The Number of Iterations [ 20    ]?
```

Figure 3.

```
Date: 10-14-1990          File=                          Time:12:21:07
-------------------------------------------------------------------------
SOLN=  .9989173   SOLP= -2.913908
-------------------------------------------------------------------------

                          RESULTS
                          ---------
                Dispersed fraction: .8304025
                Segregated fraction: 1.599598

            CALCULATION OF PARTCLE SIZE (ITERATION)
-------------------------------------------------------------------------
            C0                C2                ABS(C2 - C0)
-------------------------------------------------------------------------
            100               165.1384          65.13841
            165.1384          163.6914          1.447021
            163.6914          163.6913          4.577637E-05
            163.6913          163.6913          0
                    Particle size: 163.6913
-------------------------------------------------------------------------
     DO YOU WANT TO TRY AGAIN?
```

Figure 4.

solved with the data in hand. In such situations, a series or warnings have been included in the program. Three typical situations may occur:

1. The weight percent of the well dispersed fraction (x_1) is higher than the total weight percent of the supported material (x_3). As a consequence, the weight of the segregated fraction (x_2) would be negative. The warning that will appear under such circumstances is: *distribution NOT ACCETABLE.* Figure 5 gives a typical example.

2. None of the solutions of equation [22] satisfies the definition of a probability, that is to belong to the range 0 - 1. The following warning will appear next to the solutions of equation [22]: *Solutions NOT ACCEPTABLE.* An example in which these solutions were 1.587371 and -4.403212 is shown in Figure 6. This situation usually leads to a particle distribution that has no physical meaning (Figure 6).

3. During the determination of C_2 by iteration, no convergence takes place, and the following warning is displayed: *ATTENTION: NO CONVERGENCE.*

STEP 5: In all situtions, at the end of STEP 4, the following question appears:

DO YOU WANT TO TRY AGAIN?

If the answer is YES, press Y or y then **ENTER**. You will be prosted to provide data exactly as in STEP 3.

Note that the default answer to this question is NO, that is if you press any key, other than N or n or if you press no key, then **ENTER**, you will move to the next question:

DO YOU WANT TO SAVE DATA

If your answer is NO, press N or n then **ENTER**. ....END

The default answer here is YES. If you press any key, other than N or n, or if you press no key, then **ENTER**, the following will appear on the screen:

FILE NAME= A:

At this stage, you have to provide a name for your data file, and the last data you used will be saved. Note that all data file identifications comprise a set of a maximum of 8 characters followed by the extension .DAT. The extension is automatically added to any file name you provide.

```
  Date: 10-14-1990          File=A:PT-10.DAT                    Time:12:32:23
-------------------------------------------------------------------------------
  SOLN= -4.725732   SOLP=  .9842296
                                 RESULTS
                                 ---------
                        Dispersed fraction: 25.42908
(Distribution NOT ACCEPTABLE)!!!
                        Segregated fraction:-23.57908

                    CALCULATION OF PARTCLE SIZE (ITERATION)
-------------------------------------------------------------------------------
                    C0                  C2                ABS(C2 - C0)
-------------------------------------------------------------------------------
                   100                 280.5658          180.5658
                   280.5658            271.9846          8.581207
                   271.9846            271.9846          0
                         Particle size: 271.9846
-------------------------------------------------------------------------------
             DO YOU WANT TO TRY AGAIN?
```

Figure 5.

```
  Date: 10-14-1990          File=A:NI-1.DAT                     Time:12:30:45
-------------------------------------------------------------------------------
  SOLN=  1.587371   SOLP= -4.403212       (Solutions NOT ACCEPTABLE)!!!

                                 RESULTS
                                 ---------
                        Dispersed fraction: 110.472
(Distribution NOT ACCEPTABLE)!!!
                        Segregated fraction:-107.112

                    CALCULATION OF PARTCLE SIZE (ITERATION)
-------------------------------------------------------------------------------
                    C0                  C2                ABS(C2 - C0)
-------------------------------------------------------------------------------
                   100                 15.38965          84.61035
                   15.38965            9.975955          5.413693
                   9.975955            8.67513           1.300825
                   8.67513             8.543099          .1320305
                   8.543099            8.541583          1.516342E-03
                   8.541583            8.541583          0
                         Particle size: 8.541583
-------------------------------------------------------------------------------
             DO YOU WANT TO TRY AGAIN?
```

Figure 6.

```
Date: 10-29-1990          File=A:NO-1.DAT                    Time:17:45:17
-------------------------------------------------------------------------------
 SOLN=  .8886703   SOLP= -4.853999
                              RESULTS
                              ---------
                    Dispersed fraction: 9.806467
(Distribution NOT ACCEPTABLE)!!!
                    Segregated fraction:-.5064673

                CALCULATION OF PARTICLE SIZE (ITERATION)
-------------------------------------------------------------------------------
                 C0                C2                ABS(C2 - C0)
-------------------------------------------------------------------------------
                 100               -1.688451         101.6885
                -1.688451          -6.778126E-03     1.681673
                -6.778126E-03      -1.036803E-07     6.778022E-03
                -1.036803E-07       3.016018E-15     1.036803E-07
                 3.016018E-15      -9.383837E-20     3.016112E-15
                      Particle size:-9.383837E-20

******WARNING: SOLUTION NOT ACCEPTABLE
-------------------------------------------------------------------------------
          DO YOU WANT TO TRY AGAIN?
```

Figure 7.

```
'************************COMPUTER PROGRAM LAVCAN ************************
'                          **** JULY 1990 ****
'
'**** Abdel Sayari / Serge Kaliaguine / Universite Laval, Quebec ****
'
'Calculation of Crystal Size from XPS Data
'Grinding Procedure using TWO BET Surface Areas and TWO External
'Surface Areas
'
'*************************************************************************



GOSUB ControleEcran: :  GOSUB Cadre: : GOSUB Depart:


'INITIALIZATION DES PARAMETERS
NQUESTION = 20: NSORTIE = 3: VLOCATE = 57: LECTEUR$ = "A:"

DIM QUESTION$(NQUESTION, 2), VALEUR(NQUESTION), SORTIE$(NSORTIE, 2)
     FOR J = 1 TO 2
        FOR I = 1 TO NQUESTION: READ QUESTION$(I, J): NEXT
        FOR I = 1 TO NSORTIE:   READ SORTIE$(I, J):   NEXT

     NEXT

     FOR I = 1 TO NQUESTION: READ VALEUR(I): NEXT

 TEXTE3$(1) = "NOM DE LA FILIERE"
 TEXTE3$(2) = "         FILE NAME"
 TEXTE4$(1) = "    VOULEZ-VOUS UTILISER LES DONNEES D'UNE FILIERE"
 TEXTE4$(2) = "                  DO YOU WANT TO USE DATA FROM A FILE"
 PRINT TEXTE4$(LANGUE); : INPUT REP$
 IF REP$ = "n" OR REP$ = "N" THEN GOTO DEBUT


  TEXTE8$(1) = "VOULEZ-VOUS LA LISTE DES FILIERES"
  TEXTE8$(2) = "       DO YOU WANT FILES DIRECTORY"
  PRINT TAB(18); TEXTE8$(LANGUE); : INPUT REP$
  IF REP$ = "N" OR REP$ = "n" THEN GOTO RECOMMENCE2
  FILES LECTEUR$ + "*.DON"

RECOMMENCE2:
     PRINT TAB(34); TEXTE3$(LANGUE); "= "; LECTEUR$; : INPUT "", REP$
     IF REP$ = "" THEN GOTO RECOMMENCE2
     IF MID$(REP$, LEN(REP$) - 3,-1) = "." THEN REP$ = LEFT$(REP$, LEN(REP$) - 4)
     FILE$ = LECTEUR$ + REP$ + ".DON"

     CLOSE
        OPEN FILE$ FOR INPUT AS #3
          FOR I = 1 TO NQUESTION
          IF EOF(3) THEN GOTO DEBUT
          INPUT #3, VALEUR(I)
          NEXT

DEBUT:
     CLOSE : CLS : LOCATE 1, 38: PRINT FILE$
     GOSUB Parametres: GOSUB ParametresTravail
```

```
'CALCUL DE LA FRACTION DISPERSEE

 K = AR * (CSAR / CSAS) * (LP / LS) * DER
XB = (XB / 100) * MWPROMOTERPHASE / MWPROMOTER
T1 = 2 / (RHOS * BSA1 * .0001)
T2 = 2 / (RHOS * BSA2 * .0001)
P11 = EXP(-T1 / LS)
P12 = EXP(-T2 / LS)
B1 = K * ESA1 / ((K + Y1) * (1 - P11))
B2 = K * ESA2 / ((K + Y2) * (1 - P12))
R1 = BSA1 / BSA2
R2 = R1 ^ 2
R3 = R1 - 1
R4 = (R3 ^ 2) * P12
A0 = -B1 + B2 * (1 - R4) + R3 * ESA2
A1 = ESA1 - ESA2 * R1 + 2 * B2 * R1 * R3 * P12
A2 = P11 * B1 - (B2 * P12 * R2)


'SOLUTION DE: A2*(P0^2)+A1*P0+A0=0

B = SQR(A1 ^ 2 - 4 * A2 * A0)
SOLN = (-B - A1) / (2 * A2): SOLP = (B - A1) / (2 * A2)
P2 = 0
IF (0 < SOLN) AND (SOLN < 1) THEN P2 = SOLN
IF (0 < SOLP) AND (SOLP < 1) THEN P2 = SOLP
X1 = (1 - P2) * BSA1 * (1 - XB) * RHOR * C1 * .0001 / (1 - EXP(-C1 / LP))

 CLS : TEXTE6$(1) = "Heure:": TEXTE6$(2) = " Time:": TEXTE7$(1) = "Filiere=": TEXTE7$(2) = "
File="
 PRINT TAB(3); "Date: "; DATE$; TAB(30); TEXTE7$(LANGUE); FILE$; TAB(65); TEXTE6$(LANGUE); T
IME$
 TEXTE6$(1) = "(Solutions a REJETER)!!!": TEXTE6$(2) = "(Solutions NOT ACCEPTABLE)!!!"
 PRINT "-------------------------------------------------------------------------------"
 PRINT TAB(3); "SOLN= "; SOLN; "  SOLP= "; SOLP, : IF P2 = 0 THEN PRINT TEXTE6$(LANGUE)
 PRINT : PRINT "-------------------------------------------------------------------------------
-"
 TEXTE5$(1) = "RESULTATS": TEXTE5$(2) = " RESULTS "
 PRINT : PRINT TAB(35); TEXTE5$(LANGUE)
      PRINT TAB(35); "---------"

RESULTAT(1) = X1 * 100 * MWPROMOTER / MWPROMOTERPHASE
I = 1: GOSUB SortieEcran
X2 = XB - X1
RESULTAT(2) = X2 * 100 * MWPROMOTER / MWPROMOTERPHASE
I = 2:  GOSUB SortieEcran
B3 = K * (1 - P11 * (P2 ^ 2)) / ((K + Y1) * (1 - P11))
B4 = (P2 - B3) * ESA1 * (1 - XB) * RHOR * .0001 / X2

'DEFINITION OF FUNCTIONS

DEF FNA (X) = -EXP(-C0 / LP) - B4 * C0 + 1
DEF FNB (X) = -B4 + (EXP(-C0 / LP)) / LP
```

```
'CALCUL DE LA TAILLE DES PARTICULES, PAR ITERATION

     NCOUNT = 1
PRINT : PRINT TAB(21); "CALCULATION OF PARTCLE SIZE (ITERATION)"
      PRINT "-------------------------------------------------------------------------------"
      NCOUNT = 1

Iteration:
     IF NCOUNT > NCOUNT THEN GOTO FinIteration2
                C2 = C0 - FNA(C0) / FNB(C0)
                PRINT TAB(18); C0; TAB(35); C2; TAB(53); ABS(C2 - C0)
           IF ABS(C2 - C0) < .0000001 THEN GOTO FinIteration
                C0 = C2
        NCOUNT = NCOUNT + 1: GOTO Iteration

FinIteration:
     RESULTAT(3) = C2
     I = 3: GOSUB SortieEcran
     IF C0 > C1 THEN GOTO RECOMMENCE
    IF C0 < C1 THEN PRINT "******ATTENTION: VALEUR INACCEPTABLE": GOTO RECOMMENCE

FinIteration2:
     PRINT "******ATTENTION: NO CONVERGENCE": PRINT

RECOMMENCE:
     TEXTE1$(1) = "              VOULEZ-VOUS RECOMMENCER"
     TEXTE1$(2) = "             DO YOU WANT TO TRY AGAIN"
     PRINT TEXTE1$(LANGUE); : INPUT REP$
    IF REP$ = "O" OR REP$ = "o" OR REP$ = "Y" OR REP$ = "y" THEN GOTO DEBUT

    TEXTE2$(1) = "       VOULEZ-VOUS SAUVER LES DONNEES"
    TEXTE2$(2) = "           DO YOU WANT TO SAVE DATA"
    PRINT TEXTE2$(LANGUE); : INPUT REP$
    IF REP$ = "n" OR REP$ = "N" THEN END

RECOMMENCE1:
    PRINT TAB(30); TEXTE3$(LANGUE); "= "; LECTEUR$; : INPUT "", REP$
    IF REP$ = "" THEN GOTO RECOMMENCE1
    FILE$ = LECTEUR$ + REP$ + ".DON"

     CLOSE
     OPEN FILE$ FOR OUTPUT AS #3
          FOR I = 1 TO NQUESTION: PRINT #3, VALEUR(I): NEXT
     CLOSE #3


    END


Parametres:                          'ROUTINE DES PARAMETRES

     FOR I = 1 TO NQUESTION
          LONGPARAM = LEN(QUESTION$(I, LANGUE))
          LOCATE I + 3, VLOCATE - LONGPARAM: PRINT QUESTION$(I, LANGUE); " [";
          PRINT VALEUR(I): LOCATE I + 3, VLOCATE + 10: PRINT "]";
          INPUT REPONSE$
          IF REPONSE$ = "" THEN GOTO SuiteParametres:
          VALEUR(I) = VAL(REPONSE$)
```

```
SuiteParametres:
     NEXT
     RETURN

ControleEcran:                    'CONTROLE DE L'ECRAN
     COLOR (4), (11), (4): CLS
     RETURN



Depart:                           'TEXTE DE DEPART
     LOCATE 3, 24: PRINT " L A V A L - C A N N E T"
     LOCATE 4, 24: PRINT " ---------------------"
     LOCATE 10, 23: PRINT "CRYSTAL SIZE FROM XPS DATA"
     LOCATE 15, 20: PRINT "Abdel Sayari & Serge Kaliaguine"
     LOCATE 20, 10: PRINT "Would you like to use the english version [E]"
     LOCATE 21, 10: PRINT "Voulez-vous utiliser la version francaise [F]"
     LOCATE 23, 26: INPUT "Your choice / Votre choix: ", REP$
     LANGUE = 1
     IF REP$ = "F" OR REP$ = "f" THEN LANGUE = 1
     IF REP$ = "E" OR REP$ = "e" THEN LANGUE = 2
     RETURN

ParametresTravail:                'Identification des parametres de travail
     LP = VALEUR(1):   LS = VALEUR(2):   RHOS = VALEUR(3): RHOR = VALEUR(4)
     BSA1 = VALEUR(5): BSA2 = VALEUR(6): ESA1 = VALEUR(7): ESA2 = VALEUR(8)
     CSAS = VALEUR(9): CSAR = VALEUR(10)
     AR = VALEUR(11):  DER = VALEUR(12): C1 = VALEUR(13):  XB = VALEUR(14)
     MWPROMOTERPHASE = VALEUR(15):              MWPROMOTER = VALEUR(16)
     Y1 = VALEUR(17):  Y2 = VALEUR(18):  CO = VALEUR(19):  NCOUNT = VALEUR(20)
     RETURN

          DATA "Libre Parcours Moyen des Electrons dans le Promoteur"
          DATA "Libre Parcours Moyen des Electrons dans le Support"
          DATA "Densite du Support"
          DATA "Densite du Promoteur"
          DATA "Surface BET du Catalyseur non Broye"
          DATA "Surface BET du Catalyseur Broye"
          DATA "Surface Externe du Catalyseur non Broye"
          DATA "Surface Externe du Catalyseur Broye"
          DATA "Section Efficace du Photoelectron du Support"
          DATA "Section Efficace du Photoelectron du Promoteur"
          DATA "Rapport des Densites Atomiques np/ns"
          DATA "Rapport des Facteurs de Transmission Dp/Ds"
          DATA "Taille des petites particules"
          DATA "Teneur en %Poids"
          DATA "Masse Moleculaire de la Phase du Promoteur"
          DATA "Masse Moleculaire du Promoteur"
          DATA "Rapport d'Intensite XPS pour Catalyseur non Broye"
          DATA "Rapport d'intensite XPS pour Catalyseur Broye"
          DATA "Valeur initiale du diametre des particules externes en A"
          DATA "Nombre d'iterations"

          DATA "Fraction dispersee:"
          DATA " Fraction segreguee:"
          DATA " Diametre:"
```

```
        DATA "Mean Free Path of Photoelectron from Promoter"
        DATA "Mean Free Path of Photoelectron from Support"
        DATA "Density of Support"
        DATA "Density of Promoter"
        DATA "BET Surface Area of Unground Catalyst"
        DATA "BET Surface Area of Ground Catalyst"
        DATA "External Surface Area on Unground Catalyst"
        DATA "External Surface Area of Ground Catalyst"
        DATA "Cross Section of Photoelectron from Support"
        DATA "Cross Section of Photoelectron from Promoter"
        DATA "Atomic Density Ratio np/ns"
        DATA "Detection Efficiency Ratio Dp/Ds"
        DATA "Size of the Small Particles"
        DATA "Promotor Loading in wt%"
        DATA "Molecular Weight of the Promoter Phase"
        DATA "Molecular Weight of Promoter
        DATA "XPS Intensity Ratio for Unground Catalyst"
        DATA "XPS Intensity for Ground Catalyst"
        DATA "Initial Guess for the Particle Size in A"
        DATA "The Number of Iterations"

        DATA " Dispersed fraction:"
        DATA "Segregated fraction:"
        DATA "Particle size:"


        DATA 17.4,20.5,2.4,11.4,364
        DATA 301, 19.1, 23.8, 0.865, 15.12
        DATA 2.678, 1.121, 3, 2.43, 106.4
        DATA 106.4, 0.3017, 0.2648, 100, 20

Cadre: 'CADRE ---DRAWS FRAME FROM (ROW1,COL1) TO (ROW2,COL2)---

     CLS : ROW1 = 6: COL1 = 6: ROW2 = 17: COL2 = 70
     IF (ROW1 > ROW2) THEN PRINT "Error-frame": BEEP: RETURN
     LOCATE ROW1, COL1
     PRINT CHR$(201); STRING$(COL2 - COL1 - 1, 205); CHR$(187);
     FOR I = 1 TO (ROW2 - ROW1 - 1)
          LOCATE ROW1 + I, COL1
          PRINT CHR$(186)
          LOCATE ROW1 + I, COL2
          PRINT CHR$(186)
     NEXT I
     LOCATE ROW2, COL1
     PRINT CHR$(200); STRING$(COL2 - COL1 - 1, 205); CHR$(188);

     RETURN

SortieEcran:
          PRINT TAB(25); SORTIE$(I, LANGUE); RESULTAT(I)
          RETURN
```

APPENDIX 2

TRANSMISSION ELECTRON MICROGRAPHS AND PARTICLE SIZE STATISTICS OF SELECTED CATALYSTS

Transmission electron micrographs of two Pt/HZSM-5 and two Pd/HZSM-5 are shown in the following pages. These micrographs were obtained using the extractive replica technique. This technique allows only particles on the external surface to be observed.

Particle size histograms are also included. These histograms were calculated based on the analysis of typically 500 to 1000 particles (this figure is referred to as *counts* in the legend of the histogram). The average particle size (given in nm) is designated as *mean*.

LIST OF MICROGRAPHS AND HISTOGRAMS

Designation	Sample
140A	1.85% Pt/HZSM-5(A), prepared by ion-exchange, reduced.
140B	2.53% Pt/HZSM-5(B), prepared by ion-exchange, reduced.
142A	3.00% Pd?HZSM-5(A), prepared by ion-exchange, reduced.
151B	2.98% Pd/HZSM-5(B), prepared by gas phase adsorption-decomposition, reduced.

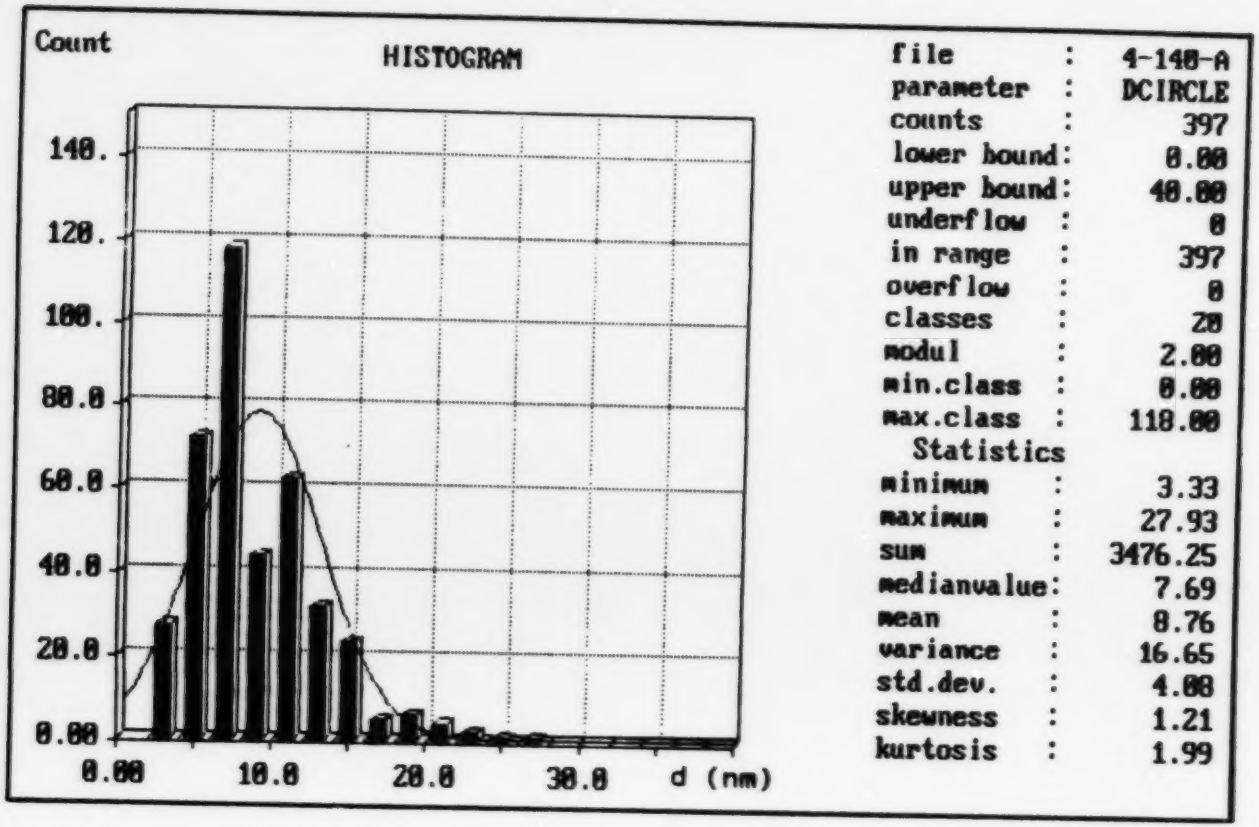

Histogram of sample 140A (1.85% Pt/HZSM-5)

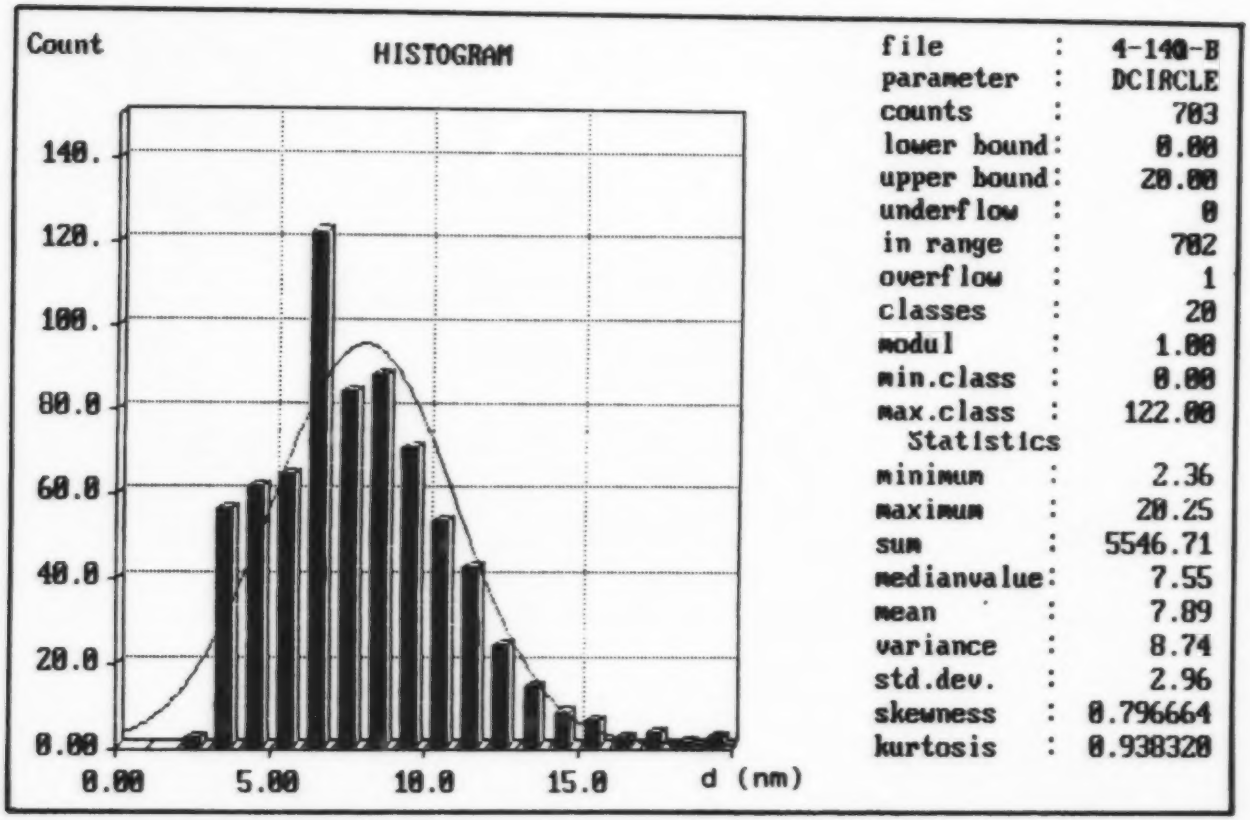

Histogram of sample 140B (2.53% Pt/HZSM-5)

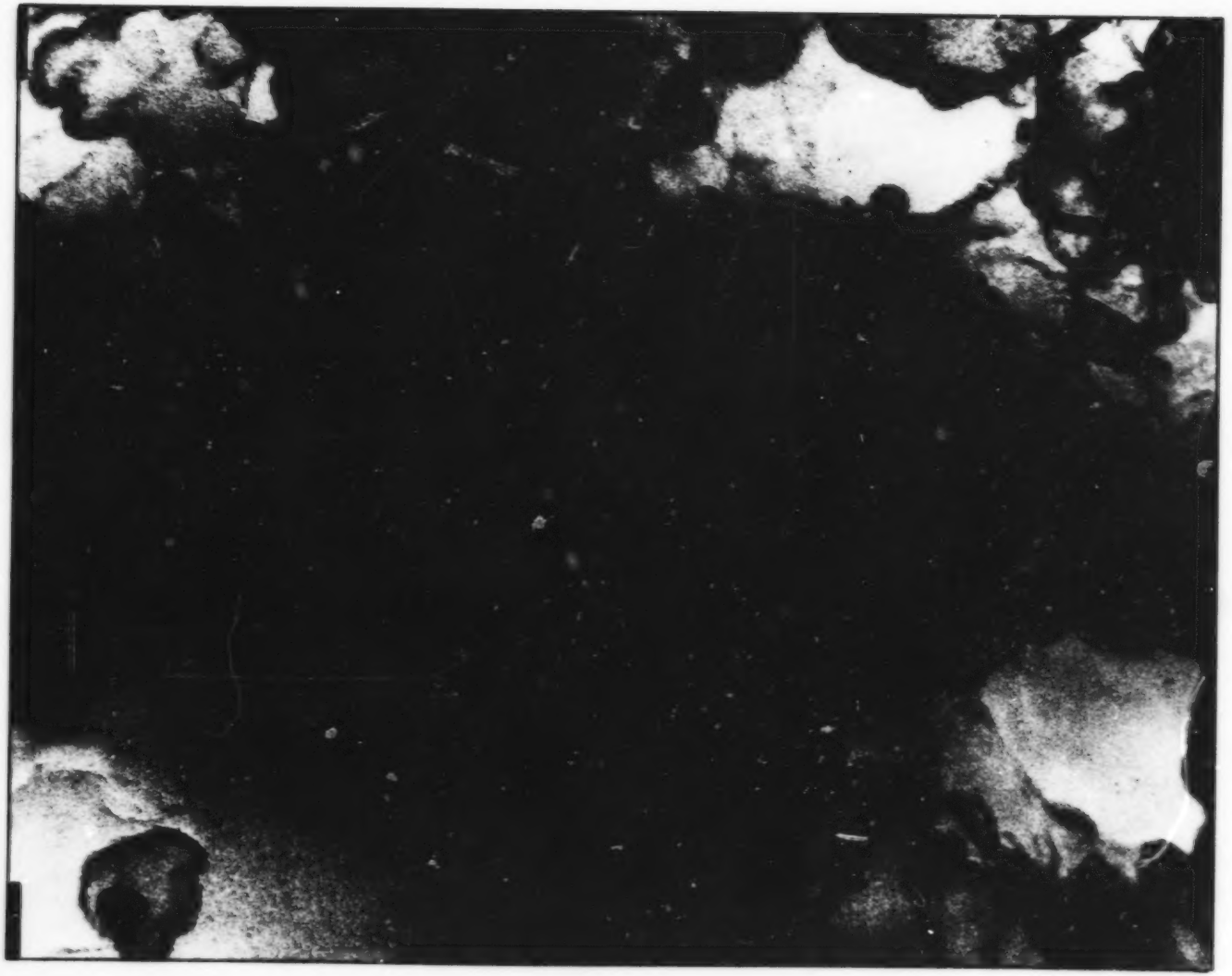

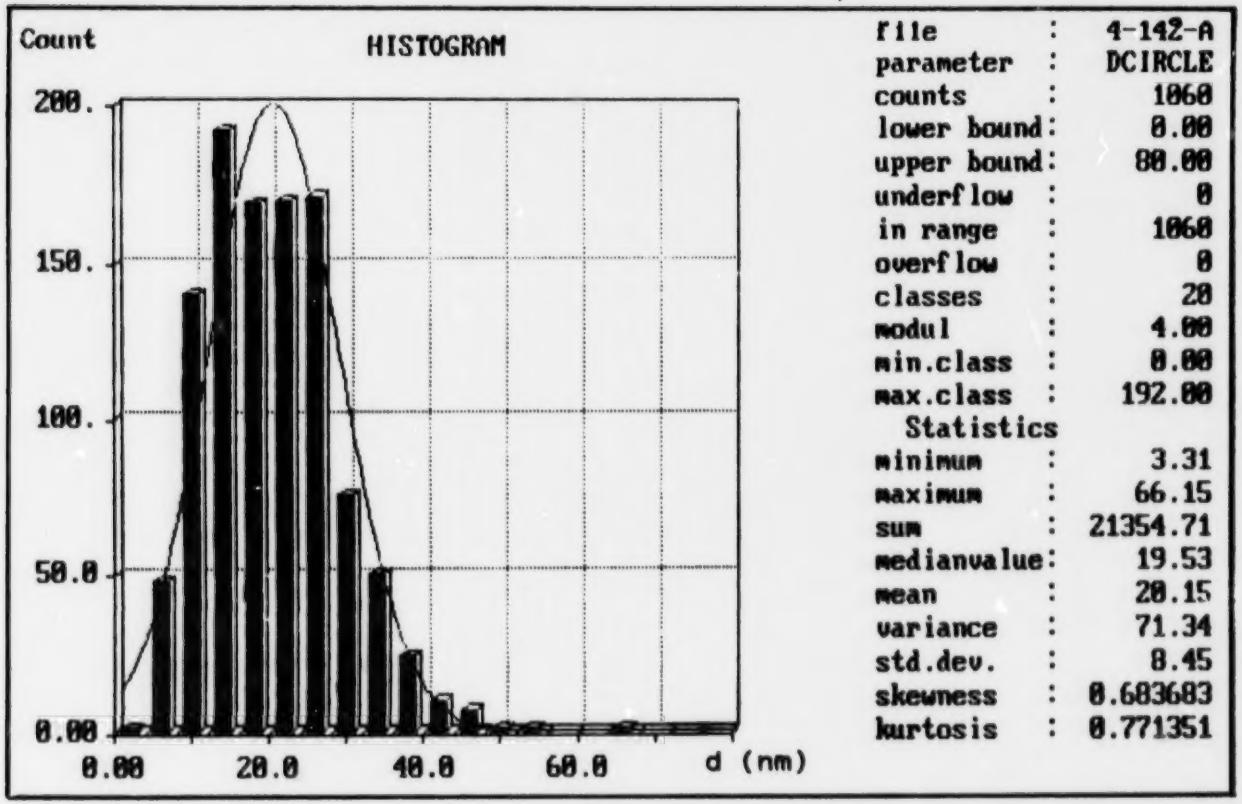

Histogram of sample 142A (3.00% PD/HZSM-5)

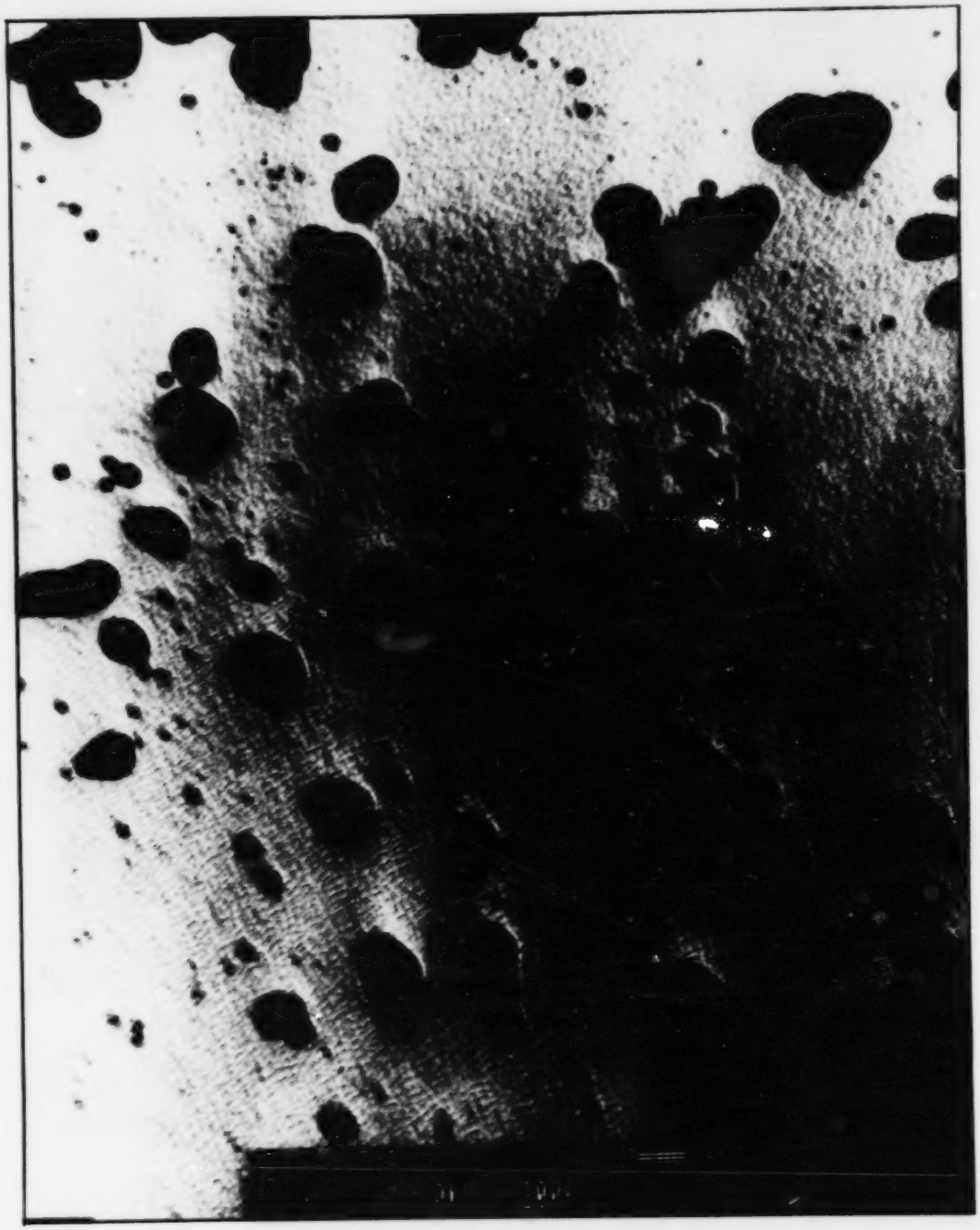

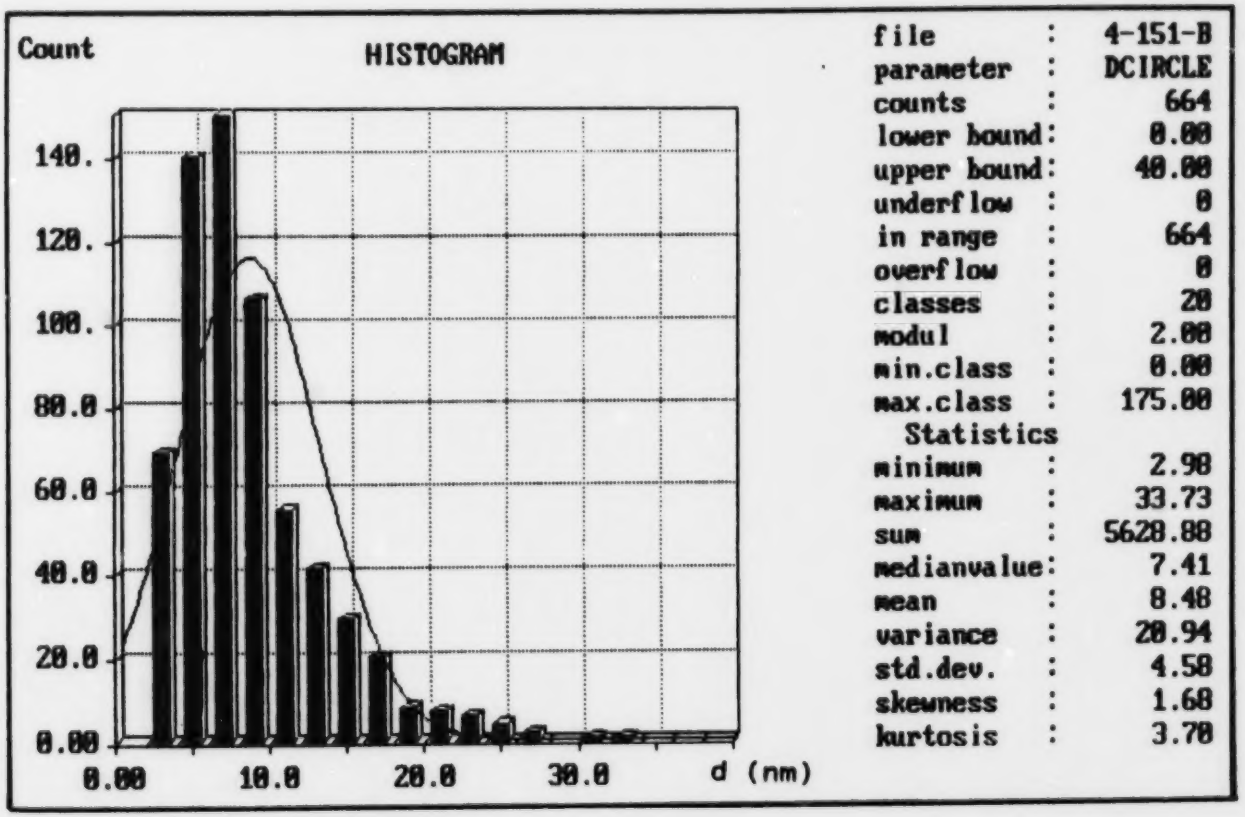

Histogram of sample 151B (3.00% PD/HZSM-5)